GlyBP: A structural model of the extracellular domain of human α1 glycine receptor

by

Zhenyu Liu

BS, Nankai University, 1998

MS, Peking University, 2001

Submitted to the Graduate Faculty of

Graduate School of Medicine in partial fulfillment of

the requirements for the degree of

Doctor of Philosophy

University of Pittsburgh

2007

UNIVERSITY OF PITTSBURGH

School of Medicine

This dissertation was presented

by

Zhenyu Liu

It was defended on

Nov. 16th, 2007

and approved by

Yan Xu, Professor, Department of Anesthesiology

Jon W. Johnson, Associate Professor, Department of Neuroscience

Gonzalo E. Torres, Assistant Professor, Department of Neurobiology

Maria Kurnikova, Assitant Professor, Department of Chemistry,

Carnegie Mellon University

Marc J. Glucksman, Professor, Department of Biochemistry and Molecular Biology,

Rosalind Franklin University

Dissertation Advisor: Michael Cascio, Associate Professor,

Department of Molecular Genetics and Biochemistry

GlyBP: A structural model of the extracellular domain of human α1 glycine receptor

Zhenyu Liu, PhD

University of Pittsburgh, 2007

The Glycine receptor (GlyR) is the major inhibitory neurotransmitter receptor in the spinal cord and brainstem. Dysfunction of GlyR causes hyperekplexia, a neurological disease characterized by an excessive startle response. However, limited structural information about this physiologically important receptor is available. Therefore, direct structural analyses at high resolution of truncated ligand binding domains, and possibly full-length GlyR, are required for further understanding of this important neurotransmitter receptor.

This study is focused on purifying and characterizing glycine binding protein (GlyBP), a mutant form of the ligand binding domain of the GlyR, in which two hydrophobic loops were replaced with corresponding hydrophilic residues in AChBP. GlyBP was overexpressed in Sf9 insect cells. GlyBP was found in both cytosolic and membrane-bound fractions after subcellular fractionation. The cytosolic fraction was misfolded. In contrast, the membrane-bound form is functional as shown by its ability to reversibly bind to 2-aminostrychnine resin. After affinity purification, membrane-bound GlyBP could be isolated in an aqueous form and a membrane-associated vesicular form. Radiolabeled binding assays showed both forms of GlyBP retained abilities to bind to its ligands, with affinities comparable to those of full-length GlyR. Furthermore, studies using chemical crosslinking, light scattering and luminescence resonance energy transfer (LRET) showed that both forms of GlyBP are oligomeric, and are very likely pentameric. The LRET studies also showed GlyBP undergoes conformational changes upon

glycine binding equivalent to changes in full-length GlyR. Further studies using chemical crosslinking coupled with mass spectrometry were conducted to probe the low resolution three-dimensional structure and inter-subunit interactions. A number of intramolecular and/or intermolecular Lys-Lys crosslinks were identified. Those crosslinks provided useful information about protein folding and validated our computationally-derived model of GlyBP.

Results from this study indicate that GlyBP adopts a native-like structure and is a structural and functional homolog of the extracellular domain of GlyRs and other members in Cys-loop receptor family. Further detailed structural studies will lead to further understanding of function of the ligand binding domain of GlyRs. In addition, efforts on resolving a high-resolution structure of GlyBP might result in detailed structural information about this physiologically important receptor and also other Cys-loop receptors.

TABLE OF CONTENTS

LIST OF TABLES

LIST OF FIGURES

PREFACE

I would like to express my deepest gratitude to my dissertation advisor, Dr. Michael Cascio. His great scientific guidance and continuous support over these years makes this dissertation possible. Mike has a great personality and a positive attitude towards life. His encouragement has been inspiring to me throughout the entire process of my graduate study.

I sincerely thank my dissertation committee members: Dr. Yan Xu, Dr. Jon W. Johnson, Dr. Gonzalo Torres and Dr. Maria Kurnikova. I appreciate all the instructive suggestions brought up by all of them at each committee meeting. I also appreciate the time Dr. Marc Glucksman has taken to serve as the outside examiner.

Thanks also go to our collaborators. I'd like to thank Dr. Maria Kurnikova from Carnegie Mellon University for her help with all the computational work, Dr. Vasanthi Jayaraman from University of Texas Health Science Center for her help with the LRET studies, and Dr. Robert O. Fox from the University of Texas Medical Branch for his support on dynamic light scattering experiment. I also wish to thank Dr. Billy Day and Dr. Mani Balasubramani in the Genomics and Proteomics Core Laboratories for their help with mass spectrometry experiments.

I'm grateful to the current and past members in Cascio Lab, Dr. Tom Tillman, Stephanie Goode and Emily Boyde for their help and friendship. I also appreciate the time shared with all my friends in Pittsburgh.

I must thank my parents, Henghua Liu and Guilian Zheng, and my sisters for their endless love and support. Finally, I thank my wife Wen Xu, for her love, understanding and support, and my 18-month old son Alex Liu, who has brought me lots of joy.

1.0   INTRODUCTION

1.1   INHIBITORY SYNAPSES AND GLYCINE SYNAPTOGENESIS

1.1.1   Synaptic neurotransmission

Neurons in the brain and at the neuromuscular junctions communicate at synapses. How synapse formation occurs became an intriguing question since the term "synapse" was introduced by Charles Sherrington more than a century ago (Shepherd and Erulkar, 1997). Synapses may be electrical or chemical. Direct neuronal communication is mediated by electrical synapses. The most common type of electrical synapses are mediated via neuronal gap junctions (Bennett and Zukin, 2004; Hormuzdi et al., 2004). Specialized gap junctions are clusters of transcellular channels composed of connexin proteins, which allow ionic current to flow directly between neurons and thus mediate electrical coupling between cells (Connors and Long, 2004). However, interneuronal and neuromuscular communication is mainly mediated by chemical synapses. A chemical synapse consists of a pair of opposing presynaptic and postsynaptic terminals. The presynaptic neuron secretes neurotransmitters, which activate a variety of ligand-gated ion channels and G-protein coupled receptors on the postsynaptic membrane (Kandel et al., 2000). The arrival of an action potential generated in the presynaptic neuron triggers fusion of neurotransmitter-

containing synaptic vesicles resulting in release of neurotransmitter into the synaptic cleft. Released neurotransmitter then binds specifically to receptors residing on the postsynaptic membrane, resulting in conformational changes in the receptor and transient opening of coupled ion channels. The open ion channels allow influx or efflux of ions causing changes in the membrane potential of the postsynaptic cells. The direction of ion flow is determined by the concentrations of ions inside and outside of the cell, the membrane potential and the permeability (P) of the membrane to those ions. Specifically, the membrane potential is described by the Goldman-Hodgkin-Katz equation:

$$V_m = \frac{RT}{F} \ln \frac{P_K[K^+]_{out} + P_{Na}[Na^+]_{out} + P_{Cl}[Cl^-]_{in}}{P_K[K^+]_{in} + P_{Na}[Na^+]_{in} + P_{Cl}[Cl^-]_{out}}$$

The resulting ion flow, in turn, affects the membrane potential. These effects could either be excitatory and inhibitory depending on the ion selectivity of the channels. Influx of cations or efflux of anions depolarizes the postsynaptic membrane, potentially resulting in generation of an action potential. In contrast, influx of anions, usually Cl⁻ ions, results in hyperpolarization of the postsynaptic membrane. Under typical conditions, the ion channels, such as AChR and glutamate receptors, which are permeable to Na^+ and K^+ ions, are excitatory, whereas GlyRs and γ-amino-butyric acid (GABA) receptors (GABARs) typically mediate inhibitory effects (Kandel et al., 2000).

1.1.2   Glycine as an inhibitory or excitatory neurotransmitter

Glycine was discovered as a neurotransmitter more than 40 years ago when Aprison and Werman found that glycine is much more concentrated in the spinal cord than elsewhere in

the brain (Aprison and Werman, 1965). Glycine is most concentrated in the ventral horn, where spinal interneuronal terminals are enriched. Thus they postulated that glycine might function as a postsynaptic inhibitory neurotransmitter. This idea was supported by electrophysiological studies, in which it was found that the action of potential firing in spinal neurons is greatly reduced when glycine is applied to these neurons (Curtis and Watkins, 1960; Werman et al., 1967). A subsequent study on the rate of glycine synthesis in the rat central nervous system demonstrated that glycine is derived by *de novo* synthesis, suggesting that spinal neurons have the ability to synthesize glycine endogenously (Shank and Aprison, 1970). In addition, isotopically labeled glycine could be released in rat spinal cord slices upon electrical stimulation (Hopkin and Neal, 1970). All those early studies demonstrated that glycine fulfilled most criteria set for a neurotransmitter molecule and functioned as an inhibitory neurotransmitter by acting on GlyRs in the spinal cord and the brainstem.

In addition to its action on GlyRs, glycine also functions as a co-agonist of N-methyl-D-aspartic acid (NMDA) receptors. The presence of glycine at nanomolar concentrations is a prerequisite for channel activation by glutamate or NMDA (Johnson and Ascher, 1987; Kleckner and Dingledine, 1988). Glycine displays different affinities within distinct NMDA receptor subtypes and the affinity of glycine can be modulated by Mg^{++} concentrations (Wang and MacDonald, 1995; Parsons et al., 1998).

1.1.3 Inhibitory synapses

A balance of excitation and inhibition is crucial for normal brain function (Cline, 2005). Disruption of this balance has been shown to be associated with a number of neurological diseases such as Parkinson's disease, autism and schizophrenia (Llinas et al., 1999; Rubenstein and Merzenich, 2003; Wassef et al., 2003). Proper control of excitability of neurons is achieved by inter-neuron communication mainly medicated by neurotransmitters. GABA and glycine are major inhibitory neurotransmitters in the brain and spinal cord (Kuhse et al., 1995; Moss and Smart, 2001; Breitinger and Becker, 2002). They both specifically bind to distinct receptors residing in the postsynaptic membrane and activate chloride-conducting channels generally resulting in a rapid hyperpolarization of postsynaptic neurons (Moss and Smart, 2001). Although they have distinct distribution patterns and functions in the nervous system, electrophysiological studies have shown that GlyRs and GABA$_A$Rs may coexist in the same neurons (Barker and Ransom, 1978; Faber et al., 1980), suggesting a synergistic role in mediation of inhibitory synaptic transmission.

In the CNS, GlyRs are predominantly located in the brainstem and spinal cord (Legendre, 2001; Breitinger and Becker, 2002). When glycine binds to GlyR on the membrane, this ion-conducting pore transiently allows passive diffusion of Cl$^-$ across the membrane. Once GlyRs are activated, the membrane potential rapidly reaches the Cl$^-$ equilibrium potential (Lynch, 2004). The Cl$^-$ flux could either depolarize or hyperpolarize the neuronal membrane depending on the Cl$^-$ equilibrium potential relative to the resting potential. At early developmental stages, the high intracellular Cl$^-$ concentration results in depolarization of neuronal membranes after GlyR activation (Flint et al., 1998). In mature neurons, the Cl$^-$ equilibrium is typically more negative and GlyR activation hyperpolarizes

the neurons in which GlyR resides (Lynch, 2004). Thus, GlyRs are generally considered to mediate inhibitory neurotransmission in the mature central nervous system. In addition to its high concentration in the spinal cord and the brainstem, GlyRs are also highly concentrated in the retina (Pourcho, 1996). In addition, immunolabeling experiments showed GlyRs are detectable in the cerebellum (Araki et al., 1988; Takahashi et al., 1992) and olfactory bulb (van den Pol and Gorcs, 1988).

The formation of functional synapses requires selective accumulation of neurotransmitter receptors at the postsynaptic site. GlyRs were found to be highly concentrated at the postsynaptic site apposed to glycinergic afferent endings (Triller et al., 1985; Seitanidou et al., 1988). At early developmental stages, newly-synthesized GlyRs are randomly distributed in the postsynaptic membrane (Hoch et al., 1989; Kirsch et al., 1993). Extensive studies have shown that the postsynaptic scaffolding protein gephyrin plays a crucial role in the formation of GlyR clusters (Kneussel and Betz, 2000). Gephyrin was originally co-purified with GlyRs (Pfeiffer et al., 1982; Graham et al., 1985) and subsequent studies showed that gephyrin directly binds to the cytoplasmic loop of GlyR β subunit (Meyer et al., 1995; Kneussel et al., 1999) and anchors the receptor to the cytoskeleton (Kirsch and Betz, 1995). In addition, a number of gephyrin binding partners, including collybistin (Kins et al., 2000), profilin (Mammoto et al., 1998) and RAFT1 (Sabatini et al., 1999), as well as the cytoskeleton, were believed to act in concert with gephyrin to mediate postsynaptic accumulation of GlyRs (Kneussel and Betz, 2000). GlyR clustering was found to be activity-dependent (Kirsch and Betz, 1998), as blockade of neuronal activity with tetrodotoxin prevents the formation of postsynaptic GlyR clusters in embryonic spinal neurons. In addition to its location on the postsynaptic membrane, GlyRs

are also found in presynaptic (Jeong et al., 2003) and non-synaptic sites (Flint et al., 1998). Activation of presynaptic GlyRs was found to facilitate transmitter release in the rat auditory brainstem nucleus (Turecek and Trussell, 2001, 2002). Non-synaptic GlyR activation seems to be crucial for development in both cortical and hippocampal neurons (Flint et al., 1998; Mori et al., 2002)

1.2   GLYCINE RECEPTOR AND OTHER PENTAMERIC CYS-LOOP RECEPTORS

1.2.1   General structure of Cys-loop receptors and their roles in the central nervous system

Cys-loop receptors, also called pentameric ligand gated ion channels (LGICs) or nicotinicoid receptors, are essential mediators of fast synaptic transmission at neuronal and neuromuscular synapses (Connolly and Wafford, 2004). The Cys-loop receptor family includes nicotinic acetylcholine receptors (nAChR), GlyRs, GABA type A and C receptors and serotonin type 3 receptors (5-HT$_3$ receptor) (Connolly and Wafford, 2004; Lester et al., 2004). Similar to other classical neurotransmitter-gated receptors, Cys-loop receptors are usually located on postsynaptic membranes and undergo a conformational change upon binding to their respective presynaptically released endogenous agonist. This binding leads to the opening of the ion channel pore at a millisecond time scale and allows passive flux of selective ions across the postsynaptic membrane. Based on their ion selectivity, the Cys-loop receptors are divided into two major categories: cation-selective and anion-selective

receptors. nAChR and 5-HT$_3$ receptor are selective for cations and mediate excitatory neurotransmission in the nervous system and muscles (Barry and Lynch, 2005). GlyR and GABA$_{A/C}$ –R channels are anion-selective and primarily conduct chloride ions, so activation of these receptors typically produce an inhibitory effect on the postsynaptic cell (Legendre, 2001; Luscher and Keller, 2004; Mody and Pearce, 2004).

All Cys-loop receptors are comprised of a pentameric assembly of subunits arranged surrounding a central ion-conducting pore. Each subunit of Cys-loop receptors shares a similar topology. The N-terminal extracellular domain is followed by four transmembrane segments (M1-M4) that comprise the transmembrane domain. This N-terminal domain harbors overlapping agonist and antagonist binding sites located at subunit interfaces. The presence of a conserved Cys-disulfide pair separated by 13 residues (Cys-loop) is the defining feature of this receptor family (Schofield et al., 1987). The M2 segment from each subunit lines the central ion-conducting pore. Each TM segment (M1-M4) is considered to be α–helical. This four helix membrane topology was originally proposed based on hydropathy analysis on nAChR (Karlin and Akabas, 1995) and was supported by the structure of the *Torpedo* nAChR as determined by cryoelectron microscopy (Miyazawa et al., 2003). However, previous studies in our lab and others showed the original four transmembrane helix model might not be entirely correct for Cys-loop receptors (Leite et al., 2000; Leite and Cascio, 2001). A large intracellular loop exists between M3 and M4 and is important for modulation of channel activity by interaction with intracellular proteins.

The nAChR is the most extensively studied receptor in the Cys-loop superfamily of LGICs. Using its competitive antagonist α–bungarotoxin, the nAChR was the first

neurotransmitter receptor to be functionally characterized at a molecular level (Changeux et al., 1970). nAChRs consist of neuronal- and muscle-type receptors found in the central and peripheral nervous systems and in neuromuscular junctions, respectively (Hogg et al., 2003). Both types of receptors respond to acetylcholine and are involved in many important physiological functions. The muscle-type nAChR on the postsynaptic membrane of muscle is the key player in neuromuscular transmission (Hogg et al., 2003). Dysfunction of the muscle-type nAChR is associated with a number of inherited and acquired diseases resulting in impaired neuromuscular transmission and muscle weakness (Kalamida et al., 2007). Myasthenia gravis and congenital myasthenic syndromes are the most studied diseases associated with muscle-type nAChR. The former is the most common autoimmune disorder of neuromuscular transmission, in which the presence of autoantibodies to muscle-type nAChRs cause loss of receptors at neuromuscular junction, leading to defects in neuromuscular transmission and muscle fatigue (Vincent et al., 2001). The neuronal-type nAChR is involved in many brain functions, such as attention, memory and cognition (Lindstrom, 2003). Defects in neuronal-type nAChR are often associated with neurodegenerative diseases such as Alzheimer's disease, Parkinson's disease and schizophrenia (Hogg and Bertrand, 2007).

GABA$_{A/C}$ receptors are the major inhibitory neurotransmitter receptors and are found in about 20-50 % of all neuronal synapses (Bloom and Iversen, 1971). GABA$_A$Rs mediate most of physiological actions of GABA (Sieghart et al., 1999). Dysfunctions of GABA$_{A/C}$R have been implicated in a variety of central nervous system disorders, such as stress, sleep disturbances, alcoholism, epilepsy, schizophrenia and insomnia (Mohler, 2006; Michels and Moss, 2007).

The 5-HT$_3$ receptor is the only ligand gated ion channel among the receptors for serotonin. 5-HT$_3$ receptors are located both presynaptically and postsynaptically (Chameau and van Hooft, 2006). Activation of presynaptic 5-HT$_3$ receptors mediates an increase in intracellular Ca^{2+}, either indirectly via the activation of voltage-gated Ca^{2+} channels or directly via Ca^{2+} entry through the 5-HT$_3$-receptor-operated ion channel, which controls the excitability of neuronal networks (Chameau and van Hooft, 2006). Dysfunction of 5-HT$_3$ receptors are involved in nausea, vomiting and autonomic cardiac defect (Costall and Naylor, 2004).

1.2.2   Molecular diversity and receptor assembly of Cys-loop receptors

1.2.2.1 Molecular diversity and assembly of GlyR

Most ion channels are usually formed by multiple identical or homologous subunits (Doyle, 2004). All Cys-loop receptors are believed to be pentameric, either homopentameric or heteropentameric. A large number of subunits of each member have been identified, which gives rise to various subunit composition and spatial arrangements within a single complex. The GlyR was originally purified from rat spinal cord (Pfeiffer and Betz, 1981; Pfeiffer et al., 1982). Subsequent studies using cDNA library screening resulted in isolation of cDNA clones that correspond to the 48 kDa (α1) and 58 kDa (β) subunits (Grenningloh et al., 1987; Grenningloh et al., 1990). To date, four α subunits (α1-4) and one β subunit have been identified (Grenningloh et al., 1990; Kuhse et al., 1990a; Akagi et al., 1991; Kuhse et al., 1991; Matzenbach et al., 1994). Cloning and isolation of these subunits were mostly

9

from humans, mice, rats (Breitinger and Becker, 2002), chicks (Boehm et al., 1997; Harvey et al., 2000) and zebrafish (Legendre and Korn, 1994; Legendre, 1997). In addition, alternative splicing contributes to the heterogeneity of GlyR subunits. All α subunits have splicing variants (Breitinger and Becker, 2002). For example, GlyR α1 has a splicing variant that contains an additional eight-amino acid insert in the large intracellular loop containing a phosphorylation site (Malosio et al., 1991a). Primary sequence of all α subunits shares about 80-90% identity (Lynch, 2004). In contrast, the β subunit only has sequence identity of less than 50% to α subunits (Grenningloh et al., 1990). While all α subunits were found to be predominantly distributed in the brainstem and spinal cord (Breitinger and Becker, 2002), the β subunit was transcribed at all developmental stages throughout spinal cord and brain (Fujita et al., 1991; Malosio et al., 1991b).

In adult mammalian animals, functional GlyR is a heteropentamer composed of α subunit and β subunit. Chemical cross-linking originally suggested it had a stoichiometry of 3α/2β (Langosch et al., 1988). However, a recent study provided evidence that synaptic GlyRs assemble in an invariant 2α/3β stoichiometry (Grudzinska et al., 2005). In heterologous expression systems, all α subunits could form functional homomeric channels with distinct pharmacological properties (Schmieden et al., 1989; Sontheimer et al., 1989; Kuhse et al., 1991; Schmieden et al., 1992; Bormann et al., 1993; Laube et al., 2002). Functional α homomeric GlyRs have been only found at extrasynaptic sites (Takahashi et al., 1992; Singer and Berger, 2000). In contrast, β subunit cannot assemble into functional receptors in the absence of α subunit (Bormann et al., 1993; Kuhse et al., 1993). It has been shown that membrane targeting of GlyRs to axonal or somatodendritic compartment is determined by their subunit composition (Deleuze et al., 2005).

1.2.2.2 Molecular diversity and assembly of other Cys-loop receptors

The nAChR subunits could be divided into two categories: α subunits (α1-9) and non-α subunits (β, γ, ε, and δ) (Corringer et al., 2000). The major difference between them is that all α subunits have two adjacent cysteines that are critical for ligand binding (Kao et al., 1984; Karlin and Akabas, 1995) and all non-α subunits do not (Sargent, 1993). Among all these subunits, when expressed heterologously, only α7 (Couturier et al., 1990), α8 (Gerzanich et al., 1994) and α9 (Elgoyhen et al., 1994) are able to form functional homopentamers.

Nineteen homologous $GABA_A$ receptor subunits have been identified, which are divided into distinct subclasses: α (1-6), β (1-3), γ (1-3), δ, ε, π, θ, and ρ (1-3) (Wilke et al., 1997; Bonnert et al., 1999; Steiger and Russek, 2004). Despite the extensive diversity of $GABA_A$ receptor subunits, the most commonly accepted stoichiometry of pentameric $GABA_A$ receptor in the brain is: $α_2β_2γ$ (Sieghart et al., 1999). As observed in other Cys-loop receptors, recombinant $GABA_A$ α1, β1, β2, γ2, or δ subunits can form homomeric receptors (Blair et al., 1988; Shivers et al., 1989; Verdoorn et al., 1990). $GABA_C$ receptor is a much less known subtype of GABA receptors. $GABA_C$ receptors have distinct pharmacological properties compared with those of $GABA_A$ receptors (Drew and Johnston, 1992; Strata and Cherubini, 1994). Similar to $GABA_A$ receptors, $GABA_C$ receptors also form homo- or hetero-oligomeric receptors when expressed heterologously (Enz and Cutting, 1998). In some cases, $GABA_C$ receptor subunits can coassemble with $GABA_A$ receptor or GlyR subunits (Koulen et al., 1998; Pan et al., 2000).

In contrast to other members of Cys-loop receptors, the molecular diversity of 5-HT_3 receptor has been much less studied. To date, only two types of 5-HT_3 receptor subunits (5-HT_{3A} and 5-HT_{3B}) have been identified (Maricq et al., 1991; Davies et al., 1999). While 5-HT_{3A} subunits form functional homomeric receptors (Hussy et al., 1994; Gill et al., 1995), 5-HT_{3B} subunits need to co-assemble with 5-HT_{3A} subunits to form functional receptors (Davies et al., 1999; Dubin et al., 1999). In addition, 5-HT_{3A} subunits are able to functionally co-assemble with the neuronal nicotinic α4 receptor subunit (van Hooft et al., 1998; Kriegler et al., 1999).

1.2.3   Structure and function of the extracellular ligand binding domain of Cys-loop receptors

Since the N-terminal extracellular domain (ECD) contains almost a half of the entire sequence and harbors the ligand binding sites, it is as important as the ion-conducting pore with regard to normal functioning of Cys-loop receptors. Although sequence alignments of the extracellular domain of all Cys-loop members show little conservation in primary sequence, a number of residues are found to be almost completely conserved (Srinivasan et al., 1999; Deane and Lummis, 2001; Jin et al., 2004). Extensive mutagenesis studies of the ECD of Cys-loop receptors, especially nAChR, have identified many important residues that are essential for ligand recognition and subsequent channel activation (Corringer et al., 2000). Before discovery of the crystal structure of AChBP and the cryo-EM structure of *Torpedo* nAChR, most structural information about the ECD of Cys-loop receptors was from photo-affinity labeling, protein modification and site-directed mutagenesis studies (Corringer et al., 2000). It is generally accepted that the ligand binding pocket is conserved

throughout the entire family of Cys-loop receptors and is formed by six distinct regions of sequence located in the interface between two neighboring subunits (Corringer et al., 2000; Grutter and Changeux, 2001; Lester et al., 2004). The principal side, also called "+" side, of this ligand binding pocket contains three loops from the same subunit (Regions A, B and C, Figure 1.1). In contrast, three β-strands, instead of loops, contribute to the formation of the complementary side (Regions D, E and F, Figure 1.1), also called "-" side. In nAChR, extensive affinity labeling and mutagenesis experiments confirmed the presence of ligand binding sites in the subunit interface and also identified various residues directly involved in ligand binding in both the principal (Kao et al., 1984; Dennis et al., 1988; Pedersen and Cohen, 1990; Middleton and Cohen, 1991; Corringer et al., 1995) and complementary sides (Chiara et al., 1998; Chiara et al., 1999). While the identified residues in regions A, B, C and D are well conserved among distinct subunits in nAChR, residues in regions E and F are relatively variable (Corringer et al., 2000).

Recently, the structure of a monomeric ECD of mouse nAChR α1 subunit was resolved at 1.9 Å resolution (Dellisanti et al., 2007), providing the first high-resolution structure of the ECD of a mammalian Cys-loop receptor. This structure reveals atomic details for a number of structural elements critical for nAChR function. Although the mouse α1 ECD retains a similar fold to that of AChBPs, the lack of structural information regarding the subunit interface limited the usefulness of the monomeric structure in understanding the quaternary structure of pentameric Cys-loop receptors.
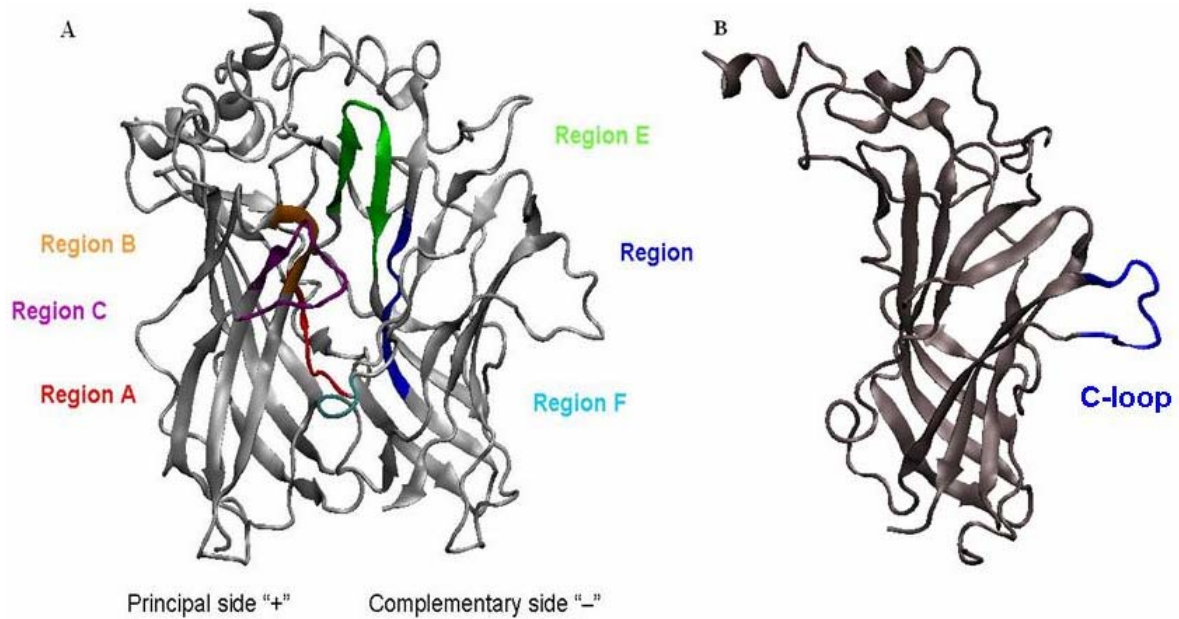
Figure 1.1 Schematic representation of structure of ligand binding pocket (A) and the C-loop (B) of Cys-loop receptors.

Figures were generated uing the program Visual Molecular Dynamics (VMD), version 1.8.6 (Humphrey et al., 1996).

1.2.4 Structure and function of transmembrane domains and gating mechanisms of Cys-loop receptors

1.2.4.1 The receptor ion pore and gating mechanisms of GlyR

As for other LGICs, GlyRs exist in at least three functional states: resting state, open state and desensitized state. In the absence of agonist, the channels are in the non-conducting resting state, which is the most stable state in the absence of bound agonist. Binding of the endogenous agonist to a ligand-gated ion channel causes transient opening of the channel,

14

also called "gating", causing the channel to exist in the short-lived conducting open state. In the long-lived desensitized state, the channels are closed and have high affinity to ligand. In the presence of agonist, GlyR cycles between these distinct conformational states and these transitions are critical for its proper functioning.

Under physiological conditions, glycine is present in the cerebrospinal fluid of rat brain in the micromolar range (Larson and Beitz, 1988; Whitehead et al., 2001). The EC_{50} value for GlyR activation ranges from 20 to 100 μM in different isolated neuronal preparations or in heterologous expression systems (Krishtal et al., 1988; Akaike and Kaneda, 1989; Sontheimer et al., 1989; Fatima-Shad and Barry, 1992; Pribilla et al., 1992; Agopyan et al., 1993). Using single channel recording techniques, ion permeation mechanisms of GlyR were studied in primary culture of embryonic mouse neurons and in rat hippocampal neurons (Bormann et al., 1987; Fatima-Shad and Barry, 1992, 1993). It was found in these studies that the relative permeabilities of anions were: $SCN^- > NO_3^- > I^- > Br^- > Cl^- > F^-$, whereas the relative conductances were: $Cl^- > Br^- > NO_3^- > I^- > SCN^- > F^-$. This sequence of permeability is proportional to the ionic hydration energy, which implies that hydration force is the major barrier to ion channel entry (Rajendra et al., 1997; Lynch, 2004). Based on these electrophysiological studies, the pore diameter of GlyR channel is estimated to be 5.2 Å in spinal neuron GlyRs (Bormann et al., 1987), 5.5–6.0 Å in hippocampal neurons (Fatima-Shad and Barry, 1993) and 5.22–5.45 Å in recombinant receptors (Rundstrom et al., 1994).

How agonist binding is coupled to channel activation has been an intriguing question for many years. Electrophysiological studies on a series of point mutants in the intracellular M1-M2 and extracellular M2-M3 loops demonstrated both loops are involved

in coupling of agonist binding and channel activation (Lynch et al., 1997). In cysteine scanning mutagenesis studies of α1 GlyR, considerable structural changes in the M2-M3 loop is observed upon channel activation (Lynch et al., 2001). In GlyRs, the involvement of the M1-M2 and M2-M3 loops in coupling of agonist binding and channel activation was also demonstrated by point mutations observed in startle diseases (Shiang et al., 1993; Rees et al., 1994; Shiang et al., 1995; Elmslie et al., 1996; Saul et al., 1999). The Cys-loop in the extracellular domain is a defining feature of the Cys-loop receptors. In both GlyR and GABA receptors, the extracellular Cys-loop is not directly inovolved in the formation of participate in agonist binding site (Vandenberg et al., 1993; Amin et al., 1994). However, mutations at Asp148, a conserved residue in this signature Cys-loop, caused a significant decrease in receptor efficacy, suggesting a functional role of this residue in channel activation (Schofield et al., 2003). In addition, molecular modeling in combination with electrophysiological studies showed that charged residues in Loops 2 and 7 interact with the M2-M3 loop and those interactions are required for signal transduction process that links ligand binding to channel activation (Absalom et al., 2003).

1.2.4.2 Structure and function of transmembrane domains and gating mechanisms of other Cys-loop receptors

The transmembrane domains (TMs) of pentameric Cys-loop receptors are the channel-forming domains that allow ion conductance across the membrane and thus play an essential role in proper receptor functioning. The second transmembrane segments (TM2) from each subunit form the ion-conducting pore. A variety of studies using cryo-EM (Unwin, 1995; Miyazawa et al., 1999) , NMR spectroscopy (Opella et al., 1999; Tang et al.,

2002) and cysteine scanning mutagenesis (Karlin and Akabas, 1998) have shown that the pore-forming TM2 segment is an α helix.

In all Cys-loop receptors, significant conformational changes occur during channel gating. In Unwin's refined structure (Unwin, 2005), the TM2-TM3 linker makes contact with extracellular loops, which is proposed to be critical for coupling of agonist binding and channels activation. In the absence of ligand, the α subunits have a different conformation from non-α subunits. When acetylcholine is bound, the α subunits convert to a non-α conformation (Unwin et al., 2002). This process is also accompanied by displacement in the C-loop (Figure 1.1B) and a 15º clockwise rotation of the inner extracellular β sheets, resulting in a more symmetrical structure. In nAChRs and GlyRs, channel gating was impaired by mutations in the M2-M3 linker (Rajendra et al., 1995a; Lynch et al., 1997; Lewis et al., 1998; Grosman et al., 2000). However, mutations in the corresponding region of non-α subunits in muscle nAChR and GlyR have no effects on channel activation properties (Grosman et al., 2000; Shan et al., 2003). In addition, a number of mutations found in this region in human diseases have also been shown to alter channel gating in Cys-loop receptors (Connolly and Wafford, 2004). Currently, the molecular mechanisms of channel gating remain controversial and poorly resolved.

1.2.5   Selective ligands and ligand binding properties of GlyRs

GlyR function is modulated by specific agonists and antagonists as well as anesthetics, neurosteroids and various drugs. The native GlyR is selectively activated by glycine, β-alanine and taurine (Legendre, 2001), all of which are released in the central nervous system (Werman et al., 1967; Rajendra et al., 1995a; Oja and Saransaari, 1996). All these

agonists bind to the N-terminal extracellular domain of GlyRs (Kuhse et al., 1990b; Schmieden et al., 1992; Vandenberg et al., 1992a). However, under typical physiological conditions, neither β-alanine nor taurine have the ability to activate synaptically located GlyRs (Legendre, 2001). The pharmacological properties of distinct α- and β-amino acids were analyzed using voltage clamp recording in heterologously expressed α1 GlyR in *Xenopus* oocytes (Schmieden and Betz, 1995). This study demonstrated that agonistic action of α-amino acids was determined by the size and polarity of their C_α-atom substitutions. In contrast, β-amino acids had both agonistic and antagonistic actions on GlyR (Schmieden and Betz, 1995). For example, taurine elicit a significant membrane current at higher concentrations and competitively inhibited glycine-induced current at lower concentrations (Schmieden et al., 1992; Schmieden and Betz, 1995; De Saint Jan et al., 2001). These β-amino acids were thus considered as partial agonists. However, antagonistic activity was not detectable for β-alanine, which is usually considered as a GlyR agonist (Laube et al., 1995). In addition, the affinities and efficacies of those agonists vary in different expression systems (Lynch, 2004).
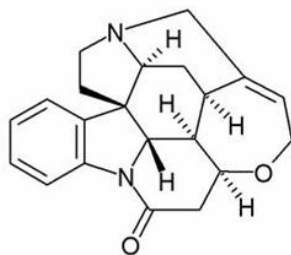
Figure 1.2 Chemical structure of strychnine.

Strychnine is a highly potent competitive antagonist of GlyRs in mature neurons (Figure 1.2) (Young and Snyder, 1973); (Ehlert, 1988). Displacement studies have shown that strychnine and glycine have overlapping, but not identical, binding sites on GlyRs (Pfeiffer et al., 1982; Graham et al., 1983; Marvizon et al., 1986). In an early study, ^{3}H-strychnine was found to bind irreversibly and photochemically label the GlyR when exposed to UV light (Graham et al., 1983). Due to its high selectivity and affinity, aminostrychnine agarose is commonly used for GlyR purification (Pfeiffer et al., 1982; Graham et al., 1985; Cascio et al., 1993; Morr et al., 1995).

As observed in all Cys-loop receptors, the ligand binding site in GlyRs is formed by three loops that contribute to the "+" side of the ligand binding pocket, and three β-sheets that belong to the "-" side of this inter-subunit pocket (Lynch, 2004) (Figure 1.1). Key residues located in regions A, B and C that correspond to the "+" side loops have been identified to be crucial for agonist binding (Vandenberg et al., 1992a; Schmieden et al., 1993; Rajendra et al., 1995b; Vafa et al., 1999; Han et al., 2001). However, the role of regions D, E and F from three β-strands on the "-" side in agonist binding have not been systematically studied (Lynch, 2004).

To date, a number of residues/fragments in the GlyR α1 subunit, including Arg52 (Ryan et al., 1994; Saul et al., 1994), Arg65 (Grudzinska et al., 2005), Ile93 (Vafa et al., 1999), Asn102 (Vafa et al., 1999; Han et al., 2001), Glu157 (Grudzinska et al., 2005), Gly160 (Kuhse et al., 1990b), Phe159-Tyr161 (Vandenberg et al., 1992b; Schmieden et al., 1993) and Lys200-Lys206 (Vandenberg et al., 1992a) have been shown to be involved in glycine binding. All identified residues are located on the regions in the binding pocket conserved throughout the entire family of Cys-loop receptors. However, most of these

studies were based on changes of EC_{50} caused by mutations introduced at those specific sites and the evidence for direct agonist-receptor binding is lacking. Compared with the α1 subunit, relatively little attention has been paid to the β subunit in terms of agonist binding. A recent report revealed that the β subunit plays a significant role in agonist-receptor binding of heterooligomeric GlyRs (Grudzinska et al., 2005). In this study, residues Arg86 and Glu180 in β subunit, which are homologous to Arg65 and Glu157 in the α1 subunit, were found to have direct interactions with glycine. In addition, the β subunit was involved in strychnine antagonism. The role of the β subunit was also confirmed by the fact that coexpression of β subunits with low affinity α1 subunit binding mutants could rescue high affinity binding (Grudzinska et al., 2005).

1.2.6 Membrane clustering of GlyR at synapses

Proper neurotransmission is highly dependent on precise location of concentrated neurotransmitter receptors at synaptic sites. It has been shown that gephyrin plays an important role in membrane clustering of synaptic GlyRs. Gephyrin is a peripheral membrane protein that was originally co-purified with GlyR (Pfeiffer et al., 1982; Schmitt et al., 1987). A variety of gephyrin isoforms exist in the CNS and in most non-neuronal tissues (Prior et al., 1992; Kawasaki et al., 1997). In brain, gephyrin colocalized with a large subset of GlyRs, especially in the spinal cord (Baer et al., 2003; Waldvogel et al., 2003). In addition, gephyrin was found to colocalize with a majority of $GABA_A$ receptor subtypes in various brain regions (Sassoe-Pognetto et al., 2000). Several lines of evidence have shown that gephyrin plays a key role in organization of the postsynaptic membrane during inhibitory synapse formation. First, gephyrin was reported to bind directly to the

cytoplasmic loop of GlyR β subunit, which connects the third and fourth transmembrane segments (Meyer et al., 1995; Kneussel et al., 1999). Second, when co-expressed with recombinant gephyrin, GlyR β subunits were targeted to intracellular gephyrin aggregates while GlyR α subunits were retained in the plasma membrane (Kirsch et al., 1995), indicating a crucial role of gephyrin in GlyR clustering via its binding to the β subunit. Third, gephyrin has been shown to bind to polymerized tubulin with a high affinity (Pfeiffer et al., 1982; Graham et al., 1985; Kirsch et al., 1991). Furthermore, abolition of gephyrin expression by antisense oligonucleotides prevents GlyR cluster formation in spinal neurons (Kirsch et al., 1993). Gephyrin knockout mice further demonstrated specific disruption of GlyR clustering while the overall morphology of glycinergic synapses and total GlyR expression level remained normal (Feng et al., 1998), corroborating the role of gephyrin in GlyR clustering.

1.2.7   Functional changes of GlyR during development

As described above, four α subunits and one β subunit of GlyRs have been identified. It was found that expression of mRNAs for rodent GlyR subunits was developmentally regulated (Malosio et al., 1991b; Watanabe and Akagi, 1995). The α1 subunit is expressed at very low levels in embryonic and neonatal rat spinal neurons and starts to become predominant at postnatal day 15. The α3 subunit displays a similar expression pattern to that of the α1 subunit during development but is less widely distributed, and the α2 mRNA accumulates prenatally and decreases after birth (Malosio et al., 1991b). The α4 subunit is expressed in embryonic neurons, although its location is restricted to the white matter instead of the grey matter where α2 usually resides at early developmental stages (Harvey

21

et al., 2000). In addition, the β subunit demonstrates a similar expression pattern to the α1 subunit, indicating a functional correlation between those two distinct types of subunits (Malosio et al., 1991b). These changes in the molecular composition of GlyR subunits during development are closely associated with changes in the functional properties of developing GlyRs in spinal cord and brainstem (Aguayo et al., 2004). In cultured mouse spinal neurons, the sensitivity of GlyR to glycine increased transiently with development (Tapia and Aguayo, 1998). Glycine-induced current was blocked by strychnine in a development-dependent manner (Ye, 2000). A model of developmental changes of the subunit composition of GlyRs was proposed based on these experimental observations (Aguayo et al., 2004). During development, the GlyR switches from homomeric α or heteromeric α2β receptors in immature neurons to α1β receptors in mature neurons, mirroring changes in functional properties of the receptors and contributing to its plasticity during development.

1.2.8   GlyR and diseases

Startle disease, also known as hereditary hyperekplexia, is a rare inherited human neuromotor disorder characterized by muscle stiffness in the neonate, hyperrelexia, and an exaggerated startle response to sensory stimuli (Zhou et al., 2002). This disease has been associated with mutations in genes *GLRA1* and *GLRB* encoding GlyR α1 and β subunits, respectively (Shiang et al., 1993; Brune et al., 1996; Humeny et al., 2002; Rees et al., 2002). *GLRA1*, localized on chromosome 5q31.2, contains over nine exons (Shiang et al., 1993; Matzenbach et al., 1994), and many of these mutations are in exons 7 and 8 that encode for amino acids ranging from M1 to the extracellular loop connecting M2 and M3

(Humeny et al., 2002). Mutations in *GLRA1* may be either dominant or recessive in familial and sporadic hyperekplexia (Saul et al., 1999; del Giudice et al., 2001; Rees et al., 2001).

Alteration in channel function caused by point mutations in the *GLRA1* gene have been confirmed by electrophysiological studies. R271 is located near at the extracellular end of M2 domain and forms part of the extracellular loop connecting the M2 and M3 transmembrane segments (the M2-M3 loop). R271L or R271Q mutations greatly reduced agonist sensitivity although ion permeation was largely unaltered (Rajendra et al., 1994). This decrease in agonist sensitivity resulted in reduced glycinergic tone in spinal cord interneurons, leading to reduction in the recurrent and reciprocal inhibitory feedback that modulates motorneuron firing in reflex arcs. Another two startle point mutations, Y279C and K276E, both also located in the M2-M3 loop, converted GlyR agonists taurine and β–alanine into competitive antagonists without alterating their binding affinities (Lynch et al., 1997). These results suggest that agonist binding and channel activation are uncoupled in these mutant GlyRs found in patients with startle diseases. W243A and I244A mutations, located in the intracellular M1-M2 loop, not only reduced agonist efficacy, but also greatly increased the desentization rate, suggesting an effect of these intracellular point mutations on coupling of channel activation and desentization (Lynch et al., 1997). Q266H, to date the only mutation in the transmembrane domain of GlyR in startle disease, greatly increased glycine EC_{50} and the single channel open time without affecting ligand binding properties (Moorhouse et al., 1999). This mutation also converted taurine into a weak partial agonist, which is consistent with the hypothesis that the agonist/antagonist behavior is determined by channel gating efficacy, not ligand binding affinities (Moorhouse et al., 1999). Thus the Q266H mutation is considered to directly affect GlyR channel gating.

Native GlyRs are typically heteropentameric structures of α and β subunits. Although the majority of GlyR point mutations found in startle disease have been identified on the α subunit, mutations in *GLRB* can also cause startle disease. A G229D mutation in GlyR β subunit greatly increased glycine EC_{50} in heterologously expressed heteromeric GlyR in HEK293 cells (Rees et al., 2002). The reduction in agonist sensitivity was attributed to either a decrease in agonist affinity or a decrease in the ability of the receptor to undergo conformational changes that open the channel.

1.3 ACETYLCHOLINE BINDING PROTEIN (ACHBP) AND CHOLINERGIC NEUROTRANSMISSION

1.3.1 Discovery of AChBP and its role in cholinergic neurotransmission

Traditionally, synaptic transmission involves participation of presynaptic and postsynaptic neurons. Neurotransmitters produced in presynaptic sites are released to the synaptic cleft and specifically bind to their cognate receptors in the postsynaptic neurons, which activate the downstream signaling cascade in the postsynaptic neurons. However, recent evidence has shown that glial cells also play a significant role in chemical neurotransmission. Glial cells are involved in the regulation of neural integration in the central nervous system (Haydon, 2001; Auld and Robitaille, 2003), in the modulation of efficacy of synaptic transmission (Mitterauer, 2000, 2001; Oliet et al., 2001) and in the generation of pacemaker rhythms (Mitterauer, 2000; Parri et al., 2001). On the basis of these experimental findings, a tripartite synapse model has been proposed (Teichberg, 1991; Araque et al., 1999;

Volterra et al., 2002). In this model, glial cells are actively involved in synaptic neurotransmission. They respond to neuronal activity with elevation of their internal Ca^{2+} concentration (Araque et al., 1999). This elevation of Ca^{2+} concentration triggers release of chemical transmitters from glial cells and thus, in turn, regulates neuronal activity.

The neuromuscular junction (NMJ) is the synapse between an axon terminal of a motorneuron and the muscular endplate. Acetylcholine released from a nerve terminal rapidly diffuses cross the synaptic cleft and binds to nAChRs on the postsynaptic muscle membrane (Martyn et al., 1992), resulting in increased cation conductance. Depolarizing cation influx allows the endplate potential at the NMJ to reach the threshold for generation of an action potential (Martyn et al., 1992). Perisynaptic Schwann cells, the glial cells at the NMJ, surround nerve terminals (Colomar and Robitaille, 2004). These cells are sensitive to neuronal activity, and high frequency nerve stimulation induces elevation of their intracellular Ca^{2+} concentration (Rochon et al., 2001). In addition, neurotransmitter release, including ACh, ATP and adenosine, activates G-protein coupled receptors in perisynaptic Schwann cells, resulting in the release of Ca^{2+} from intracellular stores (Jahromi et al., 1992; Robitaille, 1995; Robitaille et al., 1997; Bourque and Robitaille, 1998). Perisynaptic Schwann cells, in turn, also modulate synaptic neurotransmission as glial Ca^{2+} increase depresses neurotransmitter release at the NMJ (Robitaille, 1998; Castonguay and Robitaille, 2001). Synaptic modulation of perisynaptic Schwann cells has been attributed to involvement of release of chemical modulators from Schwann cells (Colomar and Robitaille, 2004). However, the identity of those modulators has not been experimentally validated, although a few candidate molecules such as glutamate and prostaglandin have been proposed to be involved in this process.

In a recent study, neurons from the CNS of the mollusc *Lymnaea stagnalis* were cultured in a triplet configuration in which the presynaptic neuron forms two synapses with postsynaptic partners (Smit et al., 2001). When co-cultured with synaptically paired neurons, glial cells specifically inhibit cholinergic neurotransmission. This inhibition is mediated by AChBP release from glial cells. AChBP is a naturally occurring homolog of the ligand-binding domains of nAChRs and other Cys-loop receptors. It is a soluble homopentamer with high affinity to x-bungarotoxin and ACh. At cholinergic synapses, AChBP captures presynaptically released ACh, and thus inhibits cholinergic synaptic transmission (Smit et al., 2001; Brejc et al., 2002).

1.3.2 Structure of AChBPs

The first X-ray structure of AChBP was resolved at 2.7 Å resolution from the freshwater snail, *Lymnaea stagnalis* (Brejc et al., 2001). Since then, the structures of AChBPs from *Aplysia californica* (Hansen et al., 2004) and the molluskan species, *Bulinus truncates* (Celie et al., 2005a) have been resolved. In addition, the structures of AChBPs with different bound nicotinic ligands, including nicotine (Celie et al., 2004), carbamylcholine (Celie et al., 2004), epibatidine (EPI), methyllycaconitine (MLA), and lobeline (LOB)(Hansen et al., 2005), as well as peptide toxins from *Elapid* snakes and *Conus* snails (Bourne et al., 2005; Celie et al., 2005b; Hansen et al., 2005), have been resolved at atomic resolution by X-ray crystallography.

Lymnaea stagnalis AChBP (Ls-AchBP) assembles as a cylindrical homopentamer with the subunits arranged radially about the central axis with a central hole having 18 Å diameter lined by hydrophilic charged residues. Each AChBP subunit has an asymmetric

shape with a size of about 62 x 47 x 34 Å. From the an N-terminus, it starts with an α–helix, two short 3_{10} helices, followed by a β–sandwich of 10 β–strands (Brejc et al., 2001). As observed in other pentameric Cys-loop receptors, the ligand binding sites in Ls-AChBP are located at the subunit interfaces. Each ligand binding site contains residues from three loops from the principal side of one subunit and three β–strands from the complementary side of an adjacent subunit. The principal side is composed of Tyr-89, Trp-143, Trp-145 and Tyr-185, which are located in distinct loops forming the ligand binding site. The complementary side of the ligand binding site contains residues Trp-53, Gln-55, Arg-104, Val-106, Leu-112, Met-114 and Tyr-164, which are located in the three β–strands. All these residues in the binding sites correlate with corresponding residues in Cys-loop receptors that have been identified to be involved in ligand binding by mutagenesis and labeling studies (Kao and Karlin, 1986; Dennis et al., 1988; Galzi et al., 1990; Middleton and Cohen, 1991; Czajkowski et al., 1993; Corringer et al., 1995; Sine et al., 1995; Martin et al., 1996). Almost all these residues are well conserved in nicotinic receptors. One exception is Tyr-164 in the loop-F region, which has low sequence conservation in this family. Sequence variation exists in this binding pocket, as this variation is essential in order to provide distinct agonist binding affinity and selectivity. The access routes to the ligand binding sites are probably from above or below the disulfide C loop (Brejc et al., 2001). In this region, the ligand binding site is buried from the solvent, which prevents access from the outside. Access of ligands with different sizes would require distinct conformational rearrangement in this region. The ligand binding properties of Ls-AChBP are similar to those of homomeric α7 nAChR, which is the closest mammalian homolog to AChBP (Smit et al., 2001). Compared with α7 nAChR, Ls-AChBP has relatively low

affinity for acetylcholine and much higher affinity for nicotine (Smit et al., 2001; Hansen et al., 2002).

In the crystal structures of Ls-AChBP in complex with the nAChR agonists carbamylcholine and nicotine (Celie et al., 2004), both ligands are bound in the interface between subunits, as predicted from studies on nAChRs (Corringer et al., 2000; Karlin, 2002; Sine, 2002). On the principal side, Trp-143 and Tyr-192 are involved in binding to both ligands, while Tyr-185 makes contacts only with carbamylcholine, but not with nicotine (Celie et al., 2004). On the complementary side, both ligands make hydrophobic contacts with Leu-112 and Met-114, while Try-53 only makes aromatic contact to nicotine and Arg-104 is only involved in binding to carbamylcholine. In comparison with the HEPES bound form of Ls-AChBP, only the C-loop displays significant backbone movement upon binding of either carbamylcholine or nicotine (Celie et al., 2004).

The AChBP of *Aplysia californica* (Ac-AChBP) only shares about 33% sequence identity with Ls-AChBP, but important functional residues that were identified in Ls-AChBP are well conserved (Celie et al., 2005b; Hansen et al., 2005). Relative to Ls-AChBP, Ac-AChBP has distinct ligand binding affinities and specificities. Ac-AChBP displays lower affinity for acetylcholine but higher affinity for the small α-conotoxin peptides including two α7-specific antagonists, natural ImI (Hansen et al., 2004) and the PnIA Ala10Leu variant (Celie et al., 2005b; Hansen et al., 2005). The crystal structures of Ac-AChBP in the apo form and as complexes with nicotinic antagonists α-conotoxin ImI and the alkaloid MLA and agonistsEPI and LOB reveals the existence of distinct conformations when Ac-AChBP is bound with agonists versus antagonists (Hansen et al., 2005). The apo form of Ac-AChBP displays very similar structure to the HEPES bound

form of Ls-AChBP. From the crystal structure of Ac-AChBP in complexes with EPI and LOB, it is evident that nicotinic agonists, including EPI and LOB, bind within discrete sites. Binding of those agonists induces C-loop closure, which might be critical for transition from agonist binding to channel activation in the nAChR (Hansen et al., 2005). In contrast, nicotinic antagonists make contacts to nonoverlapping regions of the subunit interface and antagonist binding induces an open C-loop conformation, which might be a universal feature of antagonist-receptor interaction in nAChR or possibly in other Cys-loop receptors.

The crystal structure AChBP from *Bulinus truncatus* (Bt-AChBP), a remote homolog of Ls-AChBP, reveals both conservation and variation in the ligand binding domain of Cys-loop receptor family (Celie et al., 2005a). Bt-AChBP shares 41% amino acid sequence identity with Ls-AChBP, 29% Ac-AChBP and 13-25 % with other Cys-loop receptor subunits. Similar to both Ls- and Ac-AChBPs, Bt-AChBP is well conserved in the ligand binding site. However, the residues involved in subunit interaction are much less conserved, which is also observed between other Cys-loop receptors (Brejc et al., 2001). The overall structure of Bt-AChBP is similar to that of Ls-AChBP. The variation between Bt-AChBP and Ls-AChBP is mostly within each subunit itself and relative orientation of subunits remains similar to each other. The most pronounced difference between these two AChBPs is the conformation of a number of loops located on the "bottom" side of the AChBP, including loop-2, loop-7 and the C-terminus, which correspond to membrane proximal domains in Cys-loop receptor family. The conformational difference between these two types of AChBPs is probably due to the rigid body shifts, suggesting conformational flexibility in these regions that is in agreement with sequence variations in

these regions in the entire Cys-loop receptor family. Comparison of subunit interfaces reveals that residues involved in subunit interactions share little conservation, although the surface area, hydrophobicity and accessibility of the interface between subunits are similar (Celie et al., 2005a).

1.3.3 Structural modeling of ligand gated ion channels based on crystal structure of AChBP

The discovery of AChBPs and subsequent X-ray structures of various species of AChBPs in complex with different ligands have greatly advanced our understanding of the ligand binding domain of pentameric Cys-loop receptors. Although sequence identity between AChBPs is only about 30-40%, all three types of AChBPs whose structures are known share similar structures and molecular details of ligand binding. When compared to the EM-derived structure of *Topedo* nAChR (Unwin, 2005) and all biochemical studies on ligand-receptor interaction (Smit et al., 2003; Lester et al., 2004), AChBPs mimic the ligand binding domain of nAChR very well. In addition, the ECDs of Cys-loop receptors are structurally and functionally conserved. Given the similarity of AChBPs with nAChR, AChBPs may be good structural templates for comparative homology modeling of the ligand binding domains of pentameric Cys-loop receptors. Comparative modeling predicts three-dimensional structure of a given protein based primarily on its homology to one or more proteins with known structure (Martyn et al., 1992). Based on the high resolution structure of AChBPs from different species in complexes with distinct ligands, a number of homology models have been proposed for the LBDs of nAChRs (Le Novere et al., 2002; Costa et al., 2003; Gao et al., 2004; Cheng et al., 2006a; Cheng et al., 2006b), GlyR

(Speranskiy et al., 2007), GABA$_A$-R (Cromer et al., 2002; Trudell, 2002; Ernst et al., 2005; Campagna-Slater and Weaver, 2007), GABA$_C$ receptors (Harrison and Lummis, 2006) and 5-HT$_3$ receptors (Maksay et al., 2003; Reeves et al., 2003; Maksay et al., 2004; Yan and White, 2005).

Homology modeling of α7 nAChR, the most closely related nAChR subunit to AChBP in primary sequence, was conducted using the crystal structure of Ls-AChBP as a template (Le Novere et al., 2002). Homology modeling, also known as "comparative modeling", is a classical method for building an atomic-resolution model of a target protein by aligning its amino acid sequence with proteins with known atomic structures (Marti-Renom et al., 2000). In this model, the overall size, surface area and ligand binding pocket were very similar to those of Ls-AChBP. The binding site is conserved except for a few residues that are considered to be selective for distinct ligands. Using (α7)$_5$ as a template, homology models of rat (α4)$_2$ (β2) $_3$ and (α1)$_2$β1γδ were constructed based on high sequence identity between distinct nAChR subunits. These models suggested that the ligand binding pocket is well conserved. The neuronal type of nAChR, (α3)$_2$(β4)$_3$, either in ligand-free or ligand-bound forms, were also modeled based on its sequence similarity to Ls-AChBP (Costa et al., 2003). In this model, the ligand binding site is believed to reside in the external side of the protein, which includes a number of aromatic residues on the α and β subunits, conferring agonist specificity of this type of nAChR. Agonist docking in this model showed that the agonists, ACh and nicotine, bind in a similar fashion to those observed in other types of nAChRs (Le Novere et al., 2002). Key residues on the β subunit important for pharmacological selectivity were also identified and a binding site for the allosteric modulator eserine was also proposed (Costa et al., 2003).

In collaboration with the Kurnikova lab and based on sequence alignment with both Ls- and Ac-AChBPs, a simulated annealing technique was used to build a structural model of the ECD of α1 GlyR (Speranskiy et al., 2007). In our model of the GlyR ECD, the entire β-sandwich core displays little variation relative to the structure of AChBP. However, variations exist in loops connecting neighboring β-strands, which is not unexpected since these regions are much less conserved in primary sequence. These residues are expected to confer differential ligand binding specificity and selectivity in different receptor classes in this superfamily. Docking simulations of strychnine, a potent antagonist of GlyR, showed it was restricted to the vicinity of the subunit interface. Its orientation and position clearly showed that strychnine is able to interact directly with the residues that were experimentally proved to be involved in antagonist binding (Speranskiy et al., 2007). As desribed in subsequent chapters, we have also modeled GlyBP for validation by experimental characterizations.

$(\alpha1)_2(\beta3)_2\gamma2$ GABA$_A$R was modeled based on its sequence homology with Ls-AChBP to distinguish possible assembly patterns of these five different subunits in this receptor type (Cromer et al., 2002). Of the six possible arrangements containing two α1, two β3 and one γ2 subunits, four were ruled out by biochemical and electrophysiological studies and, when viewed clockwise from an extracellular viewpoint, only γ2β3α1β3α1 or γ2α1β3α1β3 arrangements were possible (Tretter et al., 1997; Taylor et al., 2000; Klausberger et al., 2001). Models of GABA$_A$Rs corresponding to these two arrangements were constructed (Trudell, 2002), which are in mirror symmetry relative to each other. The γ2α1β3α1β3 model fits really well with these criteria that were previously set for correct subunit arrangement of heteropentameric GABA$_A$Rs (Stephenson et al., 1990; Amin et al.,

1997; Smith and Olsen, 2000), whereas the γ2β3α1β3α1 subunit arrangement clearly does not satisfy these criteria (Trudell, 2002).

Although most of the molecular models described above provide reasonable correlations with experimental observations, the accuracy of the models are limited. The main limitation arises due to low sequence identity between the ECD of Cys-loop receptors and the AChBP templates. The errors in these comparative models might be high since most of the ECDs of Cys-loop receptors share less than 30 % sequence identity with any AChBP, the template protein used in these models (Johnson and Overington, 1993; Marti-Renom et al., 2000). This results in a large number of gaps and potential errors in sequence alignments (Marti-Renom et al., 2000). Clearly, additional biochemical data are necessary to validate these models.

2.0   THESIS GOALS

Membrane proteins play an essential role in many cellular functions, such as ion conduction and transport, molecular recognition and response, energy transduction, cellular adhesion and catalysis. It is estimated that about 20 - 30 % of a cell's proteins are membrane proteins (Liang et al., 1998) and more than half of all drug targets are membrane proteins (Russell and Eggleston, 2000). Our understanding of this important protein family is circumscribed by a lack of high-resolution structural information of these very hydrophobic proteins. Although significant progress in determining the high-resolution structure of various membrane proteins has been made during the last decade, the knowledge of membrane protein structure still lags far behind that of soluble proteins. The difference may be due to the low natural expression level, high hydrophobicity and requirement for membrane mimetic environment for native-like folding of membrane proteins.

Ligand gated ion channels are a group of integral membrane proteins that open in response to binding of specific agonists, usually occurring extracellularly, and channel opening allows passage of either cations or anions across the plasma membrane. Structure and function studies of ion channels are very challenging since most experimental data are obtained from functional analyses. Although high resolution structures of a handful of ion

channels have been resolved by X-ray crystallography, structure-function relationship in ligand gated ion channels remains poorly understood.

In this study, we apply an alternative strategy and conduct direct structural studies on a truncated form of the GlyR, thus avoiding many of the difficulties associated with structural studies of full-lengh receptors. To achieve this, we overexpressed a mutant form of the extracellular domain of the GlyR and characterized it using a variety of biochemical and biophysical approaches. The long term goal of this research project is to determine the high-resolution structure of the extracellular ligand binding domain of GlyRs and to understand the structural dynamics of the ligand-receptor interactions for this receptor.

3.0 OVEREXPRESSION, PURIFICATION AND FUNCTIONAL CHARACTERIZATION OF A MUTANT FORM OF EXTRACELLULAR DOMAIN OF GLYCINE RECEPTORS

3.1 SUMMARY

Glycine binding protein (GlyBP), a mutant form of the GlyBP, a mutant form of extracellular domain of GlyR, was overexpressed in *Spodoptera frugiperda* (Sf9) insect cells. After fractionation, GlyBP was found in both cytosolic and membrane-bound fractions. The cytosolic fraction was misfolded as demonstrated by its failure to bind to 2-aminostrychnine affinity resin. The membrane-bound fraction was solubilized by 1.0 % digitonin/0.1 % deoxylcholate in the presence of 0.25 mg/ml egg phosphatidylcholine (PC). The detergent-solubilzed form of GlyBP was functional as indicated by its ability to bind 2-aminostrychine resin. The bound GlyBP on 2-aminostrychnine resin was eluted with 1.5 mM 2-aminostrychnine. After removal of detergent and salts by dialysis, GlyBP was isolated in both aqueous solution (aqueous form) and with pelleted lipid vesicles (vesicular form). Both forms of GlyBP were functional as indicated by their abilities to rebind to aminostrychnine resin and by subsequent biochemical studies. Radio-labeled binding assays showed that both forms of GlyBP retain high affinity to strychnine at nanomolar

36

level. Competitive binding assays showed that glycine, the endogenous agonist, competitively binds to both forms of GlyBP with K_i values consistent with reported values.

3.2   INTRODUCTION

GlyR, a member of the pentameric Cys-loop receptor family, is one the two major inhibitory neurotransmitter receptors in the central and peripheral nervous system. While the functional role of GlyR in inhibitory neurotransmission has been well documented, many details regarding its proper functioning remain elusive due to the lack of a high resolution structure of GlyR. However, our understanding of Cys-loop receptors has been greatly advanced by discovery of AChBPs (Brejc et al., 2001). AChBPs are secreted soluble proteins that act in the regulation of cholinergic synaptic transmission in the central nervous system (Smit et al., 2001), and are structural homologs of the extracellular domain of the Cys-loop receptors (Brejc et al., 2001; Smit et al., 2001; Sixma and Smit, 2003). The crystal structures of AChBPs in several species have been determined (Brejc et al., 2001; Celie et al., 2004; Celie et al., 2005b; Celie et al., 2005a; Hansen et al., 2006). Prior to the determination of these structures, much of our knowledge regarding the structure of the ECD of Cys-loop receptors was inferred from extensive mutagenic and crosslinking studies that had shown that agonist and competitive antagonist binding sites are located at subunit interfaces (Corringer et al., 2000; Karlin, 2002; Celie et al., 2004; Lynch, 2004). The crystal structures of AChBPs in complex with various agonists or competitive antagonists are consistent with the body of knowledge regarding the biochemistry of the intersubunit

37

ligand binding sites (Celie et al., 2004; Celie et al., 2005b; Celie et al., 2005a; Hansen et al., 2005; Ulens et al., 2006). While these crystal structures provide appropriate templates for modeling of the ligand binding domains of the Cys-loop receptor family and have greatly advanced our understanding of these domains (Brejc et al., 2001; Smit et al., 2001; Brejc et al., 2002; Maksay et al., 2003; Sixma and Smit, 2003; Smit et al., 2003; Grutter et al., 2005), the allosteric changes effected upon ligand-binding are less well-characterized and would also be expected to be critically dependent of the fine structure at the subunit interfaces, which are less well-conserved between the full-length receptors and AChBP. Expression of a soluble native-like ECD of any member of the Cys-loop superfamily has the potential to further elucidate the functional mechanism of these receptors.

Previous attempts in our lab to overexpress the ECD of the $\alpha 1$ subunit of GlyR, either as a truncated protein or fusion protein in a variety of expression systems, failed to produce soluble native-like oligomers capable of binding strychnine (unpublished observations). Given that AChBP is a secreted pentamer, we hypothesized that the ECD of GlyR might be more likely to be expressed in a native-like soluble form if two of the relatively hydrophobic membrane-proximal loops in the ECD of the full-length receptor (loops 7 and 9) were exchanged with their relatively hydrophilic counterparts in AChBP (Figure 3.1). Specifically, we substituted the two putative hydrophobic loops (Sequences N-F-P-M$_{144\text{-}147}$ and L-T-L-P-Q$_{182\text{-}186}$) in the $\alpha 1$ subunit of human GlyR with the corresponding hydrophilic loops (Sequences D-T-E-S$_{129\text{-}132}$ and S-Q-Y-S-R$_{166\text{-}170}$) in the homologous AChBP by site-directed mutagenesis. The expressed protein was designated as GlyBP.

When a recombinant membrane protein is studied, the first task is to choose an appropriate expression system. *E.coli* is used widely for heterologous protein expression due to its low cost, high expression level, multiple choices of expression vectors and the ease of scale-up. However, it is typically problematic when mammalian membrane proteins are expressed in *E.coli*. Membrane proteins expressed in *E.coli* lack post-translational modification, which is usually essential for proper functioning of mammalian membrane proteins. Recombinant membrane proteins in *E.coli* are often accumulated as misfolded proteins within inclusion bodies, which requires subsequent refolding of proteins.

In this study, we took advantage of a baculovirus expression system. Recombinant baculoviruses are widely used for heterologous expression of membrane proteins in cultured insect cells and insect larvae. For large scale expression of mammalian membrane proteins, a baculovirus expression system has many advantages over other expression vector systems: 1) Baculoviruses have a restricted host range, usually limited to some specific invertebrate species, and they are nonpathogenic to mammals and plants; 2) Production of recombinant proteins is often at high levels and is easy to scale up since insect cells are suitable for suspension culture, allowing large scale production of heterologously expressed proteins of interest; 3) Recombinant proteins produced in a baculovirus expression system can be post-translationally modified as in mammalian cell lines, which is critical for many eukaryotic proteins, especially membrane proteins.

A, Partial sequence alignment of *Lymnaea stagnalis* AChBP (GenBank accession #: AAK64377), human α7 nAChR (GenBan k accession #: NP_000737) and human α1 GlyR (GenBank accession #: P23415). Shown are Loop 7 (the Cys-loop; upper) and Loop 9 (lower) (the Cys-loop) and Loop 9 with flanking sequence. Numbering refers to residue numbers for α1 GlyR. Substituted amino acids are highlighted in gray; B, Schematic diagram showing backbone of GlyBP model with putative membrane-proximal loops facing the viewer. Substituted amino acids are highlighted in red.

Figure 3.1 Construction of GlyBP.

3.3 MATERIAL AND METHODS

3.3.1 Construction and generation of donor plasmid pFastBacGlyBP for baculovirus expression

3.3.1.1 Site directed mutagenesis

To generate a baculoviral construct encoding GlyBP, the plasmid pFastBacNGlyR encoding human α1 GlyR, residues 1-214, previously constructed in the lab, was used for site-directed mutagenesis. Two pairs of complementary primers (Table 3.1), were synthesized, which contain mutated fragments (NFPM$_{144-147}$ $\rightarrow$ DTES$_{144-147}$ and LTLPQ$_{182-186}$ $\rightarrow$ SQYSR$_{182-186}$) used in this study. The first PCR reaction was conducted with the first pair of primers (primer 1 forward and primer 1 reverse) using *Pfu Turbo* DNA polymerase and buffers included in the QuikChange Site-Directed Mutagenesis kit (STRATAGENE, La Jolla, CA). The PCR reaction mixtures with a final volume of 50 μl containing the template DNA pFastBacNGlyR, *Pfu Turbo* DNA polymerase, primers, dNTP mix and reaction buffer were incubated at 95°C for 30 sec, followed by 18 cycles with 95°C, 30 sec, 55°C 1 min, 68°C 6 min and a final incubation on ice for 2 min to cool the reaction to < 37°C. An aliquot of each PCR product was analysed by gel electrophoresis of 10 μl of the product on a 1% agarose gel. 1 μl of *Dpn* I reaction enzyme was added directly to each amplification reaction and incubated at 37°C for 1 hr to digest the parental supercoiled double strand DNA.

Table 3.1 Primers used for GlyBP construction.

All mutagenic oligonucleotides used here were purchased from MWG-Biotch.

Primer	Sequence	Mutation
Loop7 primer forward	GACACTGGCCTGCCCCATGGACTTGAAGGATACC GAGTCGGATGTCCAGACATGTATCATGCAACTGG	$NFPM_{144-147}$ ↓ $DTES_{144-147}$
Loop7 primer reverse	CCAGTTGCATGATACATGTCTGGACATCCGACTC GGTATCCTTCAAGTCCATGGGGCAGGCCAGTGTC	
Loop9 primer forward	GGAACAGGGAGCCGTGCAGGTAGCAGATGGATCACAG TACTCCCGGTTTATCTTGAAGGAAGAGAAGGACTTGAG	$LTLPQ_{182-186}$ ↓ $SQYSR_{182-186}$
Loop9 primer reverse	GGAACAGGGAGCCGTGCAGGTAGCAGATGGATCACAG TACTCCCGGTTTATCTTGAAGGAAGAGAAGGACTTGAG	

3.3.1.2 Transformation pFastBacGlyBP into XL-Blue supercompetent cells

The XL-Blue supercompetent cells were gently thawed on ice and 50 μl of cells were aliquoted to a prechilled Falcon 2059 polypropylene tubes. 1 μl of the *Dpn* I treated DNA from each PCR reaction was transferred to separate aliquots of the supercompetent cells and the mixtures were incubated on ice for 30 min, followed by a 45 sec heat pulse at 42 °C. After incubation on ice for 2 min, 0.5 ml of NZY^+ broth preheated to 42 °C was added

and the reactions were incubated at 37 °C for 1 hr with shaking at 250 rpm. Each reaction was plated on agar plates containing 50 mg/L ampicillin and incubated overnight at 37 °C.

3.3.1.3 Mini-preparation of pFastBacGlyBP DNA

DNA isolation was conducted using a Quantum Prep Plasmid Miniprep Kit (Bio-Rad Laboratories, Hercules, CA). A 3 ml culture of TB medium containing 100 μg/ml ampicillin was inoculated from single colony transformants and grown overnight at 37 °C. Cells were then pelleted at 12,900 rpm for 2 min. 200 μl of cell suspension solution was added to each tube after removal of supernatant. 200 μl of neutralization solution (1.32 M potassium acetate, pH 4.8) was added and mixed by inverting the tubes 4 times. The lysate was centrifuged at 12,900 rpm for 5 min. 1 ml of resuspended resin was added to each minicolumn/syringe assembly. Cleared lysates were transferred to the resin in each assembly and liquid was passed through by vaccuation. 2 ml of column wash solution (80 mM postassium acetate, 8.3 mM Tris-HCl, pH = 7.5, 40 μM EDTA and 50 % ethanol) was added, vaccuated and dried. After removal of the syringe barrel, minicolumns were transferred to a 1.5 ml microcentrifuge tube and centrifuged at 12,900 rpm for 2 min. Minicolumns were transferred to a new tube and 50 μl of nuclease-free water was added to each tube. The final DNA solution was collected by centrifugation at 11,000 rpm for 1 min at room temperature and stored at -20 °C. An aliquot of miniprep product of each sample was analyzed by gel electrophoresis on a 1% agarose gel and another aliquot was used for DNA sequencing to confirm correct mutation introduced by PCR amplification reactions.

3.3.2   Generation of baculovirus encoding GlyBP

3.3.2.1 Transposition of pFastBacGlyBP

DH10BAC competent cells were thawed on ice and 100 μl of cells were dispensed into 15-ml round-bottom polypropylene tubes. About 1 ng of pFastBacGlyBP plasmid (Figure 3.2) was added into the competent cells and mixed gently by tapping the side of tubes. The mixtures were incubated on ice for 30 min followed by a 45 sec heat pulse at 42 °C. After incubation on ice for 2 min, 900 μl of S.O.C medium (2% Bacto tryptone, 0.5% Bacto yeast extract, 10 mM NaCL, 2.5 mM KCl, 10 mM $MgCl_2$, 10 mM $MgSO_4$, 20 mM glucose, filter sterilized) was added. Then the mixture was placed in a shaking incubator at 37 °C for 4 hr with shaking at 225 rpm. Using S.O.C medium the cells were serially diluted to 10^{-1}, 10^{-2}, and 10^{-3}, and 100 μl of each dilution was placed and spread on the Luria agar plates containing 50 μg/ml kanamycin, 7 μg/ml gentamicin, 10 μg/ml tetracycline, 100 μg/ml Bluo-gal and 40 μg/ml IPTG. The plates were incubated for more than 24 hr until colonies were visible.
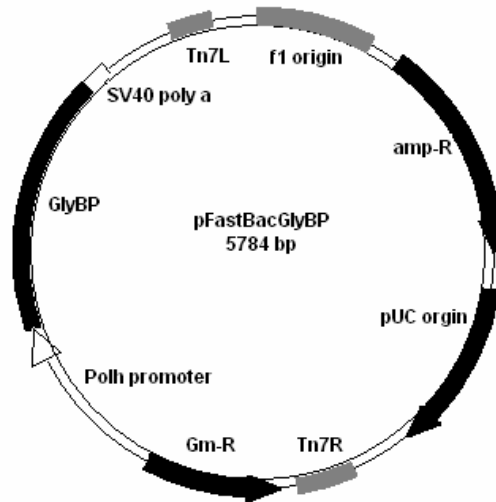
Figure 3.2 Vector map of pFastBacGlyBP donor plasmid.

3.3.2.2 Isolation of recombinant bacmid DNA encoding GlyBP

Single white colonies were inoculated into 2 ml LB medium supplemented with 50 μg/ml kanamycin, 7 μg/ml gentamicin, 10 μg/ml tetracycline and grown at 37 °C overnight to stationary phase with shaking at 250 rpm. 1.5 ml of culture was transferred to a 1.5-ml microcentrifuge tube and centrifuged at 14,000 g for 1 min. After removal of supernatant by vacuum aspiration, each pellet was resuspended in 0.3 ml of resuspension solution containg 15 mM Tris-HCl (pH 8.0), 10 mM EDTA, 100 μg/ml RNase A, mixed by gently vortexing and incubated at room temperature for 5 min. 0.3 ml of 3 M potassium acetate (pH 5.5) was slowly added, and mixed gently. A thick white precipitate formed and the sample was placed on ice for an additional 5 min. The samples were then centrifuged for 10

min at 14,000 g and the supernatant was transferred to a new tube containing 0.8 ml of absolute isopropanol. The samples were mixed by inverting the tube a few times and place on ice for 10 min. After centrifugation at 14,000 g for 15 min at room temperature, the supernatant was removed and 0.5 ml 70% ethanol was added to each tube. The tubes were inverted a few times to wash the pellet and centrifuged at 14,000 g for 5 min at room temperature. The supernatant was then removed and the pellet was air dried at room temperature. The final DNA was dissolved in 40 μl of TE buffer and stored at -20 °C. A small aliquot of each sample was analyzed by gel electrophoresis on a 1 % agarose gel.

3.3.2.3 Transfection of Sf9 insect cells with recombinant bacmid DNA encoding GlyBP

9×10^5 cells per 35-mm well of a 6-well plate were seeded in 2 ml of Sf-900 II SFM containing 50 units/ml penicillin and 50 μg/ml streptomycin. The cells used were from a 3- to 4-day-old suspension culture in mid-log phase with a viability of >97% and cells were allowed to attach at 27°C for at least 1 h. Two solutions were prepared in 12×75-mm sterile tubes: Solution A, 5 μl of mini-prep bacmid DNA was diluted into 100 μl Sf-900 II SFM without antibiotics; Solution B, 6 μl CellFECTIN® Reagent was diluted into 100 μl Sf-900 II SFM without antibiotics. For each transfection, these two solutions were combined, mixed gently, and incubated for 15 to 45 min at room temperature. The cells were washed once with 2 ml of Sf-900 II SFM without antibiotics. For each transfection, 0.8 ml of Sf-900 II SFM was added to each tube containing the lipid-DNA complexes. The samples were mixed gently and wash media was aspirated from cells. The diluted lipid-DNA complexes were overlaid onto the cells and incubated for 5 h in a 27°C incubator. Then the transfection mixtures were removed and 2 ml of Sf-900 II SFM containing

antibiotics was added and incubated in a 27°C incubator. At 72 h the baculovirus was harvested from cell culture medium and stored at 4°C or at -20°C for long term storage with addition of 2% fetal bovine serum (FBS).

3.3.2.4 Titration and amplification of recombinant baculovirus encoding GlyBP

The viral titer of baculovirus encoding GlyBP was determined by a FastPlax titer kit (Novagen, Madison, WI). 2 ml of Grace's Insect Medium supplemented with 10% fetal bovine serum (FBS) was seeded in a 6-well plate with a total of 1×10^6 cells. The three pairs of wells in the 6-well plate were labeled "-5", "-6", "-7" respectively. The cells were allowed to attach plate for 30 min at 27 °C. The viral stock was serially diluted to 10^{-5}, 10^{-6}, 10^{-7} respectively. The 2 ml medium was aspirated from each well and 100 μl of each virus dilution was added to each of the duplicate wells, drop by drop in the center starting with "-7" and then "-6", "-5". The cells were incubated at room temperature for 1 hr and then 2 ml of Grace's medium was added carefully to each well and incubated at 27 °C for 30 hr. The 2 ml of Grace's medium was aspirated and the cells were washed twice with 2 ml of PBS buffer containing 43 mM Na_2PO_4, 15 mM KH_2PO_4, 137 mM NaCl and 27 mM KCl, pH 7.4. The cells were fixed with 3.7 % formaldehyde and incubated for 15 min. After formaldehyde solution was removed, the cells were washed twice with PBS, blocked by 2 ml of 10 % gelatin in TBST (10 mM Tris-HCl, pH 8.0, 150 mM NaCl, 0.1% Tween 20) and incubated for 30 min with gentle rocking. The gelatin solution was removed and the cells were washed twice with 2 ml of PBS. 1 ml of FastPlax antibody diluted 1:10,000 in TBST was added to each well and the cells were incubated for 1 hr with gentle rocking. 1 ml of goat anti-mouse β-gal conjugate diluted 1:100 in TBST and incubated for 1 hr with gentle agitation. The cells were washed three times with 2 ml of Grace's medium for 10

min. The developing solution containing 60 μl of X-gal (50 mg/ml in 100% dimethylformamide) and 60 μl of NBT (83 mg/ml in 70% dimethylformamide) per 15 ml of PBS plus 5 mM $MgCl_2$ was added to each well and the cells were incubated at 37 °C until infected cells appeared medium blue to dark purple. The cells were then washed twice with 2 ml of TBST to stop color development and the infected cells were counted under a dissecting microscope. The titer of virus was calculated by the following formula: pfu/ml = 10 (# of infected cells/foci) (dilution factor). The final titer was obtained by the average of the 6 wells.

For amplification of viral stocks, a monolayer culture was infected at a Multiplicity of Infection (MOI) of 0.01 to 0.1 (calculated by the following formula: Inoculum required (ml) = [desired MOI (pfu/ml) × (total number of cells)]/[titer of viral inoculum (pfu/ml)]). The virus was harvested at 48 h post-infection resulting in approximately 100-fold amplification of the virus.

3.3.2.5 Infection of Sf9 insect cells with recombinant baculovirus encoding GlyBP and baculovirus tittering

Sf9 insect cells were infected at an MOI > 5 and harvested at the following time intervals: 24, 48, 72, 96 and 120 hr. For regular protein production, 750 ml of Sf9 insect cells were infected with 30 ml of viral stock solution and harvested at day 4 post-infection.

3.3.3   Insect cell culture

Sf9 insect cells were maintained and grown at 27 °C in Grace's Insect Medium (Invitrogen) supplemented with 10% fetal bovine serum (FBS) and 100 U/ml penicillin/100 μg/ml

streptomycin as either monolayer culture in T-75 flasks or suspension cultures in spinner flasks under constant rotation (120 rpm). Doubling time of Sf9 insect cells was about 36 hr. Cell density and viability were checked daily. Cell viability above 95 % was required for baculovirus infection. For monolayer cultures, Sf9 cells were passaged at confluency and typically diluted at 1:5 dilution in order to maintain log phase growth. Suspension cultures were initiated from healthy monolayer adherent cell cultures. The cells in spinner flasks were usually passaged before they reached a density of 2.0 to 2.5 x 10^6 cells/ml and diluted back to 0.7 to 1.0 x 10^6 cells/ml. Suspension cultures were grown in spinner flasks with a size range from 100 ml to 1.5 L depending on the experimental needs.

3.3.4   Expression and purification of GlyBP in insect cells

Sf9 cells were grown in Grace's Insect Medium supplemented with 10% fetal bovine serum (FBS) and 100 U/ml penicillin/100 μg/ml streptomycin at 28 °C as suspension cultures in spinner flasks under constant rotation (120 rpm). To express GlyBP in Sf9 cells, cells were infected with virus encoding GlyBP at MOI > 5. Cells were harvested 4 days post-infection.

Sf9 cells were gently pelleted by centrifugation at 1000 x g for 10 min, and washed three times with ice-cold PBS. Resuspended cell were incubated on ice for 1 hr in hypotonic solution containing 5 mM Tris (pH 8.0), 5 mM EDTA, 5 mM EGTA, 10 mM dithiothreitol, and an anti-proteolytic cocktail (APC) containing 1.6 μu/ml aprotinin, 100 μM phenylmethylsulfonyl fluoride, 1 mM benzamidine and 100μM benzethonium chloride, and then sonicated eight times for 15 sec on ice at 50% duty cycle. The disrupted cells were centrifuged at 100,000 g for 1 hr and the soluble fraction was saved as the cystolic fraction.

The insoluble fraction was solubilized by resuspending the pellet and incubating at 4 °C overnight in solubilization buffer containing 25 mM potassium phosphate buffer (KPi) (pH 7.4), 1% digitonin, 0.1% deoxycholate, 0.5 mg/ml egg PC, 500 mM KCl, 5 mM EDTA, 5 mM EGTA, 10 mM dithiothreitol, and APC. The samples were then centrifuged at 100,000 x g as before. The supernatant and the solubilized pellet were independently applied to 2-aminostrychnine agarose at 4 °C overnight with gentle agitation. The agarose was collected by gentle centrifugation, washed three times (in the case of the solubilized pellet, the wash buffer was the same as solubilization buffer except with reduced (0.1 %) digitonin), and then eluted for 2 days with elution buffer containing either 200 mM glycine or 1.5 mM 2-aminostrychnine in the solubilization buffer. In the latter case, the eluate was dialyzed against 25 mM KPi (pH 7.4) and then centrifuged at 100,000 x g. The pellet (vesicular form) was resuspended in 25 mM KPi buffer with a final protein-lipid ratio of ~1: 200 (mol: mol) and the supernatant (aqueous form) was concentrated in an Amicon Ultra-4 centrifugal filter device with a 10 KDa cutoff.

3.3.5 Protein assay - Modified Lowry assay

Protein concentrations were determined by modified Lowry assays (Peterson, 1977). Protein samples or bovine serum albumin (BSA) standards were diluted to 1.0 ml with dH_2O and proteins were precipitated by adding 0.15 ml 1.0% deoxycholate (DOC) and vortexing, and incubating for 10 min at room temperature. 0.1 ml 72% tricholoracetic acid was then added, mixed by vortexing and span at 11,000 rpm for 10 min. The supernatant was discarded and the pellet was resuspended in 0.5 ml dH_2O. 0.5 ml alkaline Cu^{2+} solution was added to each sample. The samples were mixed by vortexing and allowed to stand for

at least 15 min at room temperature. 0.05 ml phenol reagent was added rapidly and immediately mixed vigorously. The color developed for 30 min and Absorbance at 750 nm was recorded. All samples were run in duplicate. To determine protein sample concentration, the standard curve was plotted using various concentrations of BSA standard. The concentration of protein samples was determined by fitting the experimentally obtained Absorbance of protein samples to the BSA standard curve.

3.3.6 SDS-PAGE and Western blot

All protein samples were treated with SDS-PAGE sample buffer containing 2% SDS. Proteins were separated on 10% SDS-PAGE gels at a constant voltage of 200 V and transferred to a nitrocellulose membrane at 350 mA constant current for 1 hr at 4 °C. The membrane was blocked with 5% nonfat milk, washed twice and incubated with the primary antibody with a dilution of 1:5,000 (monoclonal anti-mouse antibodies against N-terminus of GlyR, Alexis Biochemicals, San Diego, CA) for 1 hr at room temperature in phosphate buffered saline with added 0.5% Tween-20 (PBST) containing 1% BSA. The membrane was again washed with PBST buffer for 15 min three times and incubated with the horseradish peroxidase (HRP)-conjugated anti-mouse secondary antibody with a dilution of 1:15,000. The membrane was again washed with PBST buffer for 15 min three times and incubated with pre-mixed NEN Chemiluminescence luminal and oxidizing reagents for 1 min at room temperature, followed by exposure to Kodak X-OMAT Blue Autoradiography Film for 5 sec to 2 min depending on signal intensity.

3.3.7 Radio-labeled ligand binding assay

For saturation binding assay, purified GlyBP, in either the aqueous form of membrane-associated form, were incubated with [^{3}H] strychnine at various concentrations on ice for 30 min in the presence and absence of excess cold strychnine. After precipitation by 15% PEG400 or PEG6000, the proteins were applied to GF/A filters and washed thoroughly with binding buffer. Radioactivity was determined by liquid scintillation spectrometry. K_d and B_{max} values were derived using the software GraphPad Prism 3.0.

For competitive binding assay, purified GlyBP was incubated with various concentrations of glycine in the presence of 100 nM of [^{3}H] strychnine overnight. After precipitation by 15% PEG6000, the proteins were applied to GF/A filters and washed thoroughly with binding buffer. Radioactivity was determined by liquid scintillation spectrometry. The IC_{50} values were determined using the software GraphPad Prism 3.0. The K_i (the concentration of the unlabeled drug that will bind to half the binding sites at equilibrium in the absence of radioligand) was calculated using the following equation (Cheng and Prusoff, 1973):

$$K_i = IC_{50}/(1 + [\text{radioligand}]/K_d)$$

3.3.8 Deglycosylation

For deglycosylation using Endo H (New England BioLabs, Ipswich, MA), purified GlyBP was denatured in denaturing buffer containing 5 % SDS and 10 % β-mercaptoethanol with

a final volume of 20 μl at 100 °C for 10 min. 2 μl of 0.5 M sodium citrate (pH 5.5) and 2 μl of 500,000 U/ml Endo H and incubated at 37 °C for 1 hr. As a control, the same amount of denatured protein sample was incubated with sodium citrate buffer only at 37 °C for 1 hr. Protein samples were separated by SDS-PAGE followed by Western blot assay.

For deglycosylation using PNGase F (glycerol free, New England BioLabs, Ipswich, MA), purified GlyBP was denatured in denaturing buffer containing 5 % SDS and 0.4 M DTT with a final volume of 20 μl at 100 °C for 10 min. 2 μl of 0.5 M sodium phosphate (pH 7.5), 2 μl of 10% NP-40 and 2 μl of 500,000 U/ml PNGase F were added to each reaction and incubated at 37 °C for 1 hr. As a control, the same amount of denatured protein sample was incubated with sodium phosphate buffer only at 37 °C for 1 hr. Protein samples were separated by SDS-PAGE followed by Western blot.

3.4   RESULTS

3.4.1   Expression of GlyBP in Sf9 insect cells

To express GlyBP in a baculoviral expression system, two pairs of specific primers were designed to generate a baculovirus encoding GlyBP by amplification of a previous construct that encoded the extracellular domain of human α1 GlyR (amino acids 1-214) with a hydrophilic randomized 30 amino acid tail appended at its C-terminus (Figure 3.3), which might increase the solubility of this mutant receptor ECD. The general strategy is summarized in Figure 3.4. After two sequential PCR amplifications, a transfer vector

containing the GlyBP construct was isolated. Transposon-mediated insertion of the GlyBP-encoding sequence into bacmid DNA (Figure 3.5) and isolation of baculovirus and viral amplification and titration were conducted as described in Material and Methods. GlyBP expression was first detected at day 1 post-infection, and expression increased over time and appeared to reach its highest level at day 4 (Fig 3.6A). After cells were harvested by centrifugation and washed, they were lysed by sonication and fractionated into cytosolic and membrane-associated fractions by ultracentrifugation. The aqueous fraction contained cytosolic proteins and the insoluble fraction contained mostly precipitated and membrane-associated proteins. GlyBP was detected in both fractions in Western immunoblots (Figure 3.6B). However, attempts to purify GlyBP from the cytosolic fraction were not successful as the protein did not bind to a 2-aminostrychnine affinity resin (Figure 3.7A), an initial step in the methodology routinely used to purify full-length GlyR (Cascio et al., 1993; Cascio et al., 2001). This indicates that GlyBP in the cytosolic fraction is not folded in a native-like conformation. In a similar study of heterologous expression of α7 nAChR ECD in *Xenopus* oocytes, secrected α7 ECD displayed a strong ability to bind ^{125}I-α-Bungarotoxin, while the intracellularly retained fraction lost its ability to bind ^{125}I-α-Bungarotoxin (Wells et al., 1998), also suggesting that the cytosolic fraction of overexpressed membrane receptors might exist in an unfolded state. In contrast, as described below in detail, GlyBP in the membrane-associated fraction after lysis and solubilization did bind to the 2-aminostrychnine resin (Fig 3.7B), suggesting that the membrane-associated GlyBP may adopt a native-like structure. The presence of a large fraction of the GlyBP in the membraneous fraction suggests that, despite replacing loops 7 and 9 of the GlyR ECD with the more hydrophilic sequences from AChBP and the

inclusion of a fairly hydrophilic long N-terminal tail, the receptor still partitions on the membrane surface (GlyBP lacks any hydrophobic transmembrane segments), consistent with a previous study on a refolded form of the extracellular domain of GlyR (Breitinger et al., 2004). The strychnine-binding capability of only the membrane-associated fraction also suggests that this partitioning may be required for proper assembly of the ECD, possibly due to the need for a high local concentration of properly oriented monomers for functional assembly. All further experiments in this study have been conducted on the fraction of overexpressed GlyBP that remains membrane-associated upon lysis of the insect cells.

A R S A P K P M S P S D F L D K L M G R T S G Y D A R I R P N F

K G P P V N V S C N I F I N S F G S I A E T T M D Y R V N I F L R

Q Q W N D P R L A Y N E Y P D D S L D L D P S M L D S I W K P

D L F F A N E K G A H F H E I T T DN K L L R I S R N G N V L Y

S I R I T L T L A C P M D L K **D T E S** D V Q T C I M Q L E S F G Y

T M N D L I F E W Q E Q G A V Q V A D G **S Q Y S R** F I L K E E K

D L R Y C T K H Y N T G K F T C I E A R F*P T S T S S L V A A A F*

E S R A C S L E A C G T K L V E K Y

Figure 3.3 Amino acid sequence of GlyBP.

Substituted residues in loops 7 and 9 are underlined in bold and the C-terminal hydrophilic randomized tail is highlighted in italics.
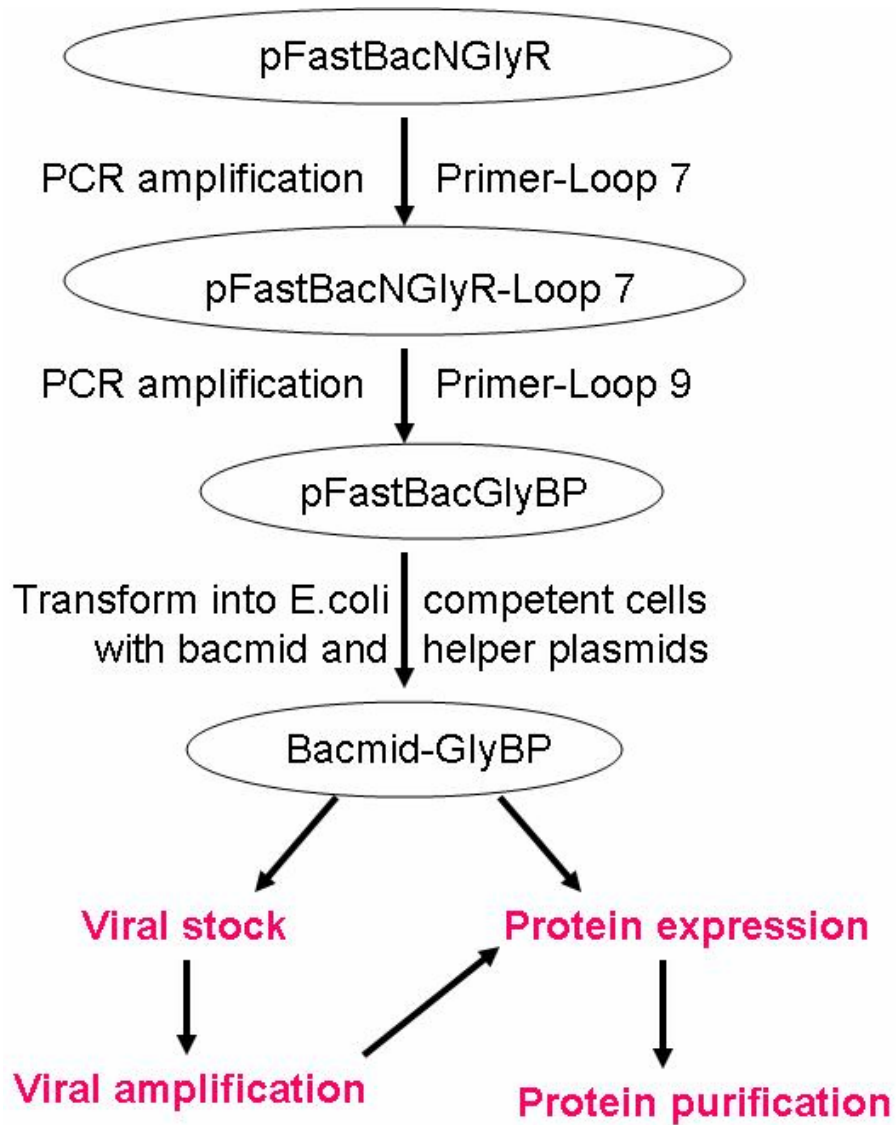
Figure 3.4 Strategy of generation of GlyBP.
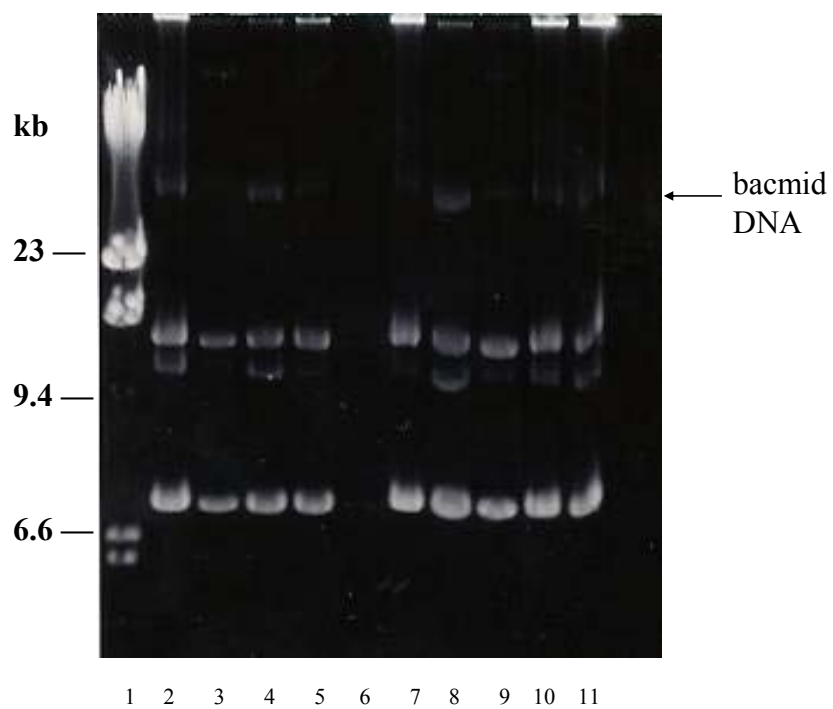
Figure 3.5 Generation of GlyBP bacmid.

Lane 1: λ-DNA/Hind III fragments; Lane 2-11: mini-preps of bacmid DNA from different white colonies.
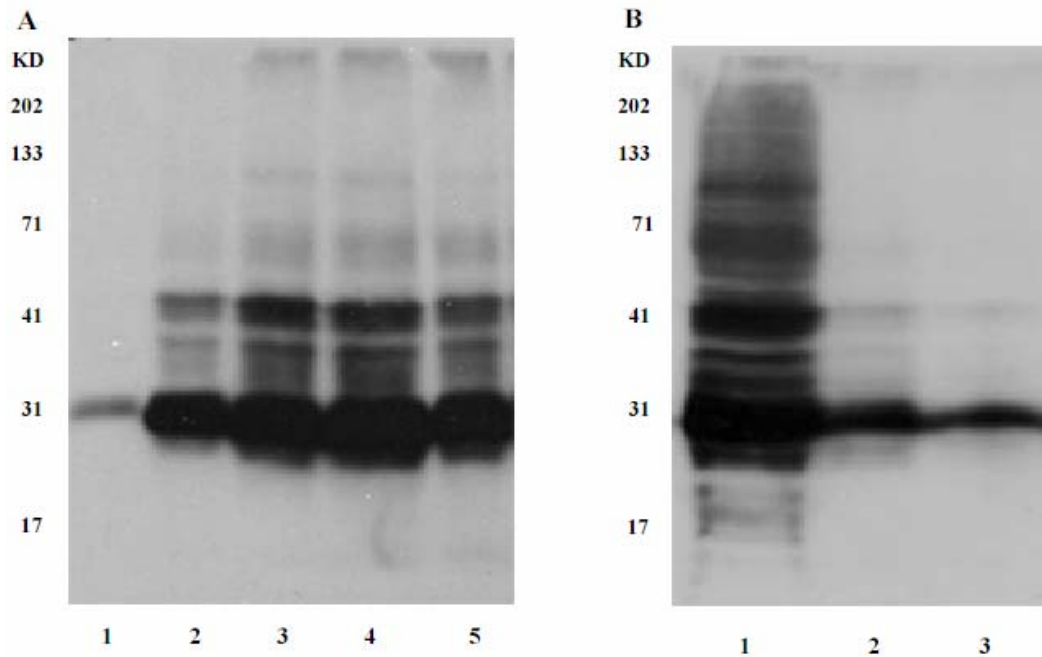
Figure 3.6 Overexpression of GlyBP in Sf9 insect cells as detected by Western immunoblot.

A, Time course of expression. Lanes 1 – 5, GlyBP expression at days 1, 2, 3, 4 and 5 post-infection, respectively; B, Subcellular fractionation of GlyBP. Lane 1, total extract, Lane 2, cytosolic fraction, Lane 3, membrane-associated pellet.
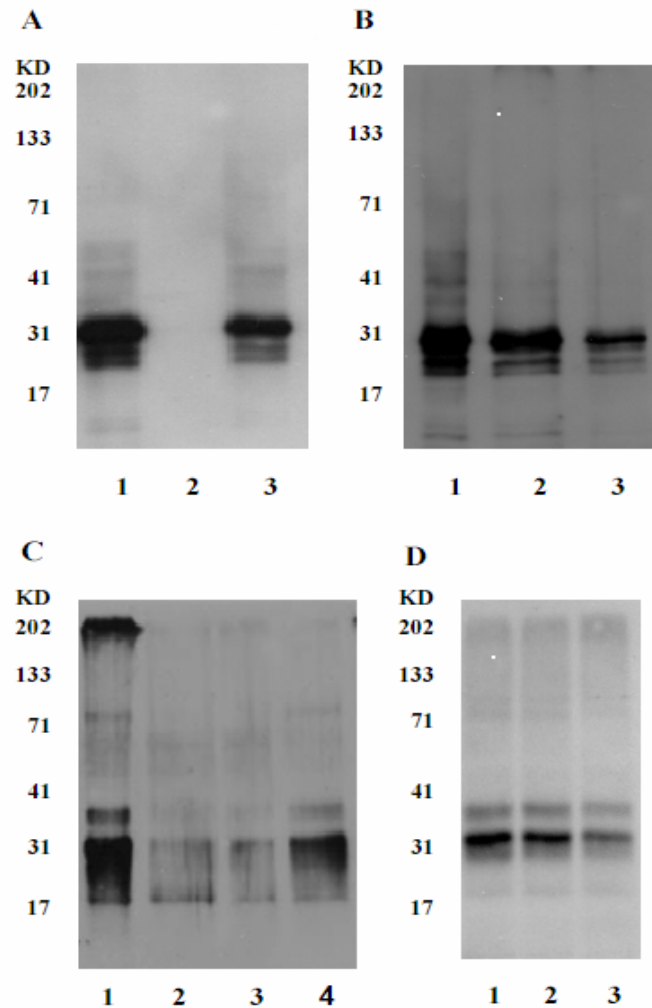
Figure 3.7 Western immunoblots of binding of GlyBP to 2-aminostrychnine affinity matrix.

A, Cytosolic fraction. Lane1: total cytosolic protein, Lane 2: protein bound to 2-AS, Lane 3: unbound protein; B, Membrane fraction. Lane 1: total membrane fraction, Lane 2: protein bound to 2-AS, Lane 3: unbound protein; C, Elution of membrane-associated GlyBP from 2-AS resin. Lane 1: GlyBP bound to 2-AS after elution with 200 mM glycine, Lane 2: protein eluate after incubation with 200 mM glycine, Lane 3: GlyBP bound to 2-AS after elution with 1.5 mM 2-AS Lane 4: protein eluate after incubation with 1.5 mM 2-AS; D, Partitioning of purified membrane-bound GlyBP after detergent dialysis (Lane 1)

and ultracentrifugation (Lanes 2 and 3). Lane 2: soluble form of GlyBP, Lane 3: vesicular form of GlyBP.

3.4.2 Purification of GlyBP

In order to purify GlyBP we first solubilized the membrane-associated fraction after lysis of the insect cells by incubation with a solubilization buffer containing 25 mM KPi (pH 7.4), 0.5 M KCl, 1% digitonin, 0.1 % deoxylcholate, 0.2 mg/ml lipid mixture, 5 mM EDTA, 5 mM EGTA, 10 mM dithiothreitol and a mixture of antiproteolytics at 4 °C overnight. This ratio of the detergents digitonin and deoxylcholate is identical to that used to solubilize full-length GlyR in previous studies (Cascio et al., 1993; Cascio et al., 2001). After ultracentrifugation, the supernatant containing GlyBP/detergent/lipid micelles was incubated with the 2-aminostrychnine affinity resin overnight. In our hands, full-length GlyR is routinely eluted from this resin by competition with 200 mM glycine. However, unlike the full-length receptor, only ~10% of the solubilized GlyBP that was bound to the aminostrychnine resin was eluted from the resin after equilibration with 200 mM glycine. Instead, an elution buffer in which 1.5 mM 2-aminostrychnine was substituted for glycine resulted in elution of > 90% of GlyBP bound to the affinity resin (Figure 3.7C).

Purified GlyBP/detergent/lipid micelles were then dialyzed against 25 mM potassium phosphate buffer (pH 7.4) to remove detergent and the relatively high concentration of salts used during purification, yielding protein and spontaneously-formed vesicles in the phosphate buffered solution. After brief probe sonication to make the vesicles small and unilamellar, the vesicles and any associated GlyBP were pelleted by ultracentrifugation. Western immunoblots of the rehydrated pellet and the supernatant were

conducted to determine the partitioning of purified GlyBP between aqueous solution and the vesicles (Figure 3.7D). Under the conditions used in this study, GlyBP was found at approximately equal levels in both the supernatant, as a soluble protein (aqueous form), and with pelleted lipid vesicles (vesicular form) (Figure 3.7D). GlyBP in both fractions retained their capability of binding aminostrychnine as assayed in rebinding studies. The aqueous form of GlyBP is thus considered to be a purified, water-soluble form of GlyBP capable of binding antagonist. The vesicular form of GlyBP is similarly a purified, vesicle-associated form of the protein that is also capable of binding antagonist. Isolation of GlyBP as a soluble protein (without potentially-interfering associated lipids and/or detergents) is especially significant as this protein may be useful in subsequent high-resolution structural studies. In our hands, partitioning of GlyBP between association with vesicles or remaining free in solution is somewhat variable, and appears to depend on salt concentration, lipid composition, and other variables. While this partitioning has not been further explored in this study, future investigations of this partitioning may provide insight into the energetics involved in interactions between the extracellular domain of GlyR and the surface of the lipid bilayer, as well as any preferential selectivity towards specific lipid headgroups. Both forms of GlyBP were used for subsequent studies in order to distinguish which (or if both) of these may be an appropriate model for the corresponding structure of the ECD in the full-length GlyR.

Both forms of GlyBP appear to run as a doublet on SDS-PAGE gels with apparent molecular weight of of 29 and 31 KDa (Figure 3.7). In addition, despite being reduced and denatured, higher order bands are observed at elevated apparent molecular weight. A similar phenomenon was also observed in full-length $\alpha 1$ GlyR that also ran as a doublet on

SDS-PAGE (Cascio et al., 1993; Griffon et al., 1999). The migration of GlyBP as a doublet on SDS-PAGE might be due to: 1) heterogeneity in the unfolding of GlyBP and/or differential binding of SDS such that two predominant species with altered shape and/or charge distribution of the monomeric protein are present giving rise to anomalous migration; or 2) differential post-translational modifications of GlyBP in insect cells; or 3) partial proteolysis of the protein *in vivo* or during sample preparation. As described in 3.3.4, treatment of both forms of GlyBP with either Endo H or PNGase F did not result in any significant molecular mass shift observed on SDS-PAGE gel (Figure 3.8), indicating that the doublet is probably not due to the presence of differential glycosylation states that causes some of the protein to migrate at a higher apparent molecular weight on SDS-PAGE. While we cannot rule out partial proteolysis or clipping, subsequent characterization of GlyBP, as well as binding assays, suggests that this event, if it occurs, does not result in misfolding of GlyBP because it continues to bind agonist and antagonist. In addition, mass fingerprinting of both bands of the analogous doublet in SDS-PAGE of full-length GlyR gave coverage over the entire primary sequence of GlyR, suggesting that the doublet, in this case, is not due to any proteolytic degradation at either the amino- or carboxy-termini of the full-length receptor (Tillman and Cascio, unpublished observation). Given these observations, we propose that the observed GlyBP doublet is most likely due to anomalous migration of GlyBP.

3.4.3   Deglycosylation of GlyBP

Glycosylation is a common post-translational modification of many membrane proteins and may play a significant role in oligomerization of membrane proteins. Both α and β subunits

of native functional GlyR are glycosylated (Pfeiffer and Betz, 1981; Pfeiffer et al., 1982). The GlyR α1 subunit has a N-glycosylation consensus site at N38, which was shown to be critical for oligomerization of homomeric α1 GlyR (Griffon et al., 1999). To determine if differential glycosylation may be responsible for the doublet observed in SDS-PAGE, enzymatic deglycosylation studies were conducted on both forms of GlyBP. Both forms of GlyBP were incubated without or with endoglycosidase H (Endo H) for 1 hr at room temperature and samples were analyzed by SDS-PAGE followed western blot as described in Material and Methods. Treatment with Endo H did not result in any significant shift in molecular weight on SDS-PAGE (Figure 3.8A). Since Endo H removes only high mannose and some hybrid types of N-linked carbohydrates, we also incuated GlyBP with N-glycosidase F (PNGase F), which has a broader substrate specificity for N-linked carbohydrates. Similarly, no molecular weight shift was observed for both forms of GlyBP after PNGase digestion (Figure 3.8B). Thus, the presence of a doublet observed in SDS-PAGE is not due to differential glycosylation.
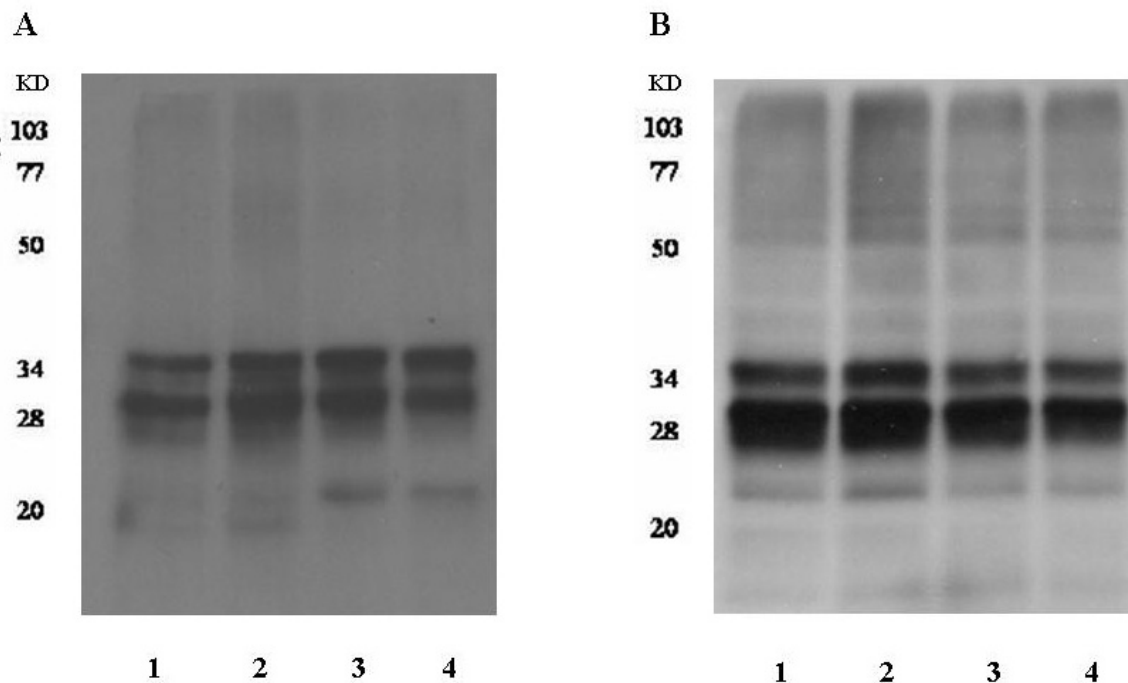
Figure 3.8 Deglycosylation of GlyBP.

A, Aqueous (lane 1 and 2) and vesicular (lane 3 and 4) GlyBP digested with Endo H (lane 2 and 4 respectively); B, Aqueous (lane 1 and 2) and vesicular (lane 3 and 4) GlyBP digested with PNGase F (lane 2 and 4 respectively).

3.4.4 Ligand binding properties of GlyBP

The affinity of a receptor to its cognate ligands (agonists/antagonists) is a defining property of that receptor and may be used as a diagnostic yardstick to assess the functionality of heterologously expressed proteins and/or the integrity of purified products. With respect to the Cys-loop receptors, the K_d is also dependent on the composition of the subunits that comprise the pentameric assembly. Given that the affinities of full-length homomeric α1

GlyR for its agonist glycine or competitive antagonist strychnine have been experimentally determined to be between 10-30 nM (strychnine, K_d) and 20-60 μM (glycine, K_i) (Graham et al., 1985; Marvizon et al., 1986; Sanes et al., 1987; Rundstrom et al., 1994; Breitinger et al., 2001; Grudzinska et al., 2005), we can assess whether the structure of GlyBP approximates that of its corresponding domain in the full-length receptor by conducting radiolabeled ligand binding assays on both forms of GlyBP and comparing their ligand-binding properties to that reported for the full-length receptor. Both aqueous and vesicular forms of GlyBP were incubated with [³H] strychnine at various concentrations for 30 min at 4°C in the presence and absence of excess cold strychnine. The vesicular form of GlyBP has a K_d of 119 ± 28 nM for strychnine while the strychnine K_d of the aqueous form of GlyBP is 230 ± 88 nM (Figure 3.9A), which are broadly consistent with the reported values (Graham et al., 1985; Sanes et al., 1987). There is no statistically significant difference in strychnine binding between these two forms of GlyBP. This experiment indicates that both forms of GlyBP retain high affinity to this potent antagonist.

Given the relatively low affinity and high dissociation rate of glycine to the receptor, as well as the unavailability of glycine radiolabeled with high activity, glycine binding assays were conducted using a displacement binding assay using [³H] strychnine as a primary ligand. Both aqueous and vesicular forms of GlyBP were incubated overnight with various concentrations of glycine competitor in the presence of 100 nM of [³H] strychnine. The displacement experiment indicated a glycine IC_{50} of 166.2 ± 29.5 μM for vesicular form and 132.1 ± 28.4 μM for aqueous form (Figure 3.9B), and calculated glycine K_i values are 90.3 ± 16.0 μM and 71.8 ± 15.4 μM, respectively, which is in agreement with reported K_i of glycine for full length α1 GlyR (Lynch et al., 1997; Breitinger et al., 2001).

These binding studies also suggest that the GlyBP subunits are forming multimers, as the binding pocket for glycine and strychnine are located at the interface between adjacent subunits.

In order to assess whether all purified protein retained the ability to bind to the GlyR ligands, we calculated B_{max} from different protein preparations. B_{max} was originally to determine the receptor density on membranes in ligand binding assays. In our case, we could determine the percentage of GlyBP that bound to strychnine. The B_{max} may be converted to a mole ratio of strychnine bound per molecule of GlyBP. From these studies, it was demonstrated that the ratios were 0.88 ± 0.14 and 0.81 ± 0.16 for vesicular and aqueous forms of GlyBP respectively (Table 3.2), strongly suggesting that most, if not all, purified protein did bind to the strychnine.

As described above, glycine was less efficient to elute GlyBP than to elute full-length GlyR bound to 2-aminostrychnine resin. However, our ligand binding experiments showed that glycine retains ability to displace pre-bound [3H] strychnine after removal of detergent and lipids. To further evaluate the ability of GlyBP to bind to its endogenous ligands, saturation and competitive binding assays were conducted in the presence of detergent, lipids and high concentration of salts. Strychnine binding affinity was largely unchanged ($K_d = 154 \pm 37$ nM for strychnine) compared to that obtained after dialysis (Figure 3.9E). Interestingly, the K_i value (calculated K_i values are 1.45 ± 0.34 mM) of glycine to displace [3H] strychnine was significantly reduced as compared to that after dialysis (Figure 3.9F), suggesting that the lack of ability of glycine to compete with strychnine during elution was due to reduction of glycine binding affinity in the presence of detergent and lipids. The possible explanation is either that high concentration of detergent,

lipids and salts somehow hinders direct contact between glycine and the receptor or that the receptor ECD structure is slightly distorted during elution. In addition, reduction of competition ability of ligands in the presence of detergent in competitive binding assays was also observed in overexpressed α7 nAChR ECD in *Xenopus* oocytes (Wells et al., 1998), which also supports our observation that the presence of detergent might have negative effects on the ability of agonist to displace bound high-affinity antagonist either by direct modification on GlyBP or its indirect effet on solvent environment.

Table 3.2 Calculated Bmax's and ratio of strychning-bound protein versus total protein in ligand binding assays

	B_{max} (nmole/mg of protein)	# of protein bound/# of total protein
GlyBP ves	31.7 ± 4.7	0.88 ± 0.14
GlyBP aqu	29.2 ± 4.6	0.81 ± 0.16
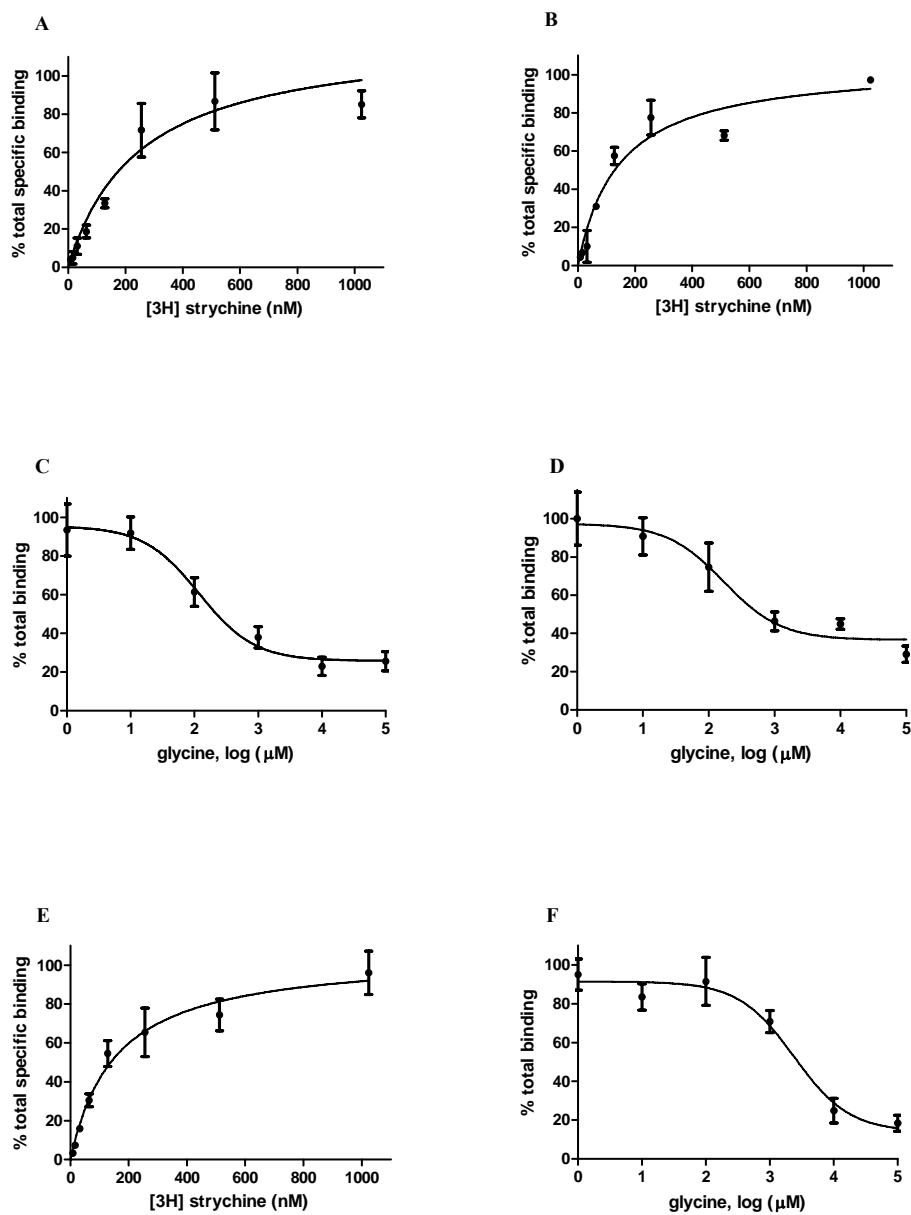
Figure 3.9 GlyBP binding assays.

[³H]Strychnine binding curves for soluble (A) and vesicular form (B) of GlyBP. Binding curves for glycine competition with [³H] strychnine-bound soluble (C) and vesicular form (D) of GlyBP. [³H]Strychnine saturation binding (E) and competitive binding (F) assays of GlyBP in the presence of detergent and lipids.

3.5   DISCUSSION

In the initial experiments, we expected to express a mutant form of the extracellular domain of GlyR and anticipated that it could function as a homopentamer. Taking advantage of baculovirus expression system, GlyBP was functionally overexpressed in Sf9 insect cells with a yield of ~ 1.0-2.0 mg of purified protein /L culture. This is a significant amount of protein for heterologously expressed ion channel proteins and might be suitable for consequent high-resolution structural studies. Heterologous expression of the ECD of a membrane protein has long been considered as an alternative strategy when direct structural studies on the integral membrane protein are not possible or practical. For Cys-loop receptors, the ligand binding domain is usually located extracellularly, and it may be expected that an overexpressed receptor ECD might be expressed as a functional secreted soluble form. However, while GlyBP was found in both cytosolic and membrane fractions after subcellular fractionation, only the membrane fraction could be affinity-purified, suggesting membrane-association property of GlyBP is required for its proper functioning. The biosynthesis of membrane proteins is a complicated and highly regulated process. GlyR is synthesized and assembled in the endoplasmic reticulum (ER) and transported to the plasma membrane. A model has been proposed for postsynaptic clustering of GlyR (Kneussel and Betz, 2000). It has been shown that molecular determinants of GlyR assembly are located in the ECD of GlyR (Griffon et al., 1999). Thus, when expressed heterologously, GlyBP is expected to be synthesized in the ER, transported to the plasma membrane and secreted to the extracellular space since the transmembrane segments are missing in GlyBP. However, after subcellular fractionation, GlyBP was present in both cytosolic and membrane fractions, but not in the culture media, indicating retention of

69

GlyBP. The presence of cytosolic pool of GlyBP might result from 1) its dramatic overexpression in a heterologous expression system; or 2) loss of ability to assemble as an functional oligomer, which is required for membrane clustering of GlyR in vivo ; or 3) alteration in its transport to plasma membrane. The failure of GlyBP in the cytosolic fraction to bind to strychnine indicates it is misfolded and/or unassembled in the cytosol. While native full-length GlyRs are integrated into the plasma membrane by mutiple hydrophobic interactions, membrane association of GlyBP might be just due to non-specific hydrophobic interaction between the lipid bilayer and one or several hydrophobic loops in GlyBP, which is probably similar to the interaction observed in many peripheral membrane proteins.

Interestingly, after detergent/lipid solubilization, GlyBP partitioned into both supernatant (aqueous form) and pellet (vesicular form) after ultracentrifugation, indicating that GlyBP might be loosely associated the membrane although this interaction is important for correct folding in insect cells. Several lines of evidence suggest that both forms of GlyBP are correctly folded. First, GlyBP was able to specifically bind to 2-aminostrychnine resin, suggesting that GlyBP was in a correct folding state and capable of binding to native ligands of GlyR. Second, radio-labeled ligand binding assay directly demonstrated that both forms of GlyBP retain ability to bind to strychnine with high affinity at nanomolar dissociation constants. Competitive binding assays further showed that glycine could competitively displace bound ^{3}H-strychnine with a K_i at micromolar levels. However, glycine seemed to be less efficient to eluate bound GlyBP on 2-aminostrychnine resin during purification. This suggested an affinity shift in the presence of detergent and lipids. Further ligand binding assay of GlyBP showed that, in the presence

of detergent, lipids and high concentration of salts, K_d for strychnine is comparable to that of soluble and vesicular forms of GlyBP, but the higher values of K_i for glycine suggests GlyBP may be slightly distorted in the presence of detergent and lipids although the presence of detergent and high salt concentration helped solubilization of GlyBP.

Based on crystal structures of GlyBPs and other mutagenesis studies, a number of connecting loops exist between neighboring β-strands, some of which are found to be involved in transition from ligand recognition to channel activation. Among these loops, loops 2, 7 (Cys-loop) and 9 (C loop) are predicted to be involved in interaction with the membrane or transmembrane domain of the receptor (Brejc et al., 2001; Unwin, 2005). In this study, replacement of hydrophobic residues in Loops 7 and 9 in the ECD of GlyR with corresponding hydrophilic ones in AChBP seemed not to affect its folding and ligand binding properties. These loops have been shown to be important for coupling agonist binding and channel activation, but are not directly involved in ligand binding sites because they reside at the "bottom" side of receptor extracellular domain.

Although two hydrophobic loops were replaced with more hydrophilic loops corresponding to those in AChBP, GlyBP still appears to partition on the surface of lipid vesicles, indicating that there may be multiple membrane association sites in the extracellular domain of GlyR in addition to loops 7 and 9. In addition, GlyBP in cytosolic fraction lost strychnine binding property while membrane associated fraction remained strychnine binding ability, which indicates that membrane association may be required for proper folding and assembly of GlyBP. Based on the crystal structure of AChBP and other studies, loop 2 is also a potential membrane-proximal segment. It might be interesting to

look at the effect of loop 2 replacement on membrane-association property of GlyR ECD, which would possibly result in increased ease of expression and solubility of GlyR ECD.

4.0 STRUCTURAL CHARACTERIZATION OF GLYBP

4.1 SUMMARY

In Chapter 3, GlyBP, a mutant ECD of GlyR, was expressed in a baculoviral expression system. GlyBP protein was observed in both cytosolic and membrane-associated fractions, but only the GlyBP in the membrane fraction could be purified by affinity chromatography. After the detergent was removed, purified GlyBP partitioned into both aqueous and vesicular phases after utltracentrifugation. Ligand binding assays showed that both forms of GlyBP retained the ability to bind ligands with affinities comparable to those of native GlyR.

In this chapter, GlyBP is biophysically and biochemically characterized. The secondary structure of GlyBP was examined by circular dichroism. Both forms of GlyBP have a globular structure with predominant β–sheet structure. Addition of either glycine or strychnine did not change their net secondary structure. In order to further characterize GlyBP, we sought to determine its oligomeric state. Chemical crosslinking experiments showed that both forms of GlyBP are oligomeric. Dynamic light scattering experiments demonstrated that the molecular size of GlyBP is consistent with it being a homopentamer.

Chemical crosslinking coupled to MALDI-TOF mass spectrometry was applied to study the protein folding and structure of the subunit interface of GlyBP. A number of K-K

73

crosslinks in GlyBP were observed after crosslinking with dimethyl suberimidate (DMS). The intramolecular crosslinks provided a number of distance constraints for GlyBP folding and validated the homology model of GlyBP. In addition, inter-subuit crosslinks gave important structural information about the subunit interface although addition of strychnine did not change the crosslinking profile of GlyBP to a significant extent.

4.2   INTRODUCTION

In Cys-loop receptors, oligomerization is essential for activity. Ligand binding sites are located at the subunit interface, and disruption of subunit-subunit interactions impairs both agonist and antagonist binding. More importantly, oligomerization of Cys-loop receptors is critical for channel activation since the ion conducting pore is formed by the M2 domains from each subunit of the receptor. A number of mutagenic and biochemical studies have shown that the Cys-loop receptors assemble as pentamers both *in vivo* and *in vitro* (Langosch et al., 1988; Karlin, 2002; Lester et al., 2004), which is further supported by the crystal structure of pentameric AChBP (Brejc et al., 2001; Hansen et al., 2004) and cryo-EM studies of nAChR (Unwin, 2003; Unwin, 2005).

Native GlyRs assemble as heteropentamers with possible stoichiometry of either 3α/2β (Langosch et al., 1988), or 2α/3β (Grudzinska et al., 2005). However, α subunits of GlyR can assemble as homopentamers when experessed heterologously (Lynch, 2004). For example, homomeric assembly of the GlyR α1 subunit resulted in a functional ion channel as demonstrated by electrophysiological studies (Gentet and Clements, 2002; Legendre et al., 2002). In addition, homomeric assembly of the GlyR α subunit results in the formation

of five identical ligand binding sites, which simplifies structural studies on ligand binding mechanisms of GlyR.

In the Cys-loop receptor family, all members share conserved pentameric assembly and similar ligand recognition mechanisms. However, the subunit interface is much less conserved, which is not unexpected since that variation in primary sequence confers selectivity to receptor assembly of any given type of receptor. Some structural information with regard to subunit interactions has been obtained for nAChR by a number of mutagenesis and crystallographic studies (Karlin, 2002; Unwin, 2005; Dellisanti et al., 2007). However, detailed analysis of the subunit interface of the nAChR and other members in this superfamily, including GlyR, is lacking.

Although X-ray crystallography and NMR are considered as the most powerful tools for understanding high resolution three-dimensional structure of proteins, there are some inherent limitations of these two techniques. Both techniques require a large mount of protein and are intrinsically time-consuming. NMR spectroscopy is applicable only to peptides and relatively small proteins of about 20-25 KD. Crystals of macromolecular complexes that refract to high resolution are very difficult to obtain, especially for membrane proteins. However, a number of alternative approaches are also available to address the questions of spatial and topological organizations of protein and protein complexes, such as chemical modification, circular dichroism and mass spectrometry.

In structural studies, chemical crosslinkers are widely used and considered as molecular rulers that can provide information on distances between crosslinked groups to define both tertiary and quaternary structures of proteins of interest (Sinz, 2006). Crosslinkers can be either homo- or hetero-bifunctional reagents. They have been used

extensively as they are soluble in aqueous solvents and can form stable inter- and intra-subunit covalent bonds. DMS, a homo-bifunctional reagent, belongs to the imidoester class of crosslinking reagents, which specifically react with primary amine groups (*i.e*., ε-amino groups of lysine residues), resulting in the formation of an amidine linkage that carries a positive charge at physiological pH (Kiehm and Ji, 1977; Wilbur, 1992). The N (amidine) to N (amidine) distance was used to determine the crosslinking span. This homo-bifunctional crosslinking reagent has been widely used to map low-resolution protein structures (Wang and Moore, 1977; Bauer et al., 1990; Dihazi and Sinz, 2003). To further understand the structure of GlyBP, chemical cross-linking studies coupled to mass spectrometric analysis was conducted, resulting in identification of a number of K-K crosslinks providing distance constraints on folding of this protein.

In collaboration with Dr. M. Kurnikova at Carnegie Mellon University, a homology model of the homopentameric GlyBP was built based on its sequence alignment with AChBP. The GlyBP homology model is similar to that of wild-type GlyR ECD (Speranskiy et al., 2007). The model provides a framework for interpretation of the crosslinking data. In addition, distance constraints obtained from chemical crosslinking coupled to mass spectrometry will also be used to validate and/or refine this model.

4.3   MATERIAL AND METHODS

4.3.1   Expression and purification of GlyBP

GlyBP was expressed and purified as described in Chapter 3.

4.3.2 Circular dichroism

CD spectra were recorded on an AVIV Model 202 spectrophotometer. CD spectra of aqueous and vesicular forms of GlyBP in 25 mM potassium phosphate buffer, pH 7.4, were all collected at a protein concentration of 0.16 - 0.2 mg/ml at 25 °C in the near-UV length region (190-280 nm). In parallel studies, concentrated stock solutions of glycine or strychnine (in 25 mM potassium phosphate buffer, pH 7.4) were diluted 100-fold by direct addition to the cuvette to give 25 mM glycine or 12 μM strychnine (much greater than the experimentally determined K_i or K_d, respectively). At least ten reproducible spectra were collected for each preparation, averaged, and smoothed (Savitzky and Golay, 1964). All reported spectra were baseline corrected by subtraction of similarly collected, averaged, and smoothed baselines of appropriate buffer, ligands and/or vesicles identically prepared, except without purified protein. Samples containing lipid vesicles were probe sonicated to minimize optical artifacts due to differential light scattering and protein to lipid ratios were minimized low to ensure negligible absorption flattening effects. The CD spectra of the protein in the near UV region were analyzed using DICHROWEB (Lobley et al., 2002; Whitmore and Wallace, 2004). Spectra were analyzed using CDSSTR (Sreerama and Woody, 2000), or CONTINLL (Provencher and Glockner, 1981) and a normalized root mean standard deviation (NRMSD) value was calculated as a measure of the fit of the calculated curve to the experimental data (Mao et al., 1982).

4.3.3 Chemical cross-linking

Purified aqueous and vesicular forms of GlyBP were incubated with various concentrations of DMS (0.2 →2 mg/ml) at room temperature for 1 hr. Protein samples were also incubated at RT without addition of DMS as controls. Reactions were quenched with addition of Tris buffer at a final concentration of 50 mM. Crosslinked products were separated by SDS-PAGE followed by Western blot.

4.3.4 Dynamic light scattering

Purified GlyBP, in 25 mM KPi (pH 7.4) and 1 mM DTT was diluted to a final monomer protein concentration of 0.4 mg/ml. Samples were filtered with a 0.22 um Millipore Millex-GV filter and analyzed in a Wyatt Protein Solutions DynaPro instrument. Dynamic light scattering data were collected in triplicate and analyzed with the Protein Solutions DynaPro software. The hydrodynamic radius (R_h) was calculated based on the following equation:

$$D = \frac{kT}{6\pi\eta_0 R_h}$$ (k: Boltzmann constant; T: temperature; η_0: solvent viscosity).

4.3.5 Silver staining and destaining

Crosslinked or non-crosslinked proteins were separated on SDS-PAGE. After electrophoresis, the gel was rinsed briefly with ultrapure water and fixed in 100 ml of fixative (40 % ethanol/10 % acetic acid) for 20 minutes with gentle rotation. The fixative

solution was decanted and washed in 30% ethanol for 10 minutes. 100 ml of Sensitizing solution was added to the washed gel in the staining container. Then the gel was incubated in the Sensitizing solution for 10 minutes and washed in 100 ml of 30% ethanol and then ultrapure water for 10 minutes respectively. The gel was incubated in 100 ml of staining solution for 15 minutes and washed with 100 ml of ultrapure water for 20-60 seconds. The gel was incubated in 100 ml of developing solution for 4-8 minutes until bands start to appear and the desired band intensity was reached. Once the appropriate staining intensity was achieved, 10 ml of Stopper directly was added to the gel still immersed in Developing solution and incubated with gentle agitation for 10 minutes. The Stopper solution was decanted and the gel was washed with 100 ml of ultrapure water for 10 minutes.

For destaining, after silver staining the gel, the gel was washed thoroughly with ultrapure water and bands of interest were carefully excised using a clean scalpel and the gel pieces were placed into a 1.5 ml sterile microcentrifuge tube. Another piece of gel of the same size from a blank region of the gel was also excised and placed into another sterile microcentrifuge tube. This will be used as a control for trypsin digestion. 50 µl of Destainer A and 50 µl of Destainer B were added to each microcentrifuge tube and incubated for 15 minutes at room temperature. The supernatant was removed using a clean pipette tip and 200 µl of ultrapure water was added to the tube and mix and incubated for 10 minutes at room temperature. This washing step was repeated twice and the gel pieces were subjected to in-gel trypsin digestion.

4.3.6 In-gel trypsin digestion

Before trypsin digestion, cysteine residues were reduced and alkylated with iodoacetamide. Briefly, the gel pieces were incubated with 100 % acetonitrile, and then 10 mM DTT, 100 mM TrisHCl, pH 8.5 at 55 °C for 1 h. After two washes with 100 mM TrisHCl, pH 8.5, the gel pieces were incubated with 15 mM iodoacetamide in 100 mM TrisHCl, pH 8.5 for 1 h in dark at room temperature.Then, the gel pieces were washed with 100 ul of wash buffer (50:50 methanol: 50 mM ammonium bicarbonate) twice for 30 min with gentle agitation. The gel plugs were dehydrated by adding 50 ul acetonitrile. After the gel plugs turned whitish, acetonitrile was removed and dried in a SpeedVac for about 15 min. 10 μl of Trypsin Buffer (20 μg/ml of porcine trypsin in 20 mM ammonium bicarbonate) was added to each sample and put on ice for 15 min and incubated overnight at 37 °C. The 10 ul Trypsin Buffer was transferred to a new tube. 60 ul of Extraction Buffer (1% TFA in 50:50 acetonitrile: H_2O) was added to the gel plugs and incubated for 30min with gentle agitation. Then the 60 uL of Extraction Buffer was transferred to same labeled sample tube and the gel plugs were incubated with 40ul of Extraction Buffer (1% TFA in 50:50 acetonitrile: H_2O) for 30 min with gentle agitation and then transferred as described above. Samples were dried in SpeedVac for about 1.5-2 hr.

4.3.7 Sample purification and spotting for MALDI-TOF MS

Prior to sample spotting, protein samples were purified and concentrated using C18 Ziptips. The Ziptip was prewet by 10 μl of 50 % acetonitrile in Milli-Q water, equilibrated with 10

µl of 0.1 % TFA in Milli-Q water. The sample was drawn up into Ziptip and pipetted up and down 5-6 times. The Ziptip was then washed twice with 10 µl of 0.1 % TFA to remove contaminants. The peptides were eluted with 3 µl of 50% acetonitrile/0.1% TFA in Milli-Q into a labeled clean vial. Those samples were used for direct spotting for MALDI-TOF analysis.

The sample preparation method used was the dried-droplet method (Karas and Hillenkamp, 1988). Briefly, in a clean microcentrifuge tube, 0.5 µl of each protein sample cleaned by C18 Ziptip was mixed with the same volume of 10 mg/ml of α–cyano-4-hydroxycinnaic acid (CHCA) (Applied Biosystems, Foster City, CA) in 50% acetonitrile/0.1% TFA by vortexing. The mixture of sample/matrix was deposited onto a welled gold sample plate. The droplets were air-dried at room temperature. A standard mixture including des-Arg^1-Bradykinin ($[M + H]^+_{mono}$ = 904.47), Angiotensin ($[M + H]^+_{mono}$ = 1296.69), Glu^1-Fibrinopeptide B ($[M + H]^+_{mono}$ = 1570.68), ACTH (1-17 clip) ($[M + H]^+_{mono}$ = 2093.09), ACTH (18-39 clip) ($[M + H]^+_{mono}$ = 2465.20) and ACTH (7-38 clip) ($[M + H]^+_{mono}$ = 3657.93) was used as external calibriants.

4.3.8   MALDI-TOF MS

Matrix-assisted laser desorption/ionization time-of-flight mass spectrometry (MALDI-TOF MS) was performed on a Voager DE Pro Biospectrometry Workstation equipped with a nitrogen laser (337 nm). The instrument was run in positive ionization mode and measurements were performed in reflector mode.

4.3.9   Data analysis of MALDI-TOF mass spectra of GlyBP after chemical crosslinking with DMS

MALDI-TOF mass spectra were analyzed by the Data Explorer ™ software version 4.5 (Applied Biosystems). Crosslinking products were identified using the General Protein Mass Analysis for Windows (GPMAW, version 6.0) (Lighthouse Data, Odense, Denmark) and the Automated Spectrum Assignment Program (ASAP) developed at the University of California at San Francisco (Young et al., 2000).

4.3.10   Homology modeling of GlyBP

In collaboration with Dr. Maria Kurnikova at Carnegie Mellon University, an approach similar to that used for wild-type GlyR ECD (Speranskiy et al., 2007) was used to generate a homology model of GlyBP. Briefly, the sequence of GlyBP was aligned with those of *L. stagnalis* AChBP and *A. californica* AChBP using Clustal W (Thompson et al., 1994). The program Modeller 7.7 was used to generate a model of the GlyBP pentamer (Sali and Blundell, 1993). All five subunits of the pentamer were modeled simultaneously with a five-fold symmetry. The Modeller's variable target function method (VTFM) and MD simulated annealing were used to generate 15 initially randomized models. The quality of these models was characterized in terms of Z-scores using the WHAT_IF program (Vriend, 1990). Z-scores are standardized statistically-derived structure quality assessment scales that include packing quality, Ramachandran plot appearance, chi-1/chi-2 rotamer normality, and backbone conformation. The inter-residue distances were calculated based

on the homology model of GlyBP using the program Visual Molecular Dynamics (VMD), version 1.8.6 (Humphrey et al., 1996). All molecular images were drawn in VMD.

4.4   RESULTS

4.4.1   Determination of secondary structure of GlyBP by circular dichroism

The net secondary structures of both forms of GlyBP were determined by circular dichroism (CD) spectroscopy. CD spectroscopy in the low-UV region (190-240 nm) is a particularly useful tool since the peptide transitions that give rise to the diagnostic net spectrum in this region are sensitive to small changes in backbone conformation. Given the achiral nature of the lipids comprising the vesicles, one may directly compare the net spectra of the aqueous and vesicle associated forms of GlyBP, providing the lipid-protein ratio is sufficiently high and that the vesicles are small and unilamellar in order to minimize absorption flattening effects and differential scattering, respectively (Mao and Wallace, 1984). Purified GlyBP in either its aqueous soluble form or associated with small unilamellar vesicles were examined in comparative CD studies. The resulting CD spectra of GlyBP in either form are nearly superimposable (Figure 4.1A), strongly suggesting their conformations are essentially equivalent.

Quantitation of the net secondary structure of both forms of GlyBP can determine if their secondary structure is consistent with that of the homologous AChBP (Brejc et al., 2001; Sixma and Smit, 2003) and validates our model. Historically, the ability of CD to accurately determine the secondary structure of proteins with reduced helical content, (as

expected for GlyBP given that AChBPs are ~ 8-10% α-helical (Brejc et al., 2001; Hansen et al., 2004; Celie et al., 2005a)), has been limited by the poor representation of some non-helical folds in the reference databases, the reduced signal of β-structures relative to that from helical components, and the structural variability of non-helical folds that gives rise to spectral diversity (Wallace et al., 2003). This has been redressed by the generation of a new reference database that more effectively covers secondary structure and fold space (Lees et al., 2006). Spectra were analyzed by two independent methods: CONTINLL (Provencher and Glockner, 1981) and CDSSTR (Sreerama and Woody, 2000). Both forms of GlyBP contained relatively little helical content and were largely composed of β–sheet, consistent with the observed crystal structure of AChBP (Table 4.1) and with the reduced helical content determined in CD studies of full-length GlyR reconstituted in vesicles (Cascio et al., 2001). It is also consistent with our model of GlyBP, using AChBP as a template. In all analyses the NRMSD value was ≤ 0.05, indicating that the reference data set is appropriate (a value below 0.10 indicates a reasonably good fit of the calculated and experimental spectra). Other reference databases gave significantly higher values for the NRMSD (typically above 0.2, data not shown).

In earlier CD studies of reconstituted full-length nicotinicoid receptors, addition of acetylcholine to nAChR (Mielke and Wallace, 1988) or the addition of glycine to GlyR (Cascio, unpublished observation) did not result in any significant changes in their CD spectra. However, in spectroscopic studies of the holoreceptor, small changes in GlyR ECD might be averaged over the net secondary structure of the entire receptor. In order to determine if changes in net secondary structure could be detected in the ECD alone, comparative CD studies were similarly conducted wherein 25 mM glycine or 12 µM

strychnine, concentrations well above each ligand's K_d or K_i (Figure 3.9), were added to both forms of GlyBP (Figure 4.1B & C). The addition of either ligand did not induce any significant changes in the CD spectra in the low UV range, indicating that the binding of agonist or antagonist does not appreciably alter the net secondary structure of GlyBP. Extensive experimental evidence has suggested the occurrence of conformational changes upon ligand binding in the ECD of Cys-loop receptors (Unwin, 2005; Sine and Engel, 2006). However, in the cryo-EM structure of *Torpedo* nAChR, addition of agonist led to rotations of inner β-sheets in the ECD without any significant changes in the composition of any secondary structural elements. Our observations on GlyBP are consistent with the cryo-EM structure of *Torpedo* nAChR. The absence of any detectable change in the net secondary structure change of GlyBP is consistent with known experimental data.
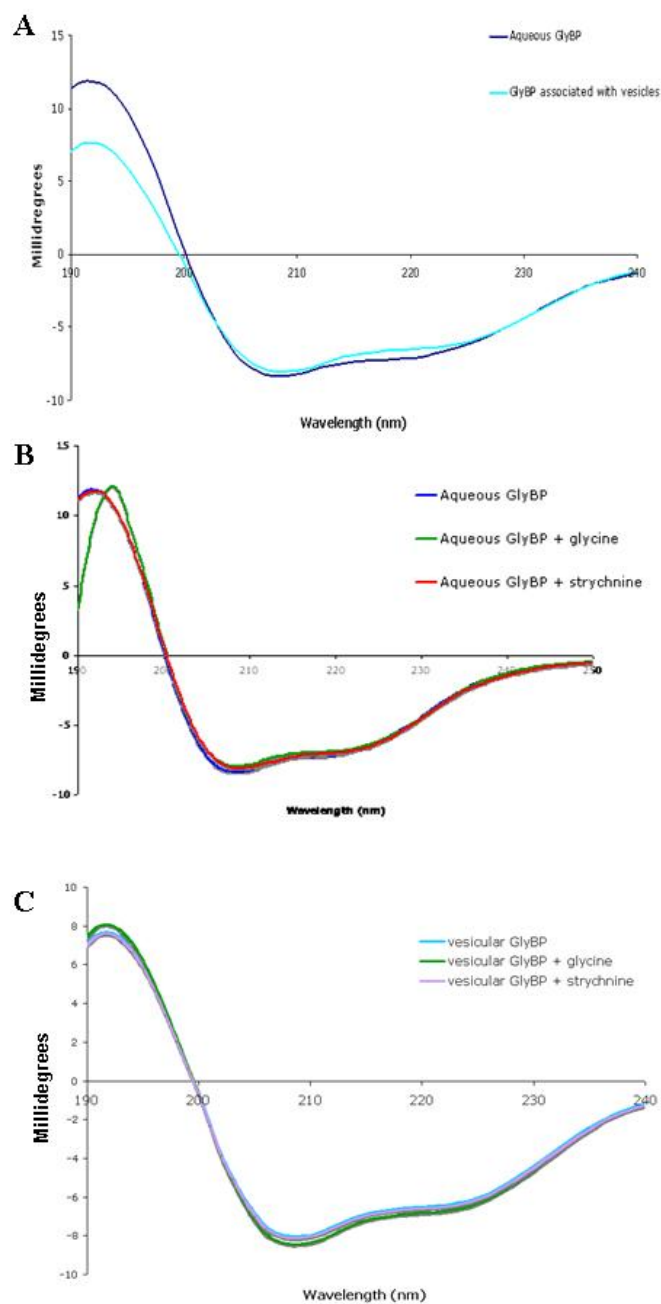
Figure 4.1 CD spectra of soluble and vesicular forms of GlyBP.

A, Comparison of CD spectra of aqueous and vesicular GlyBP; B, CD spectra of aqueous form of GlyBP in the absence and presence of glycine or strychnine; C, CD spectra of vesicular form of GlyBP in the absence and presence of glycine or strychnine.

Table 4.1 Calculated secondary structure from CD studies.

α_R and α_D are regular and distorted α-helix, respectively, as defined in Lees et al., 2006.

Reported values for β-sheet are the sum of both its regular and distorted fractions.

Sample	Method	α_R	α_D	β-sheet	β-turn	Other	NRMSD
GlyBP, aqueous form	CONTINLL	0.04	0.09	0.35	0.13	0.39	0.028
GlyBP, aqueous form	CDSSTR	0.02	0.07	0.37	0.13	0.40	0.039
GlyBP, vesicular form	CONTINLL	0.05	0.09	0.33	0.13	0.40	0.050
GlyBP, vesicular form	CDSSTR	0.03	0.04	0.41	0.10	0.40	0.044

4.4.2 Determination of oligomerization state of GlyBP

Functional GlyRs are pentameric and if GlyBP is to be considered an appropriate structural homolog of the ECD of GlyR, it, too, should be pentameric. Affinity chromatography on 2-aminostrychnine resin strongly suggests some degree of oligomerization of GlyBP since the binding sites for strychnine are situated at subunit interfaces. To further examine the oligomeric states of GlyBP, crosslinking studies were conducted with DMS, a homobifunctional agent that cross-links primary amines of lysines. Diluted preparations containing either form of purified GlyBP were incubated with increasing concentrations of DMS yielded higher order aggregates in SDS-PAGE gels as compared to control (Figure 4.2). The absence of any clear intermediate bands corresponding to dimers, trimers, and higher order oligomers upon incubation with cross-linking agents did not allow us to determine the stoichiometry of a predominant oligomeric state. Nonetheless, a common trend was observed in all experiments in that there was an obvious dose-dependent

formation of higher-order aggregates upon incubation of dilute GlyBP with increasing

levels of DMS, suggesting that both forms of GlyBP are oligomeric in nature.
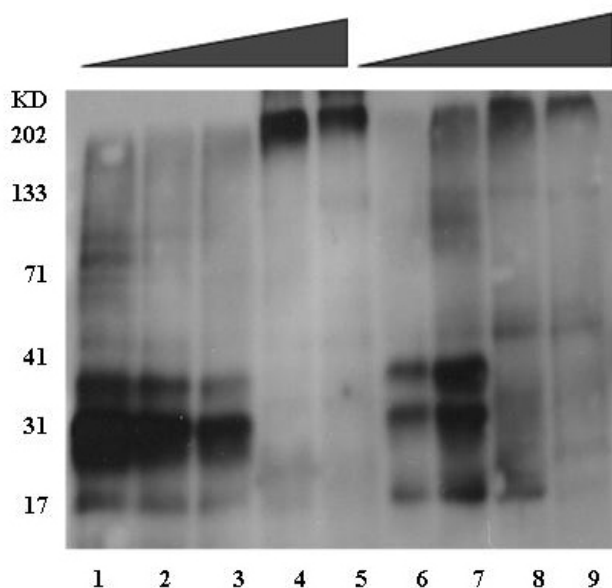
Figure 4.2 Cross-linking of purified GlyBP with DMS detected by SDS-PAGE.
Lane 1: aqueous form control; Lane 2-5: aqueous form cross-linked with 0.2, 0.5, 1, 2

mg/ml of DMS respectively; Lane 6: vesicular form control; Lane 7-9: vesicular form

cross-linked with 0.2, 1 and 2 mg/ml of DMS respectively.

Dynamic light scattering studies were conducted to better assign the oligomeric

state of the soluble form of GlyBP (the presence of vesicles precludes conducting parallel

studies on the membrane-associated form). In these studies, GlyBP was observed to have a

bimodal polydisperse distribution. A small quantity of large aggregates were present with

an hydrodynamic radius (R_h) ~20 nm. The predominant species yields a peak of R_h = 5.63

+/- 0.07 nm, with moderate polydispersity. R_h provides the radius of a hypothetical hard

sphere that diffuses at the same rate as the molecule. The polydispersity of the 5.63 nm

peaks makes a specific estimate of the molecular weight unreliable; however, the dynamic light scattering study indicates that the soluble form of GlyBP *in vitro* has a globular structure whose dimensions are consistent with those expected for a homopentamers having homology with the ECD of GlyR.

4.4.3 Determination of subunit interface and ligand-receptor interaction in GlyBP by chemical cross-linking coupled to mass spectrometry

Chemical crosslinking studies showed both forms of GlyBP are oligomeric. Furthermore, chemical crosslinking was used to examine protein folding and subunit-subunit interactions in GlyBP. A summary of the experimental design is shown in Figure 4.3. Mass spectrometry has the power to determine the sites of chemical crosslinks generated in oligomerized proteins. In GlyBP, there is a total 11 lysine residues which are reactive to the amine-specific crosslinker DMS. Lys-Lys crosslinking could ocurr intramolecularly or intermolecularly. After crosslinking of purified GlyBP with DMS, crosslinked proteins were run in SDS-PAGE, separating GlyBP lower- and higher-molecular weight bands corresponding to monomeric and oligomeric GlyBP, respectively. In the lower-molecular weight band, any crosslink must be intramolecular, whereas in the higher-molecular weight band, both intra- or inter-molecular crosslinks may exist. Lysine crosslinks were then identified by mass spectrometry. Comparison of these two crosslinking profiles might identify unique crosslinks that represent crosslinking between lysine residues from neighboring subunits, which would provide useful information about the subunit interface. All possible intramoleclar- and/or intermolecular-crosslinks are useful to validate the GlyBP homology model.
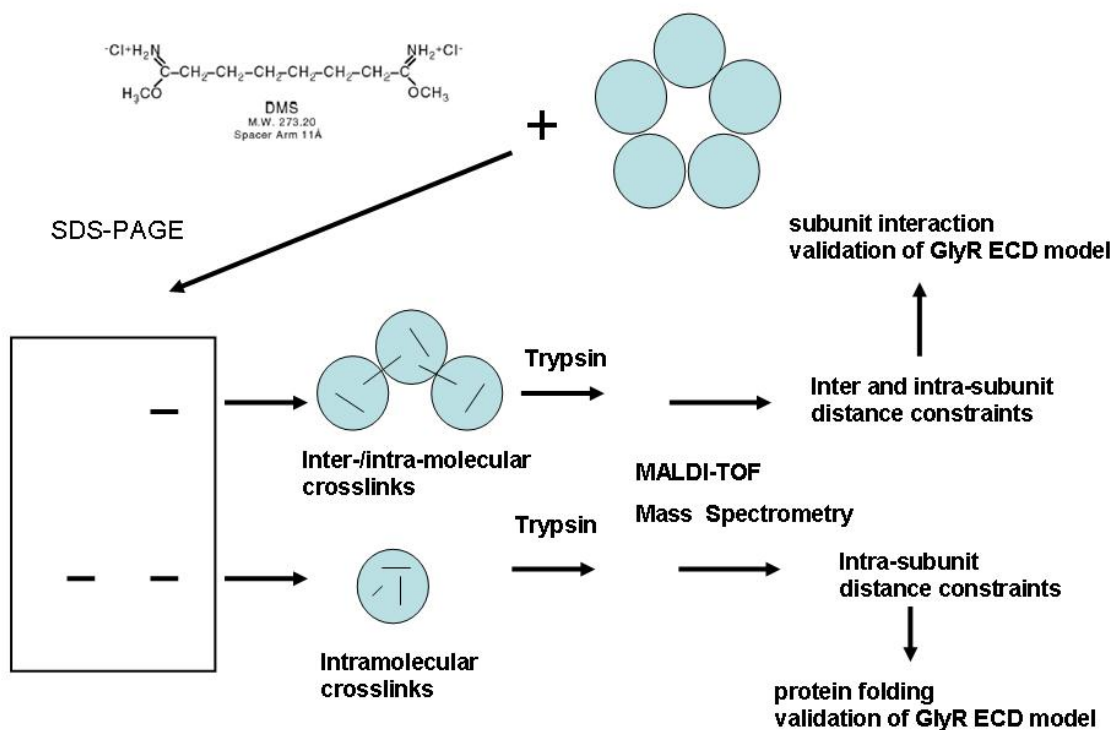
Figure 4.3 General strategy for mapping intramolecular and intermolecular crosslinks using chemical crosslinking coupled to MALDI-TOF MS.

4.4.3.1 MALDI-TOF MS analysis of GlyBP

MALDI-TOF mass spectrometry analysis was conducted on both forms of GlyBP. Purified GlyBP was separated on SDS-PAGE and stained using silver staining protocol compatible with mass spectrometry (see Material and Methods). The gel bands were excised and destained by standard protocol. After trypsin digestion, the tryptic digestion peptides were analyzed using MALDI-TOF MS in reflector mode. For both forms of GlyBP, protein

coverage of 55-80 % of entire AA sequence was usually obtained (Figure 4.4) and all lysine containing peptides were identified. Similar peaks were observed for both aqueous and vesicular GlyBPs (Figure 4.5), indicating structural similarity between aqueous and vesicular forms of GlyBP.

A R S A P K P M S P S D F L D K L M G R T S G Y D A R I R

P N F K G P P V N V S C N I F I N S F G S I A E T T M D Y R V N I

F L R Q Q W N D P R L A Y N E Y P D D S L D L D P S M L D S I

W K P D L F F A N E K G A H F H E I T T DN K L L R I S R N G N

V L Y S I R I T L T L A C P M D L K D T E S D V Q T C I M Q L E S

F G Y T M N D L I F E W Q E Q GA V Q V A D G S Q Y S R F I L K

E E K D L R Y C T K H Y N T G K F T C I E A R F P T S T S S L V A

A A F E S R A C S L E A C G T K L V E K Y

Figure 4.4 Protein sequence coverage map of GlyBP identified by MALDI-TOF MS.

Highlighted in grey are residues that are consistently observed in MALDI-TOF spectra.
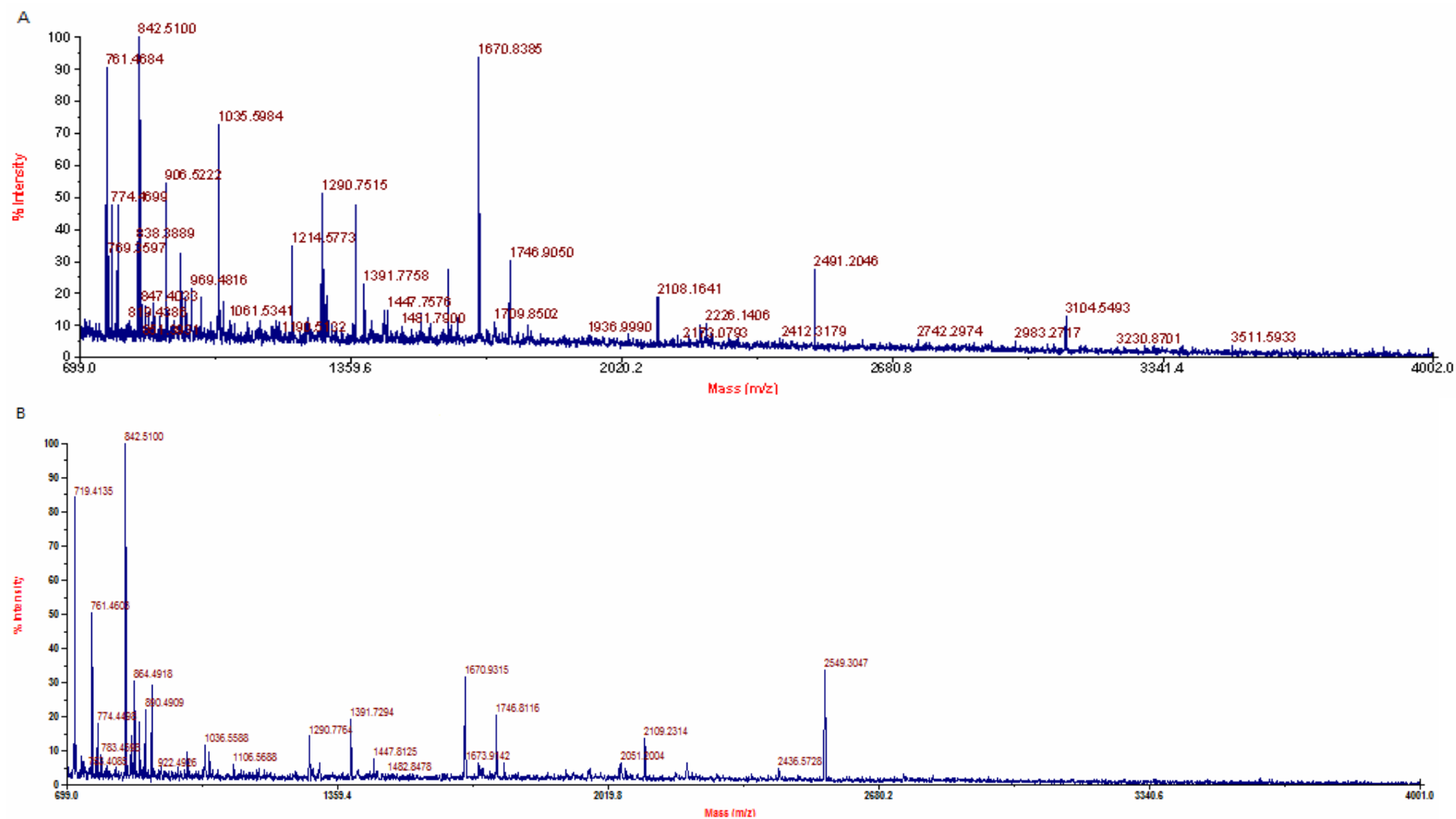
Figure 4.5 Representative spectra of MALDI-TOF MS of GlyBP without chemical crosslinking.

A, Representative mass spectrum of aqueous form of GlyBP; B, Representative spectrum of vesicular form of GlyBP.

4.4.3.2 Identification of intramolecular chemical crosslinks in GlyBP by MALDI-TOF MS

In order to obtain further structural information of GlyBP, chemical crosslinking coupled to mass spectrometry studies were conducted to provide distance constraints for Lys residues, which may be used to map the tertiary structure and quaternary structure of GlyBP. In this study, DMS, a homo-bifunctional crosslinker was used to probe the structure of GlyBP (Figure 4.6). DMS reacts with the amine groups of Lys residue and the N-terminus of a given protein. Both forms of purified GlyBP were incubated with 0.2, 0.5 and 1 mg/ml DMS or without DMS as a control, for 1 hr at room temperature. Proteins were separated on SDS-PAGE, silver-stained and then destained as described above. As described in 4.4.2, GlyBP migrated as both a monomer and as a high-order aggregate after crosslinking with DMS. Gel bands corresponding monomeric or oligomeric GlyBP were excised, washed and digested with 200 ng of trypsin per sample at 37 °C for at least 12 hr. Crosslinking reactions of GlyBP were conducted in the low micromolar range to reduce crosslinks generated between oligomer-oligomer interactions.
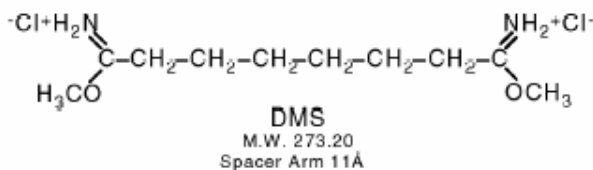
Figure 4.6 Structure of amine-specific crosslinker DMS.

Table 4.2 Intramolecular crosslinks observed from MALDI-TOF MS analysis of GlyBP crosslinked with DMS.

Parts per million (ppm) indicates the error of a percentage of the measured mass. "N" denotes the N-terminus of GlyBP.

K-K crosslinks	Theoreti m/z	Observed m/z	ΔMass, ppm	Cross-linked peptides
190-193	1498.795	1498.714	- 45	187-196
193-200	2268.040	2268.133	-41	191-196, 197-206
200-206	2357.048	2357.009	-16	197-213
N-6/16	2430.195	2430.245	-20	3- 20, 1- 2
193-206	2593.214	2593.122	36	201-213, 191-196
193-200	2652.252	2652.312	-23	194-206, 191-196
193-206	3145.452	3145.393	19	201-213 191-200
190/193-200	3153.584	3153.454	41	194-206, 187-196
193-200	3204.489	3204.330	50	194-206, 191-200
6-116	3478.711	3478.618	27	105-119, 3- 16
190/193-200/206	3646.783	3646.624	44	197-213, 187-196
N/6-116	3705.849	3705.769	22	105-119, 1- 16
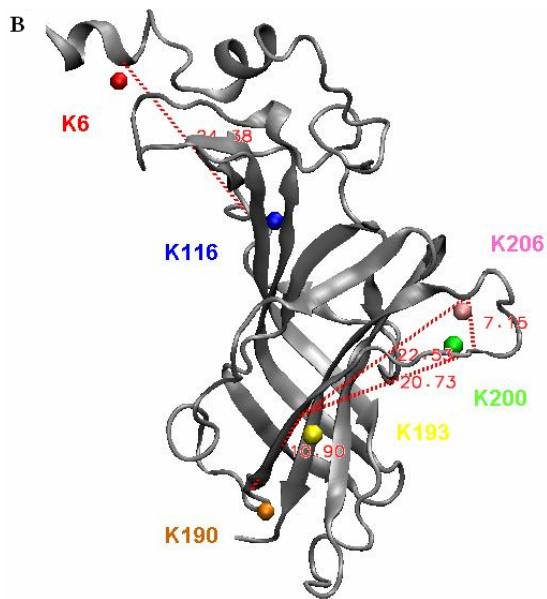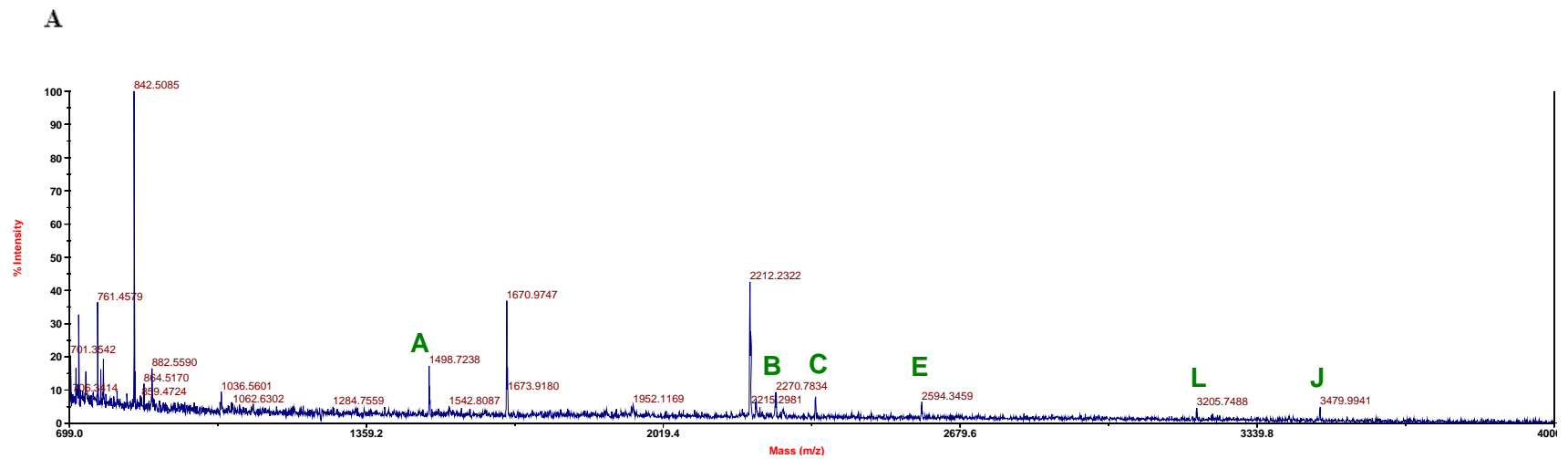
Figure 4.7 Intramolecular crosslinks observed in GlyBP after crosslinking with DMS.

A, Representative spectrum of MALDI-TOF MS of GlyBP after crosslinking with DMS; B, Schematic representation of intramolecular lysine-lysine crosslinks superimposed on the molecular model of GlyBP. A K-K pair was connected by dashed lines and distances (Å) between crosslinked K-K pairs were also provided.

95

Table 4.3 Predicted distances in GlyBP homology model of Lys-Lys pairs observed in monomeric GlyBP after chemical crosslinking with DMS followed by MALDI-TOF MS.

Crosslinked K-K pairs	C_α- C_α distances in homology model of GlyBP
K6-K116	24.3 Å
K190-K193	10.9 Å
K193-K200	20.7 Å
K193-K206	22.5 Å
K200-K206	6.6 Å

MALDI-TOF spectra were collected on a Voyager DE-Pro spectrometer in reflector mode. DMS-modified lysines will not be cleaved by trypsin due to modification of the primary amine group. Masses of tryptic peptides from crosslinked GlyBP were assigned from the mass spectra by using ASAP and GPMAW (see Material and Methods). From the MALDI spectra, most peaks observed in the absence of DMS were also obtained in the presence of the crosslinker (Figure 4.7A), indicating that modification of GlyBP by chemical crosslinking did not significantly interfere with tryptic digestion and following MS analysis. In addition, 12 masses corresponding to crosslinked peptides are listed in Table 4.2. These crosslined peptides could be divided into two classes: 2 of them (K187-196, K200-206) contain crosslinked K-K pairs within the same tryptic peptides; the rest of them have K-K pairs from distinct tryptic peptides. The K190-K193 and K200-K206 crosslinks were observed within the peptides 187-196 and 197-213 respectively. It is

expected that K190 and K193 are in close proximity since they are only separated by 2 amino acids in the primary sequence and would be expected to be crosslinked in the presence of amine-reactive chemical crosslinkers. This is also the case for the lysine pair K200 and K206.

In our GlyBP homology model, K6 and K116 were assigned to the N-terminal α–helix and β5 respectively, as shown in Figure 4.7B. The C_α- C_α inter-residue distance was predicted to be around 24 Å (Table 4.3). Considering the flexibility of Lys residues, it is expected that DMS could cross-link two lysine residues with C_α- C_α distance up to 24 Å (the arm length of DMS plus two times the length of lysine side chain, which is about 6.5 Å) (Young et al., 2000). Also, we must consider that GlyBP is dynamic and its backbone has some flexibility. The dynamic nature of GlyBP allows lysine residues to be crosslinked distances considerably shorter than that predicted in a static modeling protein molecule. K193 was crosslinked with both K200 and K206 and the distances of these two K-K pairs were similar our homology model (Table 4.3). In our GlyBP model, while K193 is located on β9, K200 and K206 are located in the C-loop region, which is critical for ligand binding and subject to significant conformational change upon ligand binding in the entire Cys-loop receptor family. Crosslinking of K193 with K200 and K206, both of which are around 20-22 Å away in the GlyBP model, indicates that the C-loop might be very flexible. Taken together, the crosslinks observed in monomeric GlyBP crosslinked provide distance constraints in GlyBP, which helps us to understand folding of GlyBP. Those data were consistent with the molecular model of GlyBP built on its homology with AChBP.

4.4.3.3 Identification of intra-/inter-molecular chemical crosslinks in GlyBP by MALDI-TOF MS

Inter-subunit crosslinks have been used for determination of the tertiary structure and arrangement of subunits within homo-oligomeric proteins and intra-subunit crosslinks for maintenance of stable tertiary structure.

As described in 4.4.3b, gel bands corresponding to the oligomeric GlyBP were excised, destained and digested with trypsin, followed by MALDI-TOF MS analysis. A representative spectrum was shown in Figure 4.8A and masses corresponding to crosslinked peptides observed in MALDI-TOF MS are presented in Table 4.4. As discussed above, K-K crosslinking of oligomeric GlyBP is expected to result in two types of crosslinks: intra- (two crosslinked lysines were crosslinked within the same protein molecule) and inter-molecular crosslinks (two crosslinked lysines were from neighbouring subunits of oligomeric GlyBP). Lower-molecular weight bands in SDS-PAGE only have intramolecular covalent crosslinks, whereas higher-molecular weight bands in SDS-PAGE may contain both intramolecular covalent crosslinks and crosslinks resulting from two neighboring subunits. Therefore, comparison of crosslinks between monomeric and oligomeric GlyBP could provide unique crosslinks that result only from inter-molecular crosslinking. These crosslinks might be important to understand the inter-subunit interaction in GlyBP oligomers, and furthermore may be used to validate/test our homology model of GlyBP. As expected, many masses listed here were also observed in the list of mass ions from monomeric GlyBP. However, several crosslinks were uniquely observed in high-order GlyBP oligomers, (Table 4.4 highlighted in grey). From this list, a few K-K pairs were found to be unique in mass spectra of crosslinked oligomeric GlyBP: K116b-

K200a, K116b-K206a, K200a-K190b and K200a-K193b (a and b denote two different neighbouring subunits). Among these crosslinks, the masses 2652.193 (EEKDLR$_{191-196}$-DLRYCTKHYNTGK$_{194-206}$) and 3153.609 (FILKEEKDLR$_{187-196}$-DLRYCTKHYNTGK$_{194-206}$) are of particular interest since both masses were fit to two crosslinked peptides that were not possible from the the same molecules since they have overlapping sequence. Both masses indicated that K200 was crosslinked to K193 in a neighbouring subunit. All crosslinks identified only from oligomeric GlyBP are consistent with the homology model of GlyBP. The calculated distances for intersubunit K-K crosslinks fall within the range of possible crosslinking distance with DMS. In contrast, our model showed that, for these crosslinked pairs, intramolecular crosslinking of these pairs is not possible since the predicted intramolecular distances by the GlyBP model are too far apart to be crosslinked by DMS (Table 4.5). One exception is the K200a-K193b pair. Although it's possible that crosslinking between K200 and K193 could occur both intra- and inter-molecularly based on the homology model, the observed mass (m/z 2652.193, EEKDLR$_{191-196}$-DLRYCTKHYNTGK$_{194-206}$) corresponded to a crosslink in which two crosslinking fragments have overlapping sequence, indicating that those two fragments must be from two neighboring subunits. For two lysines from neighbouring subunits, either lysine residue could be located either in the principal or complementary site. However, based on the GlyBP homology model, if two crosslinked lysine residues were too far away from each other, any particular orientation of the crosslinked K-K pair with a distance exceeding that predicted from GlyBP homology model could be ruled out. Therefore, a model of crosslinks observed from oligomeric GlyBP was proposed as illustrated in Figure 4.8B.

Table 4.4 Intra-/inter-molecular crosslinks observed from MALDI-TOF MS. Highlighted in grey are unique masses of K-K crosslinks that define the subunit-subunit interaction.

K-K crosslinks	Theoretical m/z	Observed m/z	ΔMass, ppm	Cross-linked peptides
190-193	1498.795	1498.743	-35	187-196
193-200	2268.040	2268.105	-29	191-196, 197-206
200-206	2357.048	2357.113	27	197-213
190-200	2385.159	2385.088	30	197-206,187-193
N-6/16	2430.195	2430.126	29	3- 20, 1- 2
193-206	2593.214	2593.177	15	201-213, 191-196
193-200	2652.252	2652.193	22	194-206, 191-196
190-200	2769.371	2769.317	20	194-206, 187-193
193-206	3145.452	3145.511	-19	201-213 191-200
190/193-200	3153.584	3153.609	-8	194-206, 187-196
193-200	3204.489	3204.405	26	194-206, 191-200
116-200	3230.549	3230.419	40	197-206, 105-119
190-200/206	3262.571	3262.502	21	197-213, 187-193
6-116	3478.711	3478.634	22	105-119, 3- 16
116-206	3555.724	3555.670	15	201-213, 105-119
116-200	3614.761	3614.823	-17	194-206, 105-119
190/193-200/206	3646.783	3646.656	35	197-213, 187-196
N/6-116	3705.849	3705.907	-16	105-119, 1- 16
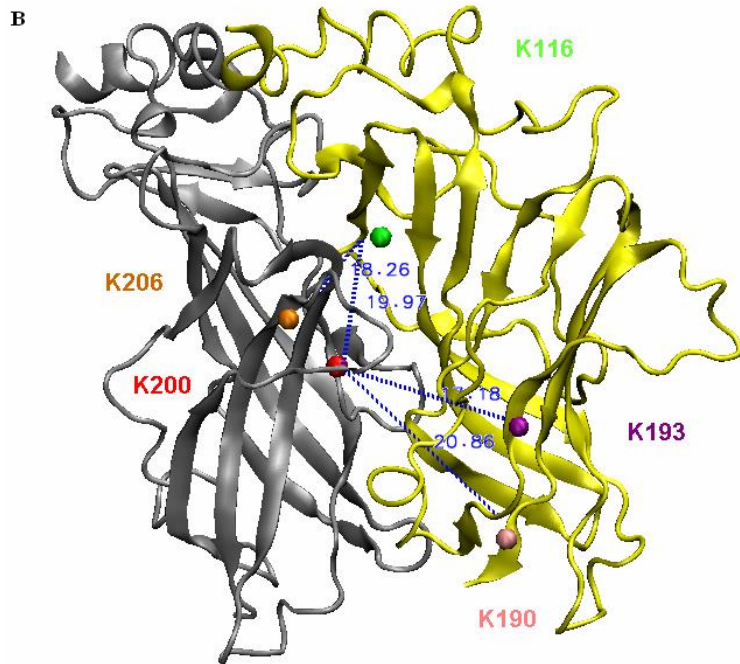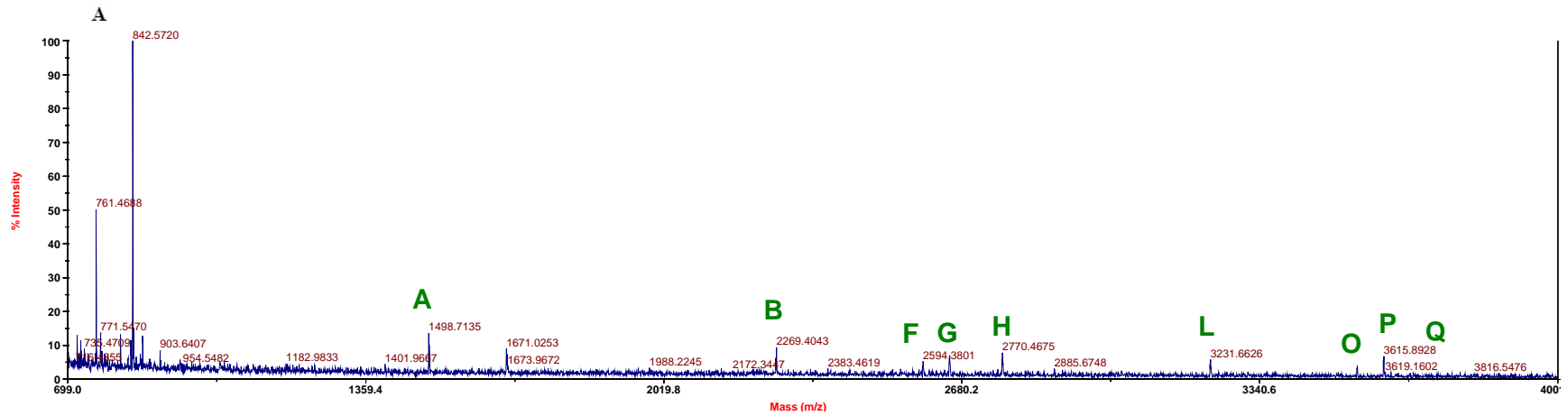
Figure 4.8 Intra-/inter-molecular crosslinks observed in GlyBP after crosslinking with DMS.

A, Representative spectrum of MALDI-TOF MS of GlyBP after crosslinking with DMS; B, Schematic representation of unique intermolecular lysine-lysine crosslinks superimposed on the molecular model of GlyBP.

101

Table 4.5 Predicted distances in GlyBP homology model of unique intermolecular Lys-Lys pairs observed in oligomeric GlyBP after chemical crosslinking with DMS followed by MALDI-TOF MS.

Crosslinked K-K pairs	Intermolecular C_α- C_α distances in homology model of GlyBP	Intramolecular C_α- C_α distances in homology model of GlyBP
K200a-K116b	19.9 Å	31.7 Å
K206a-K116b	18.2 Å	30.7 Å
K200a-K190b	20.8 Å	29.0 Å
K200a-K193b	17.1 Å	20.7 Å

4.4.3.4 Identification of intra-/intermolecular chemical crosslinks in GlyBP after incubation with strychnine by MALDI-TOF MS

As with other membrane receptors, the GlyR undergoes conformational changes upon ligand binding. It is expected that similar changes would exist in GlyBP. As shown in section 4.4.1, there is no net change in secondary structure in GlyBP upon binding of strychnine as demonstrated by CD. To test if any conformational change could be detected by K-K crosslinking coupled to mass spectrometry, GlyBP was incubated with or without strychnine for 1 hr at room temperature, and then crosslinked with DMS. The crosslinked products were then separated by SDS-PAGE, stained and gel bands were excised, destained, trypinized and analyzed by MALDI-TOF mass spectrometry (Figure 4.9). Table 4.6 and 4.7 list crosslinked peptides after incubation in the presence and absence of

strychnine. Most masses observed in the absence of strychnine were also found after incubation with strychnine (Table 4.6). Although the entire list of masses identified were not identical to those observed in the absence of strychnine, the identified crosslinked K-K pairs were identical under either condition. The crystal structure of AChBP in complex with defferent ligands and modeling studies on the ECDs of Cys-loop receptors suggest that the β–sandwich core doesn't undergo significant conformational changes. In constrast, the most obvious conformational changes occur in the C- and F-loops (Celie et al., 2004; Hansen et al., 2005; Cheng et al., 2006b). However, the similarity between identified K-K pairs in Table 4.6 and 4.7 does not absolutely indicate that no conformational changes occurred upon strychnine binding. In our crosslinking experiments, residues that were close to the C-loop and involved in crosslinking were Lys-200 and Lys-206. In the GlyBP homology model, these two lysines were located in the hinge region of the C-loop and, therefore, the position of Lys-200 or Lys-206 relative to the β–sandwich core might not be subject to significant changes upon strychnine binding.
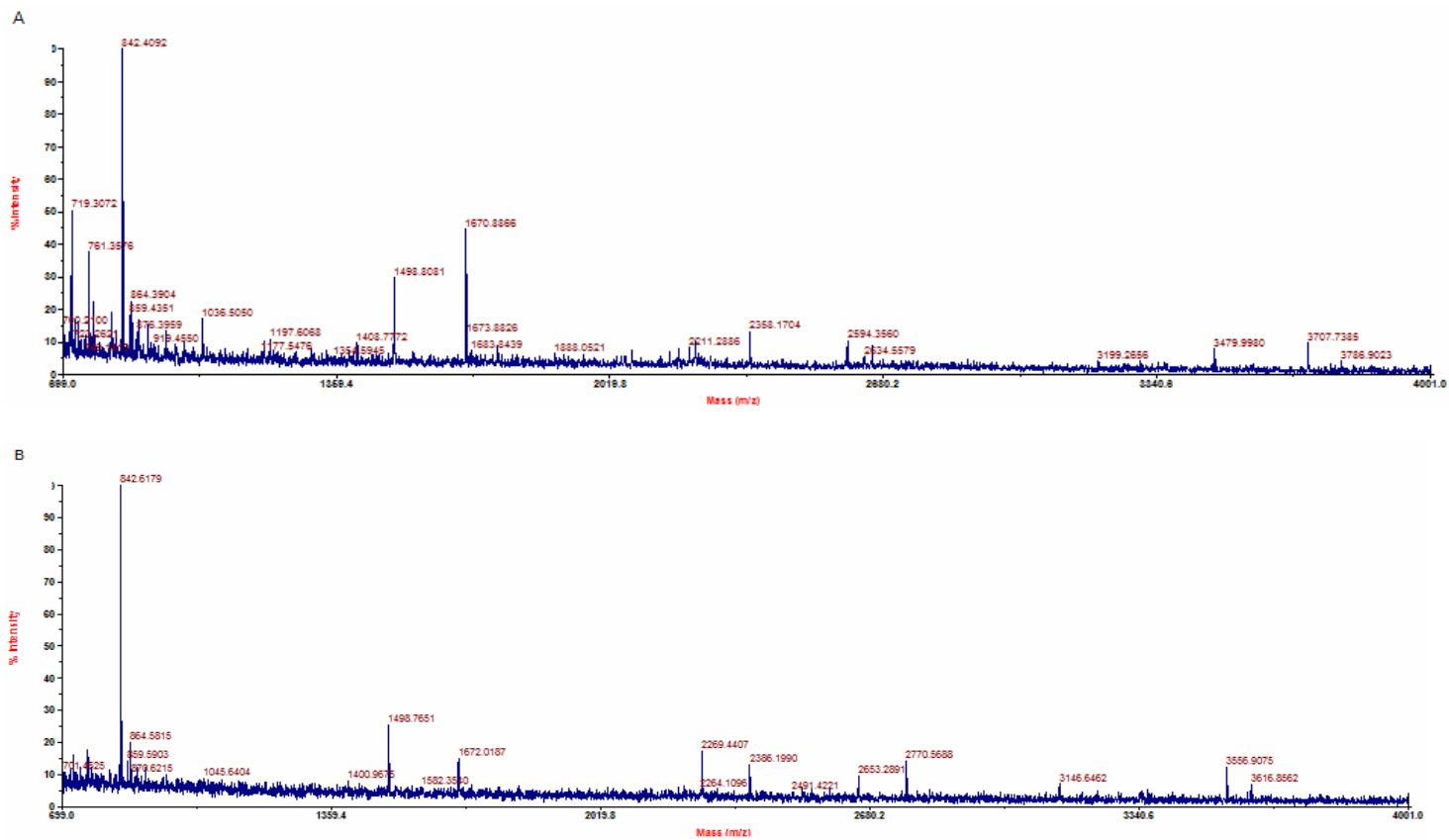
Figure 4.9 Representative spectra of MALDI-TOF MS of GlyBP after crosslinking with DMS in the presence of strychnine.

A, Representative spectrum from intramolecular crosslinking from monomeric GlyBP; B, Representative spectrum of intra-/inter-molecular crosslinking from oligomeric GlyBP.

Table 4.6 Intramolecular crosslinks observed from MALDI-TOF MS analysis of GlyBP crosslinked with DMS in the presence of strychnine.

K-K crosslinks	Theoreti m/z	Observed m/z	ΔMass, ppm	Cross-linked peptides
190-193	1498.795	1498.849	36	187-196
193-200	2268.040	2268.099	-26	191-196, 197-206
200-206	2357.048	2357.152	44	197-213
193-206	2593.214	2593.307	- 35	201-213, 191-196
193-200	2652.252	2652.177	28	194-206, 191-196
193-200	3204.489	3204.527	- 12	194-206, 191-200
6-116	3478.711	3478.627	24	105-119, 3- 16
190/193-200/206	3646.783	3646.652	36	197-213, 187-196
N/6-116	3705.849	3705.773	21	105-119, 1- 16

.

Table 4.7 Intra-/inter-molecular crosslinks observed from MALDI-TOF MS analysis of GlyBP crosslinked with DMS in the presence of strychnine.

K-K cross-link	Theoretical m/z	Observed m/z	ΔMass, ppm	Cross-linked peptides
190-193	1498.795	1498.722	-30	187-196
193-200	2268.040	2268..110	41	191-196, 197-206
200-206	2357.048	2357.002	-18	197-213
190-200	2385.159	2385.193	25	197-206,187-193
N-6/16	2430.195	2430.227	34	3- 20, 1- 2
193-206	2593.214	2593.194	-19	201-213, 191-196
193-200	2652.252	2652.122	-55	194-206, 191-196
190-200	2769.371	2769.399	22	194-206, 187-193
193-206	3145.452	3145.493	26	201-213 191-200
190-200/206	3262.571	3262.412	-43	197-213, 187-193
6-116	3478.711	3478.631	- 49	105-119, 3- 16
116-206	3555.724	3555.794	36	201-213, 105-119
116-200	3614.761	3614.809	19	197-206, 105-119

4.5   DISCUSSION

In Chapter 3, we have shown that both forms of GlyBP are correctly folded and retain the ability to bind to its ligands with affinities comparable to those observed in native full-length receptor. In this Chapter, we further demonstrated both forms of GlyBP are oligomeric, and taken together with functional data presented in Chapter 3, GlyBP is very likely pentameric. Oligomerization of GlyBP was first supported by the fact that it specifically bound to the 2-aminostrychnine resin, which strongly suggested that GlyBP is properly folded as an oligomer since it has been shown that ligand binding sites reside at the subunit interface. High affinity binding with 2-aminostrychnine resin indicated that ligand binding sites remain intact in GlyBP and the local environment around ligand binding sites mimics that of native full-length GlyR. Chemical cross-linking experiments clearly showed that it is oligomeric, although the detailed oligomeric state of GlyBP could not be inferred from chemical crosslinking experiment. Data from light scattering provided evidence that the size of GlyBP as an oligomer is consistent with it being a pentamer. In addition, LRET studies on vesicular form of GlyBP are also consistent with a pentameric structure of GlyBP. All data obtained in this study suggest that both forms of purified GlyBP are properly folded and are consistent with a pentameric structure. No pentameric structure of the ECD of any member in this receptor family has been resolved at atomic levels. AChBP has known structure, but it is just a structural homolog of the Cys-loop receptor ECD. Thus, characterization of the soluble pentameric GlyBP would provide insights into the structure and function of the ECD of GlyR and, possibly other Cys-loop receptors.

The CD experiments showed that both forms of GlyBP adopt equivalent net secondary structures. In addition, using two independent fitting programs, secondary structure analyses of the spectra of GlyBP indicated that both forms are predominantly composed of β-structure, with

little α-helix. This is consistent with expected secondary structure given the crystal structure of AChBP, a structural homolog of the ECD of Cys-loop receptors.

Mass spectrometry is a very promising tool applicable to protein structure analysis. Due to its high sensitivity, speed of analysis and ability to solve structural problems not easily handled by conventional techniques, mass spectrometry has been applied to structural studies of proteins and protein complexes (Biemann, 1995; McLafferty et al., 1999). In addition, chemical crosslinking in combination with mass spectrometric analysis has been used to provide low-resolution structure of proteins and interacting sequence within protein complexes (Young et al., 2000; Back et al., 2003; Sinz, 2003). The crosslinked K-K pairs in the crosslinking experiments were analyzed by fitting them with a homology model of GlyBP constructed in collaboration with Dr. M. Kurnikoava at CMU. All those crosslinks were found to be consistent with and validate this model.

As indicated in this study and others, crosslinking products are often of low signal intensity, which results in difficulties in identification of crosslinking product. A number of alternative strategies have been developed to help the identification of crosslinking products, including isotope-labeling of crosslinker or proteins, affinity tagged crosslinkers, fluoregenic crosslinker and chemically cleavable crosslinkers (Sinz, 2003). In this study, crosslinked products were always associated with relatively high masses, which made their identification more difficult. In the long run, might be necessary to introduce site-specific amine- (lysine) or thiol- (cysteine) reactive mutants, which would help reveal the role of any specific residue of interest and improve signal/background ratio in mass spectrometric studies.

It should be noted that chemical crosslinking methods are not only approaches for detecting proximity, but also provide information about dynamic collisions of residues involved

in crosslinking reaction (Sun and Kaback, 1997). Since lysine is a flexible residue, it's possible that formation of crosslinks occur even though they are fairly distant in the average structure. In our study, the C_α- C_α distance of a few Lys-Lys pairs are longer than the arm length of the crosslinker DMS, which is not unexpected due to the high flexibility and relatively long side chain of lysine residues.

5.0 STRUCTURAL CORRELATION BETWEEN GLYBP AND THE CORRESPONDING REGION OF FULL-LENGTH GLYR

5.1 SUMMARY

Previous studies in Chapters 3 and 4 have shown that GlyBP appear to be a structural homolog of the ECD of GlyR as evidenced by CD experiments, ligand binding assays, dynamic light scattering and crosslinking studies. In order to further examine whether GlyBP is both a structural and functional homolog of the corresponding region of full-length GlyR, comparative studies were conducted on both GlyBP and full-length GlyR using LRET. The LRET studies showed two distances were present between the intersubunit Cys-41, supporting the hypothesis that GlyBP is native-like. In addition, these two intersubunit Cys-41 distances were shortened upon glycine binding, indicating that GlyBP retains ability to undergo conformational changes upon agonist binding. Further LRET studies on full-length GlyR in intact Sf9 insect cells suggested both GlyBP and full-length GlyR have similar intersubunit Cys-41 distances and undergo the same allosteric changes upon agonist binding, which strongly suggests that GlyBP mimics the corresponding ECD of GlyR both structurally and functionally and may serve as an appropriate subject for high resolution structural studies of GlyR.

5.2   INTRODUCTION

The extracellular ligand binding domain in pentameric ligand gated ion channels is an important and inherent part of the whole protein. The receptor ECDs usually harbor the ligand binding sites and possess the determinants of ligand selectivity and specificity. In addition, the receptor ECDs are also important for pentameric assembly of the receptor (Connolly and Wafford, 2004; Lester et al., 2004). The conformational changes induced upon ligand binding are transmitted through connecting loops to the channel-forming transmembrane domains, which results in channel opening or modulation of the activity of the receptor (Connolly and Wafford, 2004).

In the previous chapters, we have shown that we are able to overexpress and purify the mutant extracellular domain of GlyR, GlyBP, in Sf9 insect cells. Further biochemical studies have shown GlyBP is a functional oligomeric protein that is a good structural model of the extracellular domain of GlyR in the resting state. However, how well this mutant protein mimics native full-length GlyR is unclear. To validate this structure, we used LRET to compare the structure of GlyBP with the corresponding region of full-length GlyR. Full-length GlyR has 7 Cys residues with four of them forming two pairs of disulfide bonds (Cys-138-Cys-152 and Cys-193-Cys-209) that are essential to activity. Each of the remaining three cysteines, Cys-41, Cys-290 and Cys-345 (Figure 5.1), has a free reactive thiol group, which might be potential sites for specific labeling studies. Since only Cys-41 is present in GlyBP, we chose to target this free cysteine residue as a labeling site for LRET studies. Cys-290 is postulated to be located in TM3 and may only be labeled appreciably in the presence of ligand (unpublished observation by R. Clarke, J. Johnson and M. Cascio). It was also found that residues in the TM2-TM3 loop, as well as the TM3 domain of the GABA$_A$ receptor were accessible only in the presence of ligands when it is heterologously expressed in *Xenopus* oocytes (Williams and Akabas, 1999, 2000),

111

suggesting that this region is less accessible in the resting state and a conformational change in TM3 is induced during channel activation. Cys-345 is located in the cytoplasmic loop connecting TM3 and TM4 and is therefore inaccessible to externally-labeled membrane-impermeant thiol-reactive reagents. Based on those facts, we hypothesized that, in studies of full-length GlyR, we could label Cys-41 in GlyR expressed in Sf9 insect cells without interference from labeling of Cys-290 and Cys-345. Then the intersubunit Cys-41 distances could be measured and compared to those obtained in GlyBP by LRET.

Förster resonance energy transfer (FRET) has been widely used to measure distances between molecules or conformational changes within an individual molecule. In this process, the excited-state energy of a fluorophore is transferred non-radiatively to a ground state acceptor fluorophore by long-range resonance coupling between the donor and acceptor transition dipoles (Clegg, 1992). The donor and acceptor molecules must be in close proximity (~10-100 Å) to allow efficient energy transfer between those fluorescent moieties (Stryer, 1978). One potential problem in these studies on membrane proteins on cell surface using free thiol as a reactive group is the presence of high background due to presence free thiol groups present on some membrane proteins other than the protein of interest. This problem has been overcome in studies on voltage-gated potassium channels expressed in Xenopus oocytes (Mannuzzu et al., 1996), in which endogenous free thiols on plasma membrane were pre-blocked by alkylating reagents before the bulk of overexpressed protein of interest reached the cell surface. We applied this approach to the baculovirus expression system used in this study to probe the intersubunit Cys-41 distances in GlyR expressed in intact Sf9 insect cells. Within ~6-24 h after infection, an infected Sf9 cell ceases synthesis of endogenous surface membrane proteins, and therefore, blockade of free thiol on the Sf9 cell surface 6 h after infection should result in only newly

synthesized GlyR on the cell surface having free cysteine residues. Thus, only Cys-41 in GlyR on plasma membrane surface could be labeled with thiol-reactive reagent and all background labeling of any other palsma membrane proteins would be minimized. By determining the intersubunit Cys-41 distances in both GlyBP and full-length GlyR, we could validate the homology model of GlyBP and determine the structural similarity between GlyBP and the corresponding region of full-length GlyR.
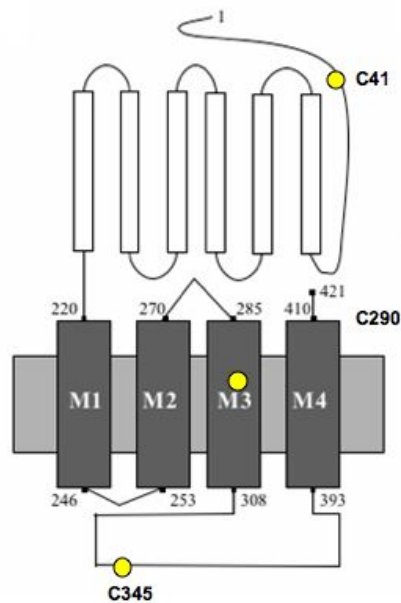
Figure 5.1 Schematic representation of Cys residues in full-length human α1 GlyR.

Cys-41, 290 and 345 are the only three Cys residue with free thiol group in native GlyR.

5.3 Material and Methods

5.3.1 Expression and purification of GlyBP

GlyBP was expressed and purified as described in Chapter 3. The vesicular form of GlyBP was reconstituted in lipid vesicles as described in Chapter 3.

5.3.2 Fluorophore labeling of purified GlyBP and GlyR in intact Sf9 insect cells

For the purified vesicular form of GlyBP, 1 μM protein in 25 mM KPi (pH 7.4) with 100 μM glycine (Sigma-Aldrich) was labeled with a 1:4 ratio of the maleimide derivatives of fluorescein (Biotium, Hayward, CA) and triethylenetetraminehexa acetic acid chelate of terbium (TTHA-Tb) (Invitrogen) for the donor:acceptor sample and with terbium chelate alone for the donor-only sample. Protein was dialyzed in phosphate buffered saline to remove excess labels.

For LRET studies on full-length GlyRs, Sf9 cells were infected with either wild-type baculovirus (no GlyR) or with baculovirus encoding full-length GlyR with a MOI > 5. Cells were pre-labeled by treatment with 10 mM iodoacetamide for 1 hr at 27 °C at 6 hr post-infection to block endogenous free thiol groups on the cell surface. Cells were collected by gentle centrifuguation at 1000 x g, washed twice with serum-free medium and then resuspended in FBS-containing medium and allowed to grow at 28 °C. Thus, only accessible extracellular Cys residues of those membrane proteins expressed on the surface after this time are available for labeling. Cells were collected 3 days post-infection by gentle centrifugation at 1000 x g, washed with extracellular buffer and labeled with the 1:4 ratio of fluorescein and terbium chelate for an

hour and a half. Cells were then washed with extracellular buffer for fluorescence lifetime measurements.

5.3.3 Fluorescence measurements and distance calculations

A TimeMaster Model TM-3M /2003 (Photon Technology International, Lawrenceville, NJ) was used for fluorescence measurements. A nitrogen/dye laser system was fiber-optically coupled to the sample compartment, which contained a thermostable cuvette holder with a microstirrer. Emitted light was collected by quartz optics and passed through a monochromator to a stroboscopic detector. Data were collected using Felix software (Photon Technologies International, Lawrenceville, NJ) and analyzed using Origin (OriginLab, Northampton, MA). The donor-only lifetimes were collected at 488 nm, whereas the LRET lifetimes were obtained by studying the sensitized emission of the acceptor, which was collected at the acceptor wavelength of 515 nm. The lifetimes calculated are an average of ~6-12 different data sets. Using the time constants of the donor fluorescence decay (τ_D) and the sensitized emission of the acceptor due to energy transfer from donor (τ_{DA}), the distances between the donor and acceptor are calculated by Förster's theory of energy transfer, with:

$$R = Ro \left(\frac{\tau_{DA}}{\tau_D - \tau_{DA}} \right)^{1/6}$$

R_o was calculated to be 60 Å using overlap integral as described previously (Du et al., 2005; Ramanoudjame et al., 2006).

5.3.4 Statistical analysis

Data from LRET are presented as mean ± SD. The difference of intersubunit Cys-41 distances was determined by two-way analysis of variance (ANOVA) for repeated measures or Student's *t*-test where applicable, and $P<0.05$ and $P<0.01$ were considered significant differences.

5.4 RESULTS

5.4.1 Determination of intersubunit Cys-41 distances and ligand-induced conformational changes of GlyBP by LRET

Since Cys-41 is the only cysteine residue with a free thiol group in GlyBP, this free cysteine may be reacted with donor or acceptor fluorophores and the LRET lifetimes were used to determine the Cys-41 distances between subunits. Terbium chelate served as the donor molecule, which is characterized by spectra with a large Stokes shift and sharp, distinct emission bands. The terbium emission spectrum overlaps well with the excitation spectrum of fluorescein (Figure 5.2). Because fluorescein emits within the "silent" regions between the terbium emission peaks, the interference from the donor emission is eliminated and the sensitized acceptor emission could be measured, which results in increased signal-to-noise ratio. In addition, terbium chelate has a very long lifetime, which makes lifetime measurements facile and highly accurate and also minimizes orientation effects. LRET studies were conducted on the vesicular form of GlyBP. The luminescence lifetime for the protein tagged with donor only (terbium chelate labeled) can be well fit by a single exponential decay (Figure 5.3A) and the lifetimes are similar in the absence

and presence of glycine (Table 5.1). The LRET lifetime for the donor: acceptor tagged protein required two exponentials (Figure 5.3B and Figure 5.4 for single exponential fit), resulting in two sensitized emission lifetimes: a shorter lifetime of 44 ± 8 µs and a longer lifetime of 241 ± 52 µs (n=12), respectively. Based on these LRET lifetimes, the intersubunit Cys-41 distances in the apo state of GlyBP are 33.8 ± 1.0 and 46.2 ± 1.6 Å (n=12).

In order to determine whether GlyBP undergoes any conformational changes upon ligand binding, intersubunit Cys-41 distances were also determined in the presence of its endogenous agonist glycine. Similarly, the LRET lifetimes were fit by a two exponential decay and the corresponding sensitized emission lifetimes are 31 ± 4 µs (n = 8) and 198 ± 14 µs (n = 8) (Table 5.1). The calculated intersubunit Cys-41 distances in GlyBP in the presence of glycine are 31.9 ± 0.6 (n =8, $p < 0.01$) and 44.4 ± 0.7 Å (n = 8, $p < 0.05$) respectively, which are significantly decreased compared with those obtained in the absence of glycine. The decrease in intersubunit Cys-41 distances in GlyBP in the presence of glycine strongly suggests that GlyBP retains the ability to undergo conformational changes upon agonist binding and this protein is also a functional homolog of the corresponding region of full-length native GlyR.

In addition, based on the geometry of polygons that are possibly formed by GlyBP monomers, the presence of two observed distances suggest a tetrameric or pentameric assembly of monomers to form GlyBP. In combination with conclusions drawn from previous binding assays, cross-linking and light scattering experiments (see Chapter 4), we conclude that GlyBP exists as a homopentamer. Furthermore, addition of glycine decreased the distances to a slight, but reproducibly degree between inter-subunit Cys-41, indicating glycine-binding induces conformational changes in GlyBP.
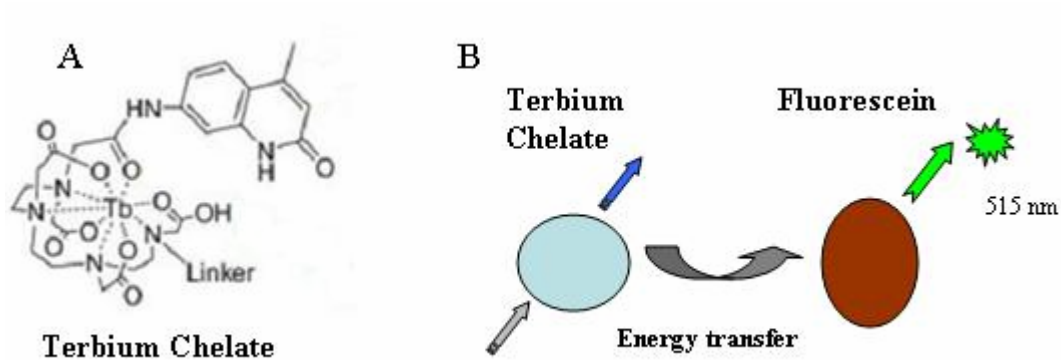
Figure 5.2 LRET of terbium chelate and fluorescein.

Schematic representation of the structure of terbium chelate (A) and energy transfer between terbium and fluorescein (B).
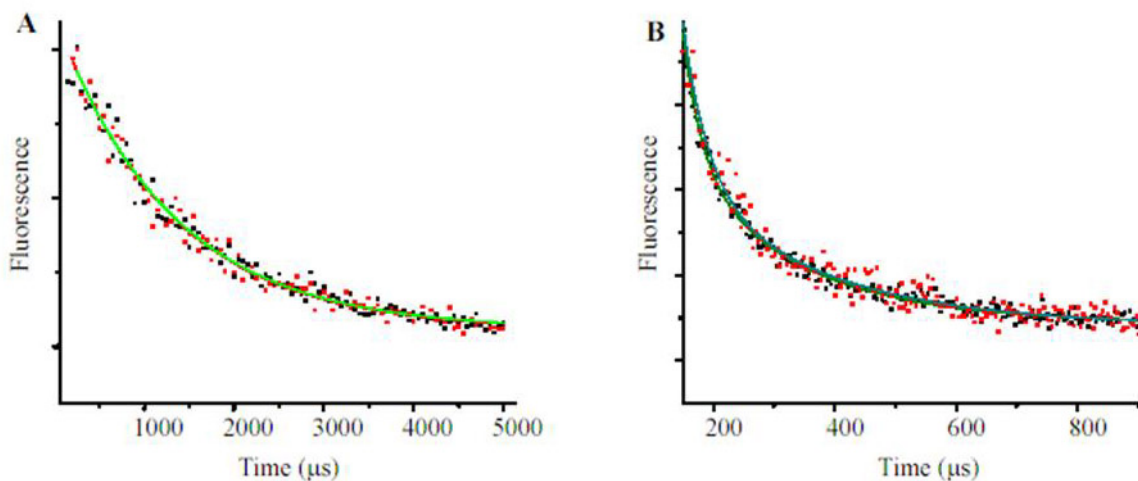
Figure 5.3 Determination of intersubunit Cys-41 distances in GlyBP by LRET.

A, The donor only lifetime; B, the LRET lifetime as measured by the sensitized emission for the apo (red) and glycine bound (black) forms of GlyBP.
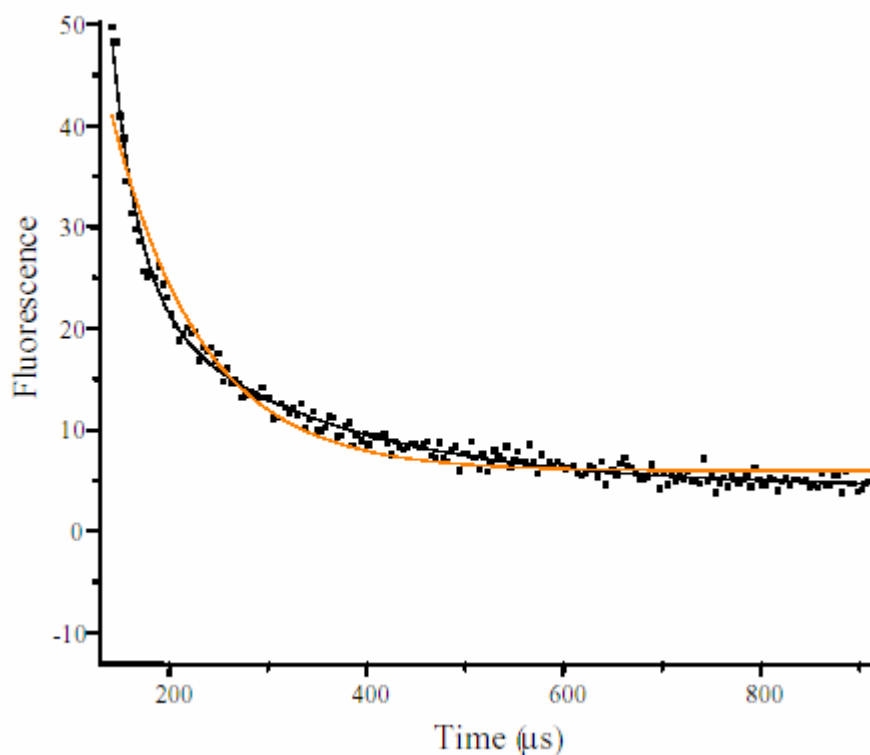
Figure 5.4 LRET lifetime of GlyBP fit by a single exponential function (red line), and by a two exponential function (black line).

5.4.2 Determination of intersubunit Cys-41 distances and ligand-induced conformational changes of GlyR in intact Sf9 cells by LRET

In order to determine whether GlyBP is an appropriate functional homolog of the extracellular domain of native GlyR, LRET studies analogous to those conducted on GlyBP were conducted on recombinant α1 GlyR expressed on the surface of baculovirus-infected Sf9 cells and the inter-subunit distances between labels on Cys-41 were measured. While the full-length

receptor contains three unpaired Cys residues, only Cys-41 is accessible to thiol-reactive compounds externally applied in the absence of ligand. As a negative control, little significant LRET signal was detectable in non-transfected Sf9 cells as compared with that obtained in Sf9 cells transfected with GlyR (Figure 5.5). Similar to studies on GlyBP, the luminescence lifetime for the protein tagged with donor only could be well represented by a single exponential decay (Figure 5.6A), while the LRET lifetime for the donor: acceptor tagged protein required two exponentials (Figure 5.6B and Table 5.1) with two sensitized emission lifetimes of 44 ± 4 and 252 ± 27 μs respectively. Based on these LRET lifetimes, the intersubunit Cys-41 distances are 33.1 ± 0.5 and 45.2 ± 1.1 Å respectively (Table 5.1).

Intersubunit Cys-41 distances were also determined in GlyR in Sf9 cells in the presence of glycine by LRET. In the presence of glycine, the sensitized emission lifetimes were 35 ± 5 (n = 12) and 225 ± 25 μs (n = 9) respectively. The calculated distances are 31.9 ± 0.7 (n = 12, $p < 0.01$) and 43.8 ± 1.0 Å (n = 9, $p < 0.01$) in the presence of glycine, which decreased significantly as compared to those obtained in the absence of glycine. Furthermore, those distances are are similar to the distances between Cys-41 in GlyBP (Table 5.1), indicating that neighboring subunits in both GlyBP and GlyR moved closer to each other with respect to Cys-41 in the presence of agonist. These LRET studies strongly suggest that GlyBP and GlyR have similar structures and most likely undergo similar allosteric changes upon binding glycine.

Table 5.1 The fluorescence lifetimes and distances for GlyBP and GlyR tagged with fluorescein (acceptor) and TTHA-Tb (Donor).

Construct	Ligand	Donor lifetime (µs)	Sensitized emission lifetime (µs)	Distance (Å)
GlyBP	Apo	1392 ± 49	44 ± 8	33.8 ± 1.0
			241 ± 52	46.2 ± 1.6
GlyBP	Glycine	1392 ± 52	31 ± 4	31.9 ± 0.6
			198 ± 14	44.4 ± 0.7
GlyR	Apo	1680 ± 51	44 ± 4	33.1 ± 0.5
			252 ± 27	45.2 ± 1.1
GlyR	Glycine	1654 ± 49	35 ± 5	31.9 ± 0.7
			225 ± 25	43.8 ± 1.0
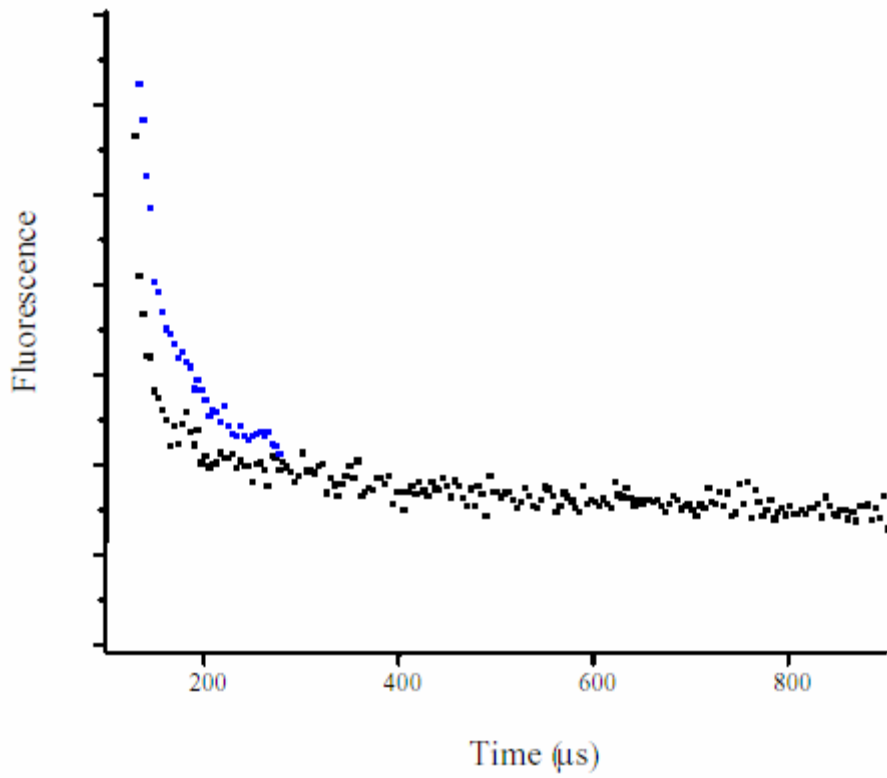
Figure 5.5 LRET lifetime of insect cells non-transfected (black) and transfected (blue) with GlyRs tagged with donor and acceptor fluorophores.
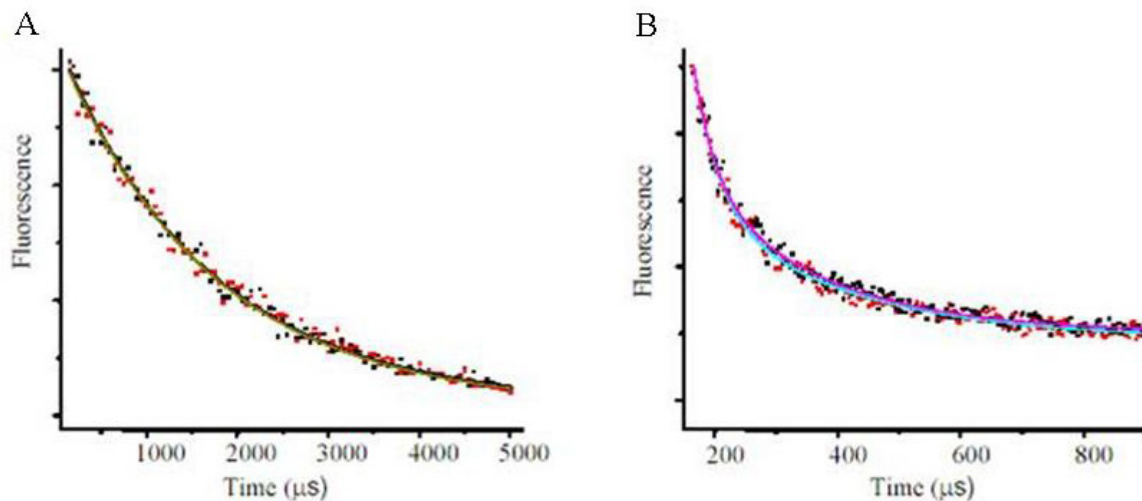
Figure 5.6 Determination of intersubunit Cys-41 distances of full-length GlyR in Sf9 cells by LRET.

A, The donor only lifetime; B, the LRET lifetime as measured by the sensitized emission for the apo (red) and glycine bound (black) forms of native GlyR expressed in Sf9 insect cells.

5.5   DISCUSSION

In this Chapter, we used LRET to study the intersubunit Cys-41 distances in both GlyBP and full-length GlyR. Due to the presence of three free Cys residues in wild-type GlyR, we took advantage of the fact that only Cys-41 could be labeled when the dye labels are applied externally. Thus, LRET studies on full-length GlyR were conducted in intact Sf9 insect cells, while GlyBP was studied with purified proteins. The presence of two distinct intersubunit Cys-41 distances strongly suggests oligomerization of GlyBP. In addition, GlyBP can only be either pentameric or tetrameric based on the possible geometry of distinct polygons that GlyBP subunits could form. Although the presence of two distances does not allow us to experimentally

123

exclude the possibility that GlyBP could be a homotetramer, we conclude that GlyBP is pentameric. First, dynamic light scattering showed the size of GlyBP is consistent with it being a pentamer. Second, the observed intersubunit Cys-41 distances fit well with values predicted from the structural models of both GlyBP and wild-type GlyR ECD (Speranskiy et al., 2007). Third, we observed nearly identical intersubunit Cys-41 distances in full-length GlyR expressed in intact Sf9 insect cells, which indicates that GlyBP adopts a native structure similar to that of full-length receptor. Those distances decreased in the presence of its endogenous agonist glycine, indicating that GlyBP is capable of undergoing conformational changes upon agonist binding, which further validated the proper functioning of GlyBP. In addition, intersubunit Cys-41 distances were decreased to a similar extent in both GlyBP and full-length GlyR, indicating they might undergo similar conformational changes upon agonist binding. Together, all of our data provide strong supporting evidence that GlyBP is pentameric and has a similar structure to the corresponding region of full-length GlyR.

In FRET studies, both donor and acceptor molecules are fluorescent. One limitation of FRET is that the signal-to-background ratio of the sensitized emission is low due to interference from the donor fluorescence and direct excitation of the acceptor. A similar technique was developed about a decade ago, in which energy transfer occurs between a luminescent donor molecule to an fluorescent acceptor molecule and was thus named luminescence resonance energy transfer (LRET) (Selvin and Hearst, 1994; Selvin et al., 1994). In LRET studies, lanthanide chelates are used as donors, which have several advantages over classical fluorophores (Selvin and Hearst, 1994). One important advantage is that, in LRET experiments, the luminescence lifetime of the donor could be determined by analyzing sensitized acceptor emission decay. The sensitized acceptor emission could be measured without significant

interference from donor emission or direct acceptor excitation since the lifetimes of lanthanide chelates are in the millisecond range whereas the lifetimes of the acceptor fluorophores are in the nanosecond range (Heyduk and Heyduk, 2001). Direct acceptor emission could be eliminated since directly excited acceptor decay to zero in a time insignificantly short compared to the lifetime of a donor, whereas directly excited donor emission could be eliminated by selecting an appropriate emission wavelength. Therefore, the decay of sensitized acceptor emission reflects only the decay properties of the donor engaged in energy transfer (Heyduk and Heyduk, 2001).

When the protein function is probed by Cys modification, it's essential to choose appropriate Cys residues in native proteins or sites at which Cys mutations are introduced. One potential problem using Cys substitutions followed by chemical modification is that the mutations might directly affect the structure and function of the protein. In some cases, a mutated residue might be crucial for subunit-subunit interaction or receptor-ligand binding. Therefore, selected Cys substitutions in this study might have a direct effect on the folding and/or ligand binding of GlyBP and full-length GlyR. With that in mind, we took advantage of the presence of native Cys residues in GlyBP and labeled native Cys residues without Cys substitution. However, this approach is limited by the location of native Cys residues in proteins of interest. It's expected the Cys residues studied are located within or near ligand binding sites or subject to significant conformational changes upon ligand binding. In LRET studies, we chose Cys-41 to study the intersubunit distances and ligand-induced conformational changes. As expected, we observed intersubunit interaction of Cys-41 by LRET and ligand-induced conformational changes as indicated by shortening of intersubunit Cys-41 distances. However, further structural information could not be obtained merely from distance changes in intersubunit Cys-41. Therefore, it seems necessary to specifically introduce Cys mutants in GlyBP in order to get

further understanding of oligomerization of GlyBP and ligand-receptor interactions. Cys mutations would be introducted close to ligand binding sites, such as essential residues in the C-loop. In combination with LRET, detailed structural information regarding to subunit interaction and conformation changes in the C-loop could be assessed by analyzing distances between introduced Cys residues.

6.0   GENERAL DISCUSSION AND FUTURE DIRECTIONS

6.1   STRUCTURAL STUDIES ON PENTAMERIC LIGAND GATED ION CHANNELS

To date, our understanding of structures of Cys-loop receptors are mainly from the following three structures: 1) the cryo-EM structure of *Torpedo* nAChR (Unwin, 2003; Unwin, 2005), 2) X-ray structures of AChBPs from different species of snail in complex with distinct ligands (Brejc et al., 2001; Smit et al., 2006), and 3) the very recently reported crystal structure of mouse α1 nAChR ECD bound to α-bungarotoxin (Dellisanti et al., 2007). The cryo-EM structures of *Torpedo* nAChR is the only resolved structure of a full-length receptor in the Cys-loop receptor family. The cryo-EM structure of nAChR provides an overall view of the whole receptor with detailed description of the ion channel in both open and closed states. However, due to the limited resolution (~ 4Å) compared to X-ray crystallography, detailed structural information regarding subunit-subunit interaction, side chain orientation and ligand-receptor interactions, and any information on the gating mechanism remain unresloved.

The crystal structures of AChBPs in complex with various ligands from a few species provides more detailed structural information since they were resolved at higher resolutions and are useful templates to model the ECDs of Cys-loop receptors. In collaboration with Dr. Maria Kurnikova, we have constructed a homology model of GlyBP based on these templates. The

AChBP structure is consistent with all previous biochemical and mutagenic data. However, the transmembrane domains, which form the ion conducting channel and are essential for receptor function, are lacking in AChBPs. Interestingly, coupling of agonist binding and channel activation was observed when AChBP was linked to the pore domain of 5-HT$_{3A}$ receptors (Bouzat et al., 2004). Thus, AChBPs are still useful models to understand the ECD of Cys-loop receptors and may even provide instructive information about the channel activation mechanisms. However, there is some controversy regarding whether these binding proteins undergo conformational changes similar to full-length Cys-loop receptors upon binding of agonist.

In addition, the most recent crystal structure of mouse α1 nAChR ECD provided the first high-resolution structure of the ECD of Cys-loop receptor subunit. This structure is similar to those of AChBPs with respect to overall folding pattern, secondary structural composition, ligand binding sites and also other essential structural features common in the entire Cys-loop receptor family, which further confirms the generally accepted concept that Cys-loop receptors are conserved in their three-dimensional structure. However, this nAChR ECD was monomeric and thus provided no information regarding the subunit interface and limited our further understanding of channel function of a whole receptor with multiple subunits. Thus, a pentameric structure of any Cys-loop receptor, even in a truncated form, is still highly desirable.

Obviously, all these structures are closely related to the structure of nicotinicoid receptors, either in part (i.e. the ECD) or the entire receptor. Other biochemical and electrophysiological studies have also been conducted on Cys-loop receptors regarding their three-dimensional structure to further understand the molecular mechanisms that gives rise to gating. To complement our understanding of structure and function of this receptor family, more

efforts need to be taken to extend structural studies on other members in this receptor family. In this study, we successfully overexpressed and purified GlyBP, a chimeric protein corresponding to the GlyR ECD in both a soluble and membrane-associated form. Biochemical and biophysical studies have shown that GlyBP is oligomeric and very likely pentameric, which is essential for proper functioning of any member of this ligand gated ion channel family. Overexpression and purification of a soluble, native-like ECD of the GlyR may enable us to provide detailed structural information and to understand the function of receptor ECD of Cys-loop receptors once further high resolution structure of this protein is achieved.

Mutations (NFPM$_{144-147}$→DTES$_{144-147}$) in the Cys-loop (loop 7) include a pair of Phe-Pro residues. From the crystal structure of mouse nAChR α1 ECD, those residues form type VI turns. Phe is packed face-to-face with Pro. Mutagenesis studies have shown that this Phe residue is critical for proper functioning of nAChR (Chakrapani et al., 2004). From the EM structure of *Torpedo* nAChR, the Cys-loop was suggested to interact with the loop between TM2 and TM3 (Unwin, 2005). In particular, a stretch of sequence F-P-F directly interacts with residues at the end of TM3. The F-P pair is conserved among all nAChR subunits and most of other Cys-loop receptor subunits, including GlyR α1 subunit. Similarly, it is very likely that, in intact GlyR, the Cys-loop also interacts with the M2-M3 loop. In LGICs, the loops connecting neighboring β-strands in the extracellular ligand binding domain are variable in primary sequence even within different subunits forming the same receptor (Unwin, 2005).

In the closed state of *Torpedo* nAChR, the C-loop is highly flexible. This is not unexpected since this loop has been implicated in acetylcholine binding, which might lock the C-loop in a specific conformation contributing to transactivation of the channel pore upon agonist binding. In our LRET studies, overall conformational changes were observed upon glycine

binding. We propose that this is due to an allosteric change which is initated in the ligand binding sites nearby the C-loop region, giving rise to the receptor residing primarily in the desensitized state. CD studies have shown that there is no detectable change in net secondary structure between the resting and desensitized states. Chemical crosslinking coupled to mass spectrometry studies also did not detect any gross conformational changes upon strychnine binding as demonstrated by unchanged Lys-Lys crosslinking pattern. This is not inconsistent with the C-loop being involved in antagonist binding and undergoing conformational changes upon strychnine binding due to the restricted locations of lysine residues probed by chemical crosslinking and also limited capacity of chemical crosslinking with respect to determination of conformational changes.

6.2   HETEROLOGOUS EXPRESSION, PURIFICATION AND CHARACTERIZATION OF CYS-LOOP RECEPTOR ECDS

As discussed earlier, due to the difficulty in crystallizing full-length membrane receptors, high-resolution structural studies on the extramembranous domains of membrane proteins have been used as alternative approaches to study the membrane protein structure at atomic levels. This has proven to be a successful strategy since a number of domains of membrane proteins have been resolved in biophysical studies, such as the X-ray crystallographic structure of the ECDs of the human growth hormone receptor (de Vos et al., 1992), the MHC-related neonatal Fc receptor (Burmeister et al., 1994), the T-cell receptor (Garboczi et al., 1996; Garcia et al., 1996) and the AMPA receptor (Armstrong and Gouaux, 2000). These structures provide detailed information

regarding ligand-receptor interactions at the atomic levels, which greatly advances our understanding of the molecular mechanisms underlying signal transduction across the plasma membrane from distinct perspectives.

Similarly, attempts have been made to overexpress a significant amount of truncated extracellular ligand binding domain of a Cys-loop receptor for further high-resolution structural studies. Among Cys-loop receptors, the nAChR is the most extensively studied receptor, and accordingly, most overexpressed ECDs were from subunits of nAChR. In addition, overexpression of $GABA_A$-R and GlyR ECDs have been reported. The expression and biochemical characterization of Cys-loop receptor ECDs are summarized in Table 6.1. However, no published reports have shown that the ECD of a Cys-loop receptor was expressed as a functional pentamer.

Common strategies for heterologous expression and purification of membrane receptor ECDs include: 1) Epitope-tagged proteins: The receptor ECDs can be attached to an epitope such as 6xHis, the FLAG peptide (DYKDDDDK); 2) Recombinant fusion proteins: The receptor ECDs may be fused with several anchorage sequences including glycosylphosphatidylinositol (GPI), the maltose binding protein and glutathione-S-transferase (GST) protein; 3) proteins without any modification: The receptor ECDs were also expressed and purified without any modification. While this strategy lacks the beneficial aspects of approaches 1) and 2), by which the purification procedure is relatively simple, it reduces the possibility that the three dimensional structure of receptor ECDs could be altered by the attached tags.

These receptor ECDs were mainly expressed in *E.coli*, *Xenopus* oocytes, yeast and insect cells. *E.coli* is one of the most commonly used expression system for recombinant membrane proteins due to high expression level of protein targets, ease of manipulation and relatively low

cost. However, the majority of expressed membrane proteins is found in the inclusion bodies and is misfolded. Thus, refolding of misfolded proteins expressed in bacteria under empirically-determined experimental conditions needs to be conducted when this approach is used to express Cys-loop receptor ECDs. ECDs of nAChR *Topedo* α1 (Schrattenholz et al., 1998; Alexeev et al., 1999) and α7 subunit (Fischer et al., 2001; Tsetlin et al., 2002), and GlyR α1 subunit were renatured from inclusion bodies of *E.coli*. However, significantly reduced ligand binding affinity was observed in several cases when those receptor ECDs are purified as refolded, which decreased the usefulness of further structural studies on those receptor ECDs.

Not surprisingly, nAChR α1 and α7 ECDs were predominant in inclusion bodies when expressed in *E.coli* (Alexeev et al., 1999). One alternative strategy for expression of receptor ECDs in *E.coli* is to take advantage of the signal sequence of proteins that are secreted into the periplasm of *E.coli*. The receptor ECD would be expressed as fusion proteins secreted into the culture medium in a correct folding state. However, receptor ECDs expressed as fusion proteins might have distorted three dimensional structures and also reduced ligand binding affinities. One key problem with heterologously expressed Cys-loop receptor ECDs is protein aggregation at higher concentration, which limited further structural characterization. Interestingly, nAChR α7 C116S mutant decreased the aggregation and increased the stability of expressed proteins in solutions (Tsetlin et al., 2002).

ECDs of nAChR α1 were often expressed as monomers since assembly of native full-length nAChR requires incorporation of other subunits. However, nAChR α7 nAChR has been known to be able to form a homo-oligomeric ion channel (Couturier et al., 1990). It seems that it is more suitable for heterologous expression of a functional receptor ECD. Several independent studies reported overexpression of α7 nAChR in different expression systems (Wells et al., 1998;

132

Fischer et al., 2001). In our studies, GlyBP was expressed as an oligomer, very likely a pentamer. Although the most recent crystal structure of mouse α1 ECD of nAChR provided the first structure of Cys-loop receptor ECD, high-resolution structural determination of oligomeric GlyBP and/or α7 nAChR ECD would provide direct detailed structural information on ligand binding sites and subunit-subunit interaction.

Secondary structural analysis of expressed receptor ECDs indicated β–structure contributes substantially to the conformation of Cys-loop receptor ECDs although the percentages of each secondary structural element vary in distinct receptor ECDs (Table 6.1). This difference might reflect subtle differences in the secondary structure of distinct subunits of any given type of Cys-loop receptor or possibly result from distinct experimental conditions in circular dichroism studies. In our study, we observed comparable percentage of secondary structural elements in GlyBP although reduced α-helix was detected in GlyBP. The similarity between secondary structure of GlyBP and that of nAChR subunits and AChBPs further confirms that all members in this receptor family share similar fold. ECDs of nAChR subunits expressed in other expressional systems such as *Xenopus* oocytes, yeast were usually correctly folded, and able to be modified post-translationally. These receptor ECDs retained high affinity with ligands and had similar secondary structures, which is more suitable for further high-resolution structural determination. A problem using these expressional systems is the difficulty in obtaining a sufficient amount of purified proteins for further structural studies, which hindered the progress on high-resolution determintation of those important receptors.

The ligand binding of any given receptor ECD is a good index of receptor functionality. For many heterologously expressed Cys-loop receptor ECDs, reduced ligand binding affinity was observed. This reduction might be due to any of the following: 1) The three dimensional

133

structure of recombinant receptor ECDs was slightly distorted under different experimental conditions; 2) The overall strucuture of receptor ECDs was similar to native full-length receptors, but the presence of tags or linker sequence interfered with ligand binding properties of purified proteins in solutions; 3) For ECDs of nAChR subunits, they were usually expressed as monomers; lack of subunit interface interactions might decrease ligand binding affinity although monomeric nAChR subunits still retained the ability to bind α-bungaroxin with relatively high affinity. High-resolution structure of any kind of Cys-loop receptor ECD could still provide insight into the detailed three-dimensional structure of the ligand binding domain and also ligand-receptor interaction, if the receptor ECD is resolved as an oligomeric form.

Table 6.1 Summary of expression and biochemical characterization of the ECD of Cys-loop receptor subunits in various expression systems.

Receptor	Subunit	Expression constructs	Expression system	Oligomerization state	Ligand binding affinity, Kd	Secondary structure	Reference
GlyBP		Hydrophilic replacements Hydrophilic tail	Sf9 insect cells	Oligomeric (pentameric)	110-130 nM for strychnine	~9-14% α-helix, ~35-40% β-sheet	Chapter 3 & 4
nAChR	*Torpedo* α1-209	No modification	Refolded in E.coli	monomeric	4 nM for α - bungarotoxin	15% α-helix, 45% β-sheet	(Schrattenholz et al., 1998)
	Torpedo α1-209	His tag	Refolded in E.coli	monomeric	130 nM for α - bungarotoxin	15% α-helix, 32-35% β-sheet	(Alexeev et al., 1999)
	mouse muscle α1 1-210	GPI-linked	*Xenopus* oocytes, CHO cells	monomeric	3 nM for α - bungarotoxin	12-14% α-helix, 51% β-sheet	(West et al., 1997)
	mouse muscle α1 1-211	No modification	yeast	monomeric	0.2 nM for α - bungarotoxin	14% α-helix, 46% β-sheet	(Yao et al., 2002)
	human muscle α1 1-210	No modification	yeast	monomeric	5.1 nM for α - bungarotoxin	N/A	(Psaridi-Linardaki et al., 2002)
	chicken α7 1-208	No modification	*Xenopus* oocytes	oligomeric	0.4 nM for α - bungarotoxin	N/A	(Wells et al., 1998)
	rat α7 1-196	Fusion proteins	Refolded in E.coli	High-molecular mass aggregate	2.5 μM for α - bungarotoxin	41% α-helix, 16% β-sheet	(Fischer et al., 2001)
	rat α7 1-208	Fusion protein	Refolded in E.coli	Oligomeric, High-order aggregate	310 nM for α - bungarotoxin	22% α-helix, 45% β-sheet	(Tsetlin et al., 2002)
	human α7	His tag	yeast	Oligomeric	57 nM for α -	N/A	(Avramopoulou

	1-208				bungarotoxin		et al., 2004)
	human muscle β 1-221	FLA/His tag	yeast	dimeric	N/A	significant % β-sheet structure	(Kostelidou et al., 2006)
	human muscle γ1-218	FLA/His tag	yeast	oligomeric	N/A	N/A	(Kostelidou et al., 2006)
	human muscle ε1-219	FLA/His tag	yeast	oligomeric	N/A	N/A	(Kostelidou et al., 2006)
	Complex of *Torpedo* α, β, γ and δ ECDs	No modification	Insect cells	oligomeric	N/A	N/A	(Tierney and Unwin, 2000)
GlyR	human α1 1-219	His tag	Refolded in E.coli	oligomeric	110-130 nM for strychnine	15% α-helix, 48% β-sheet	(Breitinger et al., 2004)

6.3   EFFECTS OF LIPID COMPOSITION AND DETERGENT ON ION CHANNEL STRUCTURE AND FUNCTION

The lipid bilayer of a cell membrane is not just a physical barrier separating the cell from the outside world, but provides an environment for membrane proteins which are important for many inter- or intra-cellular processes. It has been shown that lipid composition of a lipid bilayer in cell membranes has a significant effect on the functionality of membrane proteins, including ion channels (Tillman and Cascio, 2003). Among ligand gated ion channels, the effect of lipid composition on receptor structure and function of nAChRs has attracted much attention

(Barrantes, 2002; Barrantes, 2004). Biochemical studies showed that a low protein/lipid ratio caused a loss of nAChR activity (Jones et al., 1988; Jones and McNamee, 1988). The conformational transitions between opening, closing and desensitization were significantly affected by lipid composition (Grassi et al., 1995; Lasalde et al., 1996; Barrantes, 2004). Effects of the lipid microenvironment on functional properties of the nAChR have been extensively examined by mutagenesis studies (Li et al., 1992; Ortiz-Miranda et al., 1997; Tamamizu et al., 2000; Santiago et al., 2001). Early studies on ion channels and other membrane proteins were mostly conducted in reconstituted systems, in which individual contribution of various types of lipids could be examined. Using ESR spectroscopy, it was found that the nAChR displayed specificity of interaction with spin-labeled neutral and anionic lipid molecules in native membranes (Mantipragada et al., 2003). nAChR reconstituted lipid vesicles containing only phosphatidylcholine (PC) displayed almost no activity (Ochoa et al., 1983; Criado et al., 1984; Fong and McNamee, 1986). Addition of cholesterol and anionic lipids such as phosphatidic acid (PA) and phosphatidyl serine (PS) restored its capacity to respond to agonists (Baenziger et al., 2000). The recovery of functionality of nAChR was attributed to the formation of a lipid bilayer with optimal fluidity and special requirement of PA and PS, which are critical for maintenance of normal receptor function (Bhushan and McNamee, 1993). However, controversy exists regarding the exact effect of distinct types of phosholipids on nAChR functionality. Using chemical labeling and radio-labeled ligand binding assays, it was proposed that anionic lipids were able to stabilize distinct functional states in nAChRs (McCarthy and Moore, 1992). nAChRs reconstituted in either egg PC/cholesterol or egg PC alone existed in a desensitized state (Ryan et al., 1996), whereas in either dioleoylphosphatidylcholine (DOPC)/dioleoylphosphatidic acid (DOPA) or DOPC alone, nAChRs adopted a resting conformation (Rankin et al., 1997; Raines

and Krishnan, 1998). In contrast, FTIR studies showed that neutral or anionic lipids in egg PC membranes is sufficient to maintain the functionality of nAChR (Baenziger et al., 2000). In addition, a variety of structurally diverse neutral and anionic lipids in DOPC membranes all showed an ability to maintain nAChR activity (Sunshine and McNamee, 1994). A recent study also proposed that the relatively low levels of PA or cholesterol in a reconstituted membrane could affect the equilibrium between distinct conformational states of nAChR (Baenziger et al., 2000). With increasing levels of PA or cholesterol in egg PC membrane, nAChRs displayed an enhanced ability to undergo a conformation transition from resting state to desensitized state (Ryan and Baenziger, 1999; Baenziger et al., 2000). Those influences on the equilibria between different conformational states of the nAChR were probably due to non-specific effects on some bulk property of the membrane since addition of other lipid molecules such as phosphatidyl serine (PS) and squalene in reconstituted egg PC membrane also affected nAChR conformational equilibria, and a mixture of other neural and anionic lipids could replace PA or cholesterol to maintain nAChR functionality (Sunshine and McNamee, 1994; Ryan et al., 1996).

From studies on nAChRs, it is obvious that lipid composition has a significant effect on receptor structure and function. Lipid composition is also expected to affect GlyR structure and function, given that GlyRs share similar structural folds and conserved mechanisms of channel activation and modulation with nAChR. In this study, we attempted to express a soluble extracellular domain of GlyR which might be suitable for high-resolution structural studies. However, GlyBP, an extracellular ligand binding domain mutant of GlyR with introduction of two hydrophilic loops and one hydrophilic tail postulated to be membrane-proximal in native full-length GlyR, still retains ability to bind to the membrane after subcellular fractionation. In addition, this membrane-association property helps proper folding of GlyBP as demonstrated by

the loss of functionality of GlyBP in the cytosolic fraction. This observation suggested that GlyBP is not completely separate from the plasma membrane or other proteins residing on the plasma membrane. From crystal structures of AChBP in complex with various ligands and other biochemical mutagenesis studies, it has been proposed that Loops 2, 7 and 9 are possible sites of contact with transmembrane domains or lipid bilayer in Cys-loop receptors (Brejc et al., 2001; Karlin, 2002; Unwin, 2005). Since the hydrophobic residues in Loop 7 and 9 were mutated to hydrophilic ones, it is anticipated that Loop 2 and other additional sequences might be involved in membrane association. Membrane-association of this GlyR ECD mutant also indicated that lipid-protein interaction is critical for proper folding of GlyR. In this study, we reconstituted GlyBP in lipid vesicles containing egg PC, a major component of native lipid bilayer. However, as discussed above, lipid composition plays a significant role in maintenance of receptor functionality. Thus, it would be interesting to examine what effects addition of other lipid molecules with distinct biophysical properties would have on protein folding and ligand binding properties of GlyBP or wild type GlyR ECD if either of them could be successfully overexpressed in a suitable expressional system.

6.4   FUTURE DIRECTIONS

6.4.1   High resolution structural studies on GlyBP

The best way to examine the structure of the ECD of GlyR at high resolution would be to obtain its structure using X-ray crystallography. Since the protein yield of GlyBP expressed in Sf9 insect cells is moderate (~1.0-2.0 mg/L cell culture), it is possible to conduct crystallization trials

on GlyBP and these efforts are currently under way in the laboratory. However, problems exist regarding crystallization of GlyBP: 1) Conditions that are best for solubilization and purification might not be the best ones for crystallization. In order to successfully crystallize GlyBP, it is necessary to conduct a number of preliminary experiments to obtain the best buffering conditions for crystallization of GlyBP. 2) Protein heterogeneity. GlyBP appears to migrate on SDS-PAGE of GlyBP as a doublet. Although other studies suggest that this does not necessarily mean heterogeneity of GlyBP, further analysis will be required to confirm the homogeneity of GlyBP, which would be the key factor that determines if a good crystal can be obtained. Otherwise, further purification procedure will be conducted to produce a more homogenous GlyBP. 3) Since GlyBP retained membrane-association properties, it's possible that the presence of detergent and/or lipids might help crystallization of GlyBP. However, the presence of any type of detergent and/or lipids would make crystal growth more difficult.

6.4.2   Dynamics of GlyBP

In parallel with crystallization trial studies, further biochemical and biophysical studies would be helpful to further understanding of the dynamic nature of GlyBP. The more information we obtain about its dynamic structure, the more chance we would gain success on crystallization since better crystallization conditions would be designed based on our understanding of its other structural features.

Our crosslinking studies in combination with mass spectrometry provided a significant number of distance constraints in GlyBP, which helped us to generate a structural model on the ECD of GlyR. All those crosslinks obtained fit well with a structural model of GlyBP built in collaboration with Dr. M. Kurnikova at CMU. However, limited dynamic structural information

has been obtained since incubation with strychnine did not yield detectable conformational changes as demonstrated by the crosslinking data. This might be due to the low resolution of chemical crosslinking with respect to stuctural determination of this complex receptor. Another reason is that the locations of lysine residues studied are not optimized to probe conformational changes upon ligand binding. Thus, in order to study the dynamic nature of GlyBP in greater detail, introduction of lysine (or other chemical moieties) mutants at specific sites might be required. As suggested in the structural models of GlyR ECD and the ECDs of other Cys-loop receptor using AChBPs as templates, the C-loop region is proposed to be highly flexible and undergoes putatively significant conformational changes upon ligand binding. In our crosslinking studies, changes in the distances between K193 and the neighbouring K200 or K206 cold not be detected upong strychnine binding. Given the relatively long distance between K193 and K200/K206 in the neighboring subunit, those two pairs are not the best ones for examination of conformational changes upon ligand binding. Therefore, new pairs of lysine residues could be introduced in the tip of the C-loop and the neighboring β1, β2 or β5. Chemical crosslinking studies on GlyBP with those newly introduced lysine pairs would provide insight into how the C-loop contributes to global conformational changes in the GlyR ECD upon ligand binding. Simiarly, Lys-Lys or even Cys-Lys pairs located in other important sites in the GlyR ECD could also be introduced and subsequent analysis by chemical crosslinking would provide more detailed dynamic information about the structure of GlyR ECD. In addition, only one crosslinker was used in this study, which might limit the power of crosslinking to assess protein structure. Crosslinker with different arm lengths could provide more accurate distance constraints for GlyBP.

In our LRET studies, we examined the intersubunit Cys-41 distances and found that those distances were changed upon agonist binding, indicating conformational changes in GlyBP upon ligand binding. However, those distance changes were subtle and Cys-41 might not be located in a region which undergoes dramatic changes upon agonist binding. Therefore, systematic introduction of Cys mutations at other specific sites might be helpful to further understand the assembly state, ligand-receptor interaction, and more detailed three dimensional structures.

In addition, in our preliminary LRET study, when strychnine was applied to GlyR-infected Sf9 cells, the inter-subunit Cys-41 distances were exactly the same as those obtained from the apo state GlyR. Currently, the mechanism of strychnine inhibition is unknown, but our results suggest that the strychnine binds to GlyR in a resting state and the antagonism of strychnine is due to stabilization of the resting state of the receptor. Further studies wherein single cysteine mutants are systematically introduced to GlyR in intact Sf9 insect cells and subjected to LRET studies will provide insight into detailed molecular mechanisms of channel gating.

BIBLIOGRAPHY

Absalom NL, Lewis TM, Kaplan W, Pierce KD, Schofield PR (2003) Role of Charged Residues in Coupling Ligand Binding and Channel Activation in the Extracellular Domain of the Glycine Receptor. J Biol Chem 278:50151-50157.

Agopyan N, Tokutomi N, Akaike N (1993) Protein kinase A-mediated phosphorylation reduces only the fast desensitizing glycine current in acutely dissociated ventromedial hypothalamic neurons. Neuroscience 56:605-615.

Aguayo LG, van Zundert B, Tapia JC, Carrasco MA, Alvarez FJ (2004) Changes on the properties of glycine receptors during neuronal development. Brain Research Reviews Chemical and Electrical Synapses 47:33-45.

Akagi H, Hirai K, Hishinuma F (1991) Cloning of a glycine receptor subtype expressed in rat brain and spinal cord during a specific period of neuronal development. FEBS Letters 281:160-166.

Akaike N, Kaneda M (1989) Glycine-gated chloride current in acutely isolated rat hypothalamic neurons. J Neurophysiol 62:1400-1409.

Alexeev T, Krivoshein A, Shevalier A, Kudelina I, Telyakova O, Vincent A, Utkin Y, Hucho F, Tsetlin V (1999) Physicochemical and immunological studies of the N-terminal domain of the Torpedo acetylcholine receptor alpha-subunit expressed in Escherichia coli. European Journal of Biochemistry 259:310-319.

Amin J, Dickerson I, Weiss D (1994) The agonist binding site of the gamma-aminobutyric acid type A channel is not formed by the extracellular cysteine loop. Mol Pharmacol 45:317-323.

Amin J, Brooks-Kayal A, Weiss DS (1997) Two tyrosine residues on the alpha subunit are crucial for benzodiazepine binding and allosteric modulation of gamma-aminobutyric acidA receptors. Mol Pharmacol 51:833-841.

Aprison MH, Werman R (1965) The distribution of glycine in cat spinal cord and roots. Life Sciences 4:2075-2083.

Araki T, Yamano M, Murakami T, Wanaka A, Betz H, Tohyama M (1988) Localization of glycine receptors in the rat central nervous system: an immunocytochemical analysis using monoclonal antibody. Neuroscience 25:613-624.

Araque A, Parpura V, Sanzgiri RP, Haydon PG (1999) Tripartite synapses: glia, the unacknowledged partner. Trends Neurosci 22:208-215.

Armstrong N, Gouaux E (2000) Mechanisms for Activation and Antagonism of an AMPA-Sensitive Glutamate Receptor: Crystal Structures of the GluR2 Ligand Binding Core. Neuron 28:165-181.

Auld DS, Robitaille R (2003) Glial cells and neurotransmission: an inclusive view of synaptic function. Neuron 40:389-400.

Avramopoulou V, Mamalaki A, Tzartos SJ (2004) Soluble, oligomeric, and ligand-binding extracellular domain of the human alpha7 acetylcholine receptor expressed in yeast: replacement of the hydrophobic cysteine loop by the hydrophilic loop of the ACh-binding protein enhances protein solubility. J Biol Chem 279:38287-38293.

Back JW, de Jong L, Muijsers AO, de Koster CG (2003) Chemical Cross-linking and Mass Spectrometry for Protein Structural Modeling. Journal of Molecular Biology 331:303-313.

Baenziger JE, Morris M-L, Darsaut TE, Ryan SE (2000) Effect of Membrane Lipid Composition on the Conformational Equilibria of the Nicotinic Acetylcholine Receptor. J Biol Chem 275:777-784.

Baer K, Waldvogel HJ, During MJ, Snell RG, Faull RL, Rees MI (2003) Association of gephyrin and glycine receptors in the human brainstem and spinal cord: an immunohistochemical analysis. Neuroscience 122:773-784.

Barker JL, Ransom BR (1978) Pentobarbitone pharmacology of mammalian central neurones grown in tissue culture. J Physiol 280:355-372.

Barrantes FJ (2002) Lipid matters: nicotinic acetylcholine receptor-lipid interactions (Review). Molecular Membrane Biology 19:277 - 284.

Barrantes FJ (2004) Structural basis for lipid modulation of nicotinic acetylcholine receptor function. Brain Research Reviews

Chemical and Electrical Synapses 47:71-95.

Barry PH, Lynch JW (2005) Ligand-gated channels. IEEE Trans Nanobioscience 4:70-80.

Bauer PI, Buki KG, Hakam A, Kun E (1990) Macromolecular association of ADP-ribosyltransferase and its correlation with enzymic activity. Biochem J 270:17-26.

Bennett MVL, Zukin RS (2004) Electrical Coupling and Neuronal Synchronization in the Mammalian Brain. Neuron 41:495-511.

Bhushan A, McNamee MG (1993) Correlation of phospholipid structure with functional effects on the nicotinic acetylcholine receptor. A modulatory role for phosphatidic acid. Biophys J 64:716-723.

Biemann K (1995) The coming of age of mass spectrometry in peptide and protein chemistry. Protein Sci 4:1920-1927.

Blair LA, Levitan ES, Marshall J, Dionne VE, Barnard EA (1988) Single subunits of the GABAA receptor form ion channels with properties of the native receptor. Science 242:577-579.

Bloom FE, Iversen LL (1971) Localizing 3H-GABA in Nerve Terminals of Rat Cerebral Cortex by Electron Microscopic Autoradiography. 229:628-630.

Boehm S, Harvey RJ, Hoist A, Rohrer H, Betz H (1997) Glycine Receptors in Cultured Chick Sympathetic Neurons are Excitatory and Trigger Neurotransmitter Release. The Journal of Physiology 504:683-694.

Bonnert TP, McKernan RM, Farrar S, le Bourdelles B, Heavens RP, Smith DW, Hewson L, Rigby MR, Sirinathsinghji DJS, Brown N, Wafford KA, Whiting PJ (1999) Theta , a novel gamma -aminobutyric acid type A receptor subunit. Proc Natl Acad Sci U S A 96:9891-9896.

Bormann J, Hamill OP, Sakmann B (1987) Mechanism of anion permeation through channels gated by glycine and gamma-aminobutyric acid in mouse cultured spinal neurones. J Physiol 385:243-286.

Bormann J, Rundstrom N, Betz H, Langosch D (1993) Residues within transmembrane segment M2 determine chloride conductance of glycine receptor homo- and hetero-oligomers. Embo J 12:3729-3737.

Bourne Y, Talley TT, Hansen SB, Taylor P, Marchot P (2005) Crystal structure of a Cbtx-AChBP complex reveals essential interactions between snake alpha-neurotoxins and nicotinic receptors. Embo J 24:1512-1522.

Bourque MJ, Robitaille R (1998) Endogenous peptidergic modulation of perisynaptic Schwann cells at the frog neuromuscular junction. J Physiol 512 (Pt 1):197-209.

Bouzat C, Gumilar F, Spitzmaul G, Wang H-L, Rayes D, Hansen SB, Taylor P, Sine SM (2004) Coupling of agonist binding to channel gating in an ACh-binding protein linked to an ion channel. 430:896-900.

Breitinger HG, Becker CM (2002) The inhibitory glycine receptor-simple views of a complicated channel. Chembiochem 3:1042-1052.

Breitinger HG, Villmann C, Becker K, Becker CM (2001) Opposing effects of molecular volume and charge at the hyperekplexia site alpha 1(P250) govern glycine receptor activation and desensitization. J Biol Chem 276:29657-29663.

Breitinger U, Breitinger HG, Bauer F, Fahmy K, Glockenhammer D, Becker CM (2004) Conserved high affinity ligand binding and membrane association in the native and refolded extracellular domain of the human glycine receptor alpha1-subunit. J Biol Chem 279:1627-1636.

Brejc K, van Dijk WJ, Smit AB, Sixma TK (2002) The 2.7 A structure of AChBP, homologue of the ligand-binding domain of the nicotinic acetylcholine receptor. Novartis Found Symp 245:22-29; discussion 29-32, 165-168.

Brejc K, van Dijk WJ, Klaassen RV, Schuurmans M, van Der Oost J, Smit AB, Sixma TK (2001) Crystal structure of an ACh-binding protein reveals the ligand-binding domain of nicotinic receptors. Nature 411:269-276.

Brune W, Weber RG, Saul B, von Knebel Doeberitz M, Grond-Ginsbach C, Kellerman K, Meinck HM, Becker CM (1996) A GLRA1 null mutation in recessive hyperekplexia challenges the functional role of glycine receptors. Am J Hum Genet 58:989-997.

Burmeister WP, Gastinel LN, Simister NE, Blum ML, Bjorkman PJ (1994) Crystal structure at 2.2 A resolution of the MHC-related neonatal Fc receptor. 372:336-343.

Campagna-Slater V, Weaver DF (2007) Molecular modelling of the GABAA ion channel protein. J Mol Graph Model 25:721-730.

Cascio M, Schoppa NE, Grodzicki RL, Sigworth FJ, Fox RO (1993) Functional expression and purification of a homomeric human alpha 1 glycine receptor in baculovirus-infected insect cells. J Biol Chem 268:22135-22142.

Cascio M, Shenkel S, Grodzicki RL, Sigworth FJ, Fox RO (2001) Functional reconstitution and characterization of recombinant human alpha 1-glycine receptors. J Biol Chem 276:20981-20988.

Castonguay A, Robitaille R (2001) Differential regulation of transmitter release by presynaptic and glial Ca2+ internal stores at the neuromuscular synapse. J Neurosci 21:1911-1922.

Celie PH, van Rossum-Fikkert SE, van Dijk WJ, Brejc K, Smit AB, Sixma TK (2004) Nicotine and carbamylcholine binding to nicotinic acetylcholine receptors as studied in AChBP crystal structures. Neuron 41:907-914.

Celie PH, Klaassen RV, van Rossum-Fikkert SE, van Elk R, van Nierop P, Smit AB, Sixma TK (2005a) Crystal structure of acetylcholine-binding protein from Bulinus truncatus reveals

the conserved structural scaffold and sites of variation in nicotinic acetylcholine receptors. J Biol Chem 280:26457-26466.

Celie PH, Kasheverov IE, Mordvintsev DY, Hogg RC, van Nierop P, van Elk R, van Rossum-Fikkert SE, Zhmak MN, Bertrand D, Tsetlin V, Sixma TK, Smit AB (2005b) Crystal structure of nicotinic acetylcholine receptor homolog AChBP in complex with an alpha-conotoxin PnIA variant. Nat Struct Mol Biol 12:582-588.

Chakrapani S, Bailey TD, Auerbach A (2004) Gating Dynamics of the Acetylcholine Receptor Extracellular Domain. J Gen Physiol 123:341-356.

Chameau P, van Hooft JA (2006) Serotonin 5-HT(3) receptors in the central nervous system. Cell Tissue Res 326:573-581.

Changeux JP, Kasai M, Lee CY (1970) Use of a snake venom toxin to characterize the cholinergic receptor protein. Proc Natl Acad Sci U S A 67:1241-1247.

Cheng X, Lu B, Grant B, Law RJ, McCammon JA (2006a) Channel opening motion of alpha7 nicotinic acetylcholine receptor as suggested by normal mode analysis. J Mol Biol 355:310-324.

Cheng X, Wang H, Grant B, Sine SM, McCammon JA (2006b) Targeted molecular dynamics study of C-loop closure and channel gating in nicotinic receptors. PLoS Comput Biol 2:e134.

Cheng Y, Prusoff WH (1973) Relationship between the inhibition constant (K1) and the concentration of inhibitor which causes 50 per cent inhibition (I50) of an enzymatic reaction. Biochem Pharmacol 22:3099-3108.

Chiara DC, Middleton RE, Cohen JB (1998) Identification of tryptophan 55 as the primary site of [3H]nicotine photoincorporation in the [gamma]-subunit of the Torpedo nicotinic acetylcholine receptor. FEBS Letters 423:223-226.

Chiara DC, Xie Y, Cohen JB (1999) Structure of the Agonist-Binding Sites of the Torpedo Nicotinic Acetylcholine Receptor: Affinity-Labeling and Mutational Analyses Identify gamma-Tyr-111/delta-Arg-113 as Antagonist Affinity Determinants. Biochemistry 38:6689-6698.

Clegg RM (1992) Fluorescence resonance energy transfer and nucleic acids. Methods Enzymol 211:353-388.

Cline H (2005) Synaptogenesis: a balancing act between excitation and inhibition. Curr Biol 15:R203-205.

Colomar A, Robitaille R (2004) Glial modulation of synaptic transmission at the neuromuscular junction. Glia 47:284-289.

Connolly CN, Wafford KA (2004) The Cys-loop superfamily of ligand-gated ion channels: the impact of receptor structure on function. Biochem Soc Trans 32:529-534.

Connors BW, Long MA (2004) Electrical synapses in the mammalian brain. Annual Review of Neuroscience 27:393-418.

Corringer PJ, Le Novere N, Changeux JP (2000) Nicotinic receptors at the amino acid level. Annu Rev Pharmacol Toxicol 40:431-458.

Corringer PJ, Galzi JL, Eisele JL, Bertrand S, Changeux JP, Bertrand D (1995) Identification of a new component of the agonist binding site of the nicotinic alpha 7 homooligomeric receptor. J Biol Chem 270:11749-11752.

Costa V, Nistri A, Cavalli A, Carloni P (2003) A structural model of agonist binding to the alpha3beta4 neuronal nicotinic receptor. Br J Pharmacol 140:921-931.

Costall B, Naylor RJ (2004) 5-HT3 receptors. Curr Drug Targets CNS Neurol Disord 3:27-37.

146

Couturier S, Bertrand D, Matter JM, Hernandez MC, Bertrand S, Millar N, Valera S, Barkas T, Ballivet M (1990) A neuronal nicotinic acetylcholine receptor subunit (alpha 7) is developmentally regulated and forms a homo-oligomeric channel blocked by alpha-BTX. Neuron 5:847-856.

Criado M, Eibl H, Barrantes F (1984) Functional properties of the acetylcholine receptor incorporated in model lipid membranes. Differential effects of chain length and head group of phospholipids on receptor affinity states and receptor- mediated ion translocation. J Biol Chem 259:9188-9198.

Cromer BA, Morton CJ, Parker MW (2002) Anxiety over GABA(A) receptor structure relieved by AChBP. Trends Biochem Sci 27:280-287.

Curtis DR, Watkins JC (1960) The excitation and depression of spinal neurones by structurally related amino acids. Journal of Neurochemistry 6:117-141.

Czajkowski C, Kaufmann C, Karlin A (1993) Negatively charged amino acid residues in the nicotinic receptor delta subunit that contribute to the binding of acetylcholine. Proc Natl Acad Sci U S A 90:6285-6289.

Davies PA, Pistis M, Hanna MC, Peters JA, Lambert JJ, Hales TG, Kirkness EF (1999) The 5-HT3B subunit is a major determinant of serotonin-receptor function. 397:359-363.

De Saint Jan D, David-Watine B, Korn H, Bregestovski P (2001) Activation of human {alpha}1 and {alpha}2 homomeric glycine receptors by taurine and GABA. J Physiol 535:741-755.

de Vos A, Ultsch M, Kossiakoff A (1992) Human growth hormone and extracellular domain of its receptor: crystal structure of the complex. Science 255:306-312.

Deane CM, Lummis SCR (2001) The Role and Predicted Propensity of Conserved Proline Residues in the 5-HT3 Receptor. J Biol Chem 276:37962-37966.

del Giudice EM, Coppola G, Bellini G, Cirillo G, Scuccimarra G, Pascotto A (2001) A mutation (V260M) in the middle of the M2 pore-lining domain of the glycine receptor causes hereditary hyperekplexia. Eur J Hum Genet 9:873-876.

Deleuze C, Runquist M, Orcel H, Rabie A, Dayanithi G, Alonso G, Hussy N (2005) Structural difference between heteromeric somatic and homomeric axonal glycine receptors in the hypothalamo-neurohypophysial system. Neuroscience 135:475-483.

Dellisanti CD, Yao Y, Stroud JC, Wang ZZ, Chen L (2007) Crystal structure of the extracellular domain of nAChR alpha1 bound to alpha-bungarotoxin at 1.94 A resolution. Nat Neurosci.

Dennis M, Giraudat J, Kotzyba-Hibert F, Goeldner M, Hirth C, Chang JY, Lazure C, Chretien M, Changeux JP (1988) Amino acids of the Torpedo marmorata acetylcholine receptor alpha subunit labeled by a photoaffinity ligand for the acetylcholine binding site. Biochemistry 27:2346-2357.

Dihazi GH, Sinz A (2003) Mapping low-resolution three-dimensional protein structures using chemical cross-linking and Fourier transform ion-cyclotron resonance mass spectrometry. Rapid Commun Mass Spectrom 17:2005-2014.

Doyle DA (2004) Structural changes during ion channel gating. Trends in Neurosciences 27:298-302.

Drew CA, Johnston GAR (1992) Bicuculline- and Baclofen-Insensitive Gamma-Aminobutyric Acid Binding to Rat Cerebellar Membranes. Journal of Neurochemistry 58:1087-1092.

Du M, Reid SA, Jayaraman V (2005) Conformational changes in the ligand-binding domain of a functional ionotropic glutamate receptor. J Biol Chem 280:8633-8636.

Dubin AE, Huvar R, D'Andrea MR, Pyati J, Zhu JY, Joy KC, Wilson SJ, Galindo JE, Glass CA, Luo L, Jackson MR, Lovenberg TW, Erlander MG (1999) The pharmacological and functional characteristics of the serotonin 5-HT(3A) receptor are specifically modified by a 5-HT(3B) receptor subunit. J Biol Chem 274:30799-30810.

Ehlert F (1988) Estimation of the affinities of allosteric ligands using radioligand binding and pharmacological null methods. Mol Pharmacol 33:187-194.

Elgoyhen AB, Johnson DS, Boulter J, Vetter DE, Heinemann S (1994) Alpha 9: an acetylcholine receptor with novel pharmacological properties expressed in rat cochlear hair cells. Cell 79:705-715.

Elmslie F, Hutchings S, Spencer V, Curtis A, Covanis T, Gardiner R, Rees M (1996) Analysis of GLRA1 in hereditary and sporadic hyperekplexia: a novel mutation in a family cosegregating for hyperekplexia and spastic paraparesis. J Med Genet 33:435-436.

Enz R, Cutting GR (1998) Molecular composition of GABAC receptors. Vision Research 38:1431-1441.

Ernst M, Bruckner S, Boresch S, Sieghart W (2005) Comparative Models of GABAA Receptor Extracellular and Transmembrane Domains: Important Insights in Pharmacology and Function. Mol Pharmacol 68:1291-1300.

Faber DS, Kaars C, Zottoli SJ (1980) Dual transmission at morphologically mixed synapses: evidence from postsynaptic cobalt injections. Neuroscience 5:433-440.

Fatima-Shad K, Barry PH (1992) A patch-clamp study of GABA- and strychnine-sensitive glycine-activated currents in post-natal tissue-cultured hippocampal neurons. Proc Biol Sci 250:99-105.

Fatima-Shad K, Barry PH (1993) Anion permeation in GABA- and glycine-gated channels of mammalian cultured hippocampal neurons. Proc Biol Sci 253:69-75.

Feng G, Tintrup H, Kirsch J, Nichol MC, Kuhse J, Betz H, Sanes JR (1998) Dual requirement for gephyrin in glycine receptor clustering and molybdoenzyme activity. Science 282:1321-1324.

Fischer M, Corringer P-J, Schott K, Bacher A, Changeux J-P (2001) A method for soluble overexpression of the alpha 7 nicotinic acetylcholine receptor extracellular domain. Proc Natl Acad Sci 98:3567-3570.

Flint AC, Liu X, Kriegstein AR (1998) Nonsynaptic Glycine Receptor Activation during Early Neocortical Development. Neuron 20:43-53.

Fong TM, McNamee MG (1986) Correlation between acetylcholine receptor function and structural properties of membranes. Biochemistry 25:830-840.

Fujita M, Sato K, Sato M, Inoue T, Kozuka T, Tohyama M (1991) Regional distribution of the cells expressing glycine receptor [beta] subunit mRNA in the rat brain. Brain Research 560:23-37.

Galzi JL, Revah F, Black D, Goeldner M, Hirth C, Changeux JP (1990) Identification of a novel amino acid alpha-tyrosine 93 within the cholinergic ligands-binding sites of the acetylcholine receptor by photoaffinity labeling. Additional evidence for a three-loop model of the cholinergic ligands-binding sites. J Biol Chem 265:10430-10437.

Gao F, Bren N, Burghardt TP, Hansen S, Henchman RH, Taylor P, McCammon JA, Sine SM (2004) Agonist-mediated conformational changes in ACh-binding protein revealed by simulation and intrinsic tryptophan fluorescence. J Biol Chem.

Garboczi DN, Ghosh P, Utz U, Fan QR, Biddison WE, Wiley DC (1996) Structure of the complex between human T-cell receptor, viral peptide and HLA-A2. 384:134-141.

Garcia KC, Degano M, Stanfield RL, Brunmark A, Jackson MR, Peterson PA, Teyton L, Wilson IA (1996) An alpha beta T Cell Receptor Structure at 2.5 A and Its Orientation in the TCR-MHC Complex. Science 274:209-219.

Gentet LJ, Clements JD (2002) Binding site stoichiometry and the effects of phosphorylation on human alpha1 homomeric glycine receptors. J Physiol 544:97-106.

Gerzanich V, Anand R, Lindstrom J (1994) Homomers of alpha 8 and alpha 7 subunits of nicotinic receptors exhibit similar channel but contrasting binding site properties. Mol Pharmacol 45:212-220.

Gill CH, Peters JA, Lambert JJ (1995) An electrophysiological investigation of the properties of a murine recombinant 5-HT3 receptor stably expressed in HEK 293 cells. Br J Pharmacol 114:1211-1221.

Graham D, Pfeiffer F, Betz H (1983) Photoaffinity-Labelling of the Glycine Receptor of Rat Spinal Cord. European Journal of Biochemistry 131:519-525.

Graham D, Pfeiffer F, Simler R, Betz H (1985) Purification and characterization of the glycine receptor of pig spinal cord. Biochemistry 24:990-994.

Grassi F, Palma E, Mileo AM, Eusebi F (1995) The desensitization of the embryonic mouse muscle acetylcholine receptor depends on the cellular environment. Pflugers Arch 430:787-794.

Grenningloh G, Pribilla I, Prior P, Multhaup G, Beyreuther K, Taleb O, Betz H (1990) Cloning and expression of the 58 kd [beta] subunit of the inhibitory glycine receptor. Neuron 4:963-970.

Grenningloh G, Rienitz A, Schmitt B, Methfessel C, Zensen M, Beyreuther K, Gundelfinger ED, Betz H (1987) The strychnine-binding subunit of the glycine receptor shows homology with nicotinic acetylcholine receptors. 328:215-220.

Griffon N, Buttner C, Nicke A, Kuhse J, Schmalzing G, Betz H (1999) Molecular determinants of glycine receptor subunit assembly. Embo J 18:4711-4721.

Grosman C, Salamone FN, Sine SM, Auerbach A (2000) The extracellular linker of muscle acetylcholine receptor channels is a gating control element. Journal of General Physiology 116:327-339.

Grudzinska J, Schemm R, Haeger S, Nicke A, Schmalzing G, Betz H, Laube B (2005) The beta subunit determines the ligand binding properties of synaptic glycine receptors. Neuron 45:727-739.

Grutter T, Changeux JP (2001) Nicotinic receptors in wonderland. Trends Biochem Sci 26:459-463.

Grutter T, Prado de Carvalho L, Virginie D, Taly A, Fischer M, Changeux JP (2005) A chimera encoding the fusion of an acetylcholine-binding protein to an ion channel is stabilized in a state close to the desensitized form of ligand-gated ion channels. C R Biol 328:223-234.

Han NL, Haddrill JL, Lynch JW (2001) Characterization of a glycine receptor domain that controls the binding and gating mechanisms of the beta-amino acid agonist, taurine. J Neurochem 79:636-647.

Hansen SB, Talley TT, Radic Z, Taylor P (2004) Structural and ligand recognition characteristics of an acetylcholine-binding protein from Aplysia californica. J Biol Chem 279:24197-24202.

Hansen SB, Sulzenbacher G, Huxford T, Marchot P, Taylor P, Bourne Y (2005) Structures of Aplysia AChBP complexes with nicotinic agonists and antagonists reveal distinctive binding interfaces and conformations. Embo J 24:3635-3646.

Hansen SB, Sulzenbacher G, Huxford T, Marchot P, Bourne Y, Taylor P (2006) Structural characterization of agonist and antagonist-bound acetylcholine-binding protein from Aplysia californica. J Mol Neurosci 30:101-102.

Hansen SB, Radic Z, Talley TT, Molles BE, Deerinck T, Tsigelny I, Taylor P (2002) Tryptophan fluorescence reveals conformational changes in the acetylcholine binding protein. J Biol Chem 277:41299-41302.

Harrison NJ, Lummis SC (2006) Molecular modeling of the GABA(C) receptor ligand-binding domain. J Mol Model 12:317-324.

Harvey RJ, Schmieden V, von Holst A, Laube B, Rohrer H, Betz H (2000) Glycine receptors containing the alpha4 subunit in the embryonic sympathetic nervous system, spinal cord and male genital ridge. European Journal of Neuroscience 12:994-1001.

Haydon PG (2001) GLIA: listening and talking to the synapse. Nat Rev Neurosci 2:185-193.

Heyduk T, Heyduk E (2001) Luminescence energy transfer with lanthanide chelates: interpretation of sensitized acceptor decay amplitudes. Anal Biochem 289:60-67.

Hoch W, Betz H, Becker CM (1989) Primary cultures of mouse spinal cord express the neonatal isoform of the inhibitory glycine receptor. Neuron 3:339-348.

Hogg RC, Bertrand D (2007) Partial agonists as therapeutic agents at neuronal nicotinic acetylcholine receptors. Biochemical Pharmacology 73:459-468.

Hogg RC, Raggenbass M, Bertrand D (2003) Nicotinic acetylcholine receptors: from structure to brain function. Rev Physiol Biochem Pharmacol 147:1-46.

Hopkin JM, Neal MJ (1970) Thr release of 14C-glycine from electrically stimulated rat spinal cord slices. Br J Pharmacol 40:136P-138P.

Hormuzdi SG, Filippov MA, Mitropoulou G, Monyer H, Bruzzone R (2004) Electrical synapses: a dynamic signaling system that shapes the activity of neuronal networks. Biochimica et Biophysica Acta (BBA) - Biomembranes
The Connexins 1662:113-137.

Humeny A, Bonk T, Becker K, Jafari-Boroujerdi M, Stephani U, Reuter K, Becker CM (2002) A novel recessive hyperekplexia allele GLRA1 (S231R): genotyping by MALDI-TOF mass spectrometry and functional characterisation as a determinant of cellular glycine receptor trafficking. Eur J Hum Genet 10:188-196.

Humphrey W, Dalke A, Schulten K (1996) VMD: visual molecular dynamics. J Mol Graph 14:33-38, 27-38.

Hussy N, Lukas W, Jones KA (1994) Functional properties of a cloned 5-hydroxytryptamine ionotropic receptor subunit: comparison with native mouse receptors. J Physiol 481 (Pt 2):311-323.

Jahromi BS, Robitaille R, Charlton MP (1992) Transmitter release increases intracellular calcium in perisynaptic Schwann cells in situ. Neuron 8:1069-1077.

Jeong H-J, Jang I-S, Moorhouse AJ, Akaike N (2003) Activation of presynaptic glycine receptors facilitates glycine release from presynaptic terminals synapsing onto rat spinal sacral dorsal commissural nucleus neurons. J Physiol 550:373-383.

Jin P, Walther D, Zhang J, Rowe-Teeter C, Fu GK (2004) Serine 171, a Conserved Residue in the {gamma}-Aminobutyric Acid Type A (GABAA) Receptor {gamma}2 Subunit, Mediates Subunit Interaction and Cell Surface Localization. J Biol Chem 279:14179-14183.

Johnson JW, Ascher P (1987) Glycine potentiates the NMDA response in cultured mouse brain neurons. Nature 325:529-531.

Johnson MS, Overington JP (1993) A Structural Basis for Sequence Comparisons : An Evaluation of Scoring Methodologies. Journal of Molecular Biology 233:716-738.

Jones OT, McNamee MG (1988) Annular and nonannular binding sites for cholesterol associated with the nicotinic acetylcholine receptor. Biochemistry 27:2364-2374.

Jones OT, Eubanks JH, Earnest JP, McNamee MG (1988) A minimum number of lipids are required to support the functional properties of the nicotinic acetylcholine receptor. Biochemistry 27:3733-3742.

Kalamida D, Poulas K, Avramopoulou V, Fostieri E, Lagoumintzis G, Lazaridis K, Sideri A, Zouridakis M, Tzartos SJ (2007) Muscle and neuronal nicotinic acetylcholine receptors. Structure, function and pathogenicity. FEBS Journal 274:3799-3845.

Kandel ER, Schwartz JH, Jessell TM (2000) Principles of Neural Science, 4th Edition. New York: McGraw-Hill.

Kao P, Dwork A, Kaldany R, Silver M, Wideman J, Stein S, Karlin A (1984) Identification of the alpha subunit half-cystine specifically labeled by an affinity reagent for the acetylcholine receptor binding site. J Biol Chem 259:11662-11665.

Kao PN, Karlin A (1986) Acetylcholine receptor binding site contains a disulfide cross-link between adjacent half-cystinyl residues. J Biol Chem 261:8085-8088.

Karas M, Hillenkamp F (1988) Laser desorption ionization of proteins with molecular masses exceeding 10,000 daltons. Anal Chem 60:2299-2301.

Karlin A (2002) Emerging structure of the nicotinic acetylcholine receptors. Nat Rev Neurosci 3:102-114.

Karlin A, Akabas MH (1995) Toward a structural basis for the function of nicotinic acetylcholine receptors and their cousins. Neuron 15:1231-1244.

Karlin A, Akabas MH (1998) Substituted-cysteine accessibility method. Methods Enzymol 293:123-145.

Kawasaki BT, Hoffman KB, Yamamoto RS, Bahr BA (1997) Variants of the receptor/channel clustering molecule gephyrin in brain: distinct distribution patterns, developmental profiles, and proteolytic cleavage by calpain. J Neurosci Res 49:381-388.

Kiehm DJ, Ji TH (1977) Photochemical cross-linking of cell membranes. A test for natural and random collisional cross-links by millisecond cross-linking. J Biol Chem 252:8524-8531.

Kins S, Betz H, Kirsch J (2000) Collybistin, a newly identified brain-specific GEF, induces submembrane clustering of gephyrin. Nat Neurosci 3:22-29.

Kirsch J, Betz H (1995) The postsynaptic localization of the glycine receptor-associated protein gephyrin is regulated by the cytoskeleton. J Neurosci 15:4148-4156.

Kirsch J, Betz H (1998) Glycine-receptor activation is required for receptor clustering in spinal neurons. Nature 392:717-720.

Kirsch J, Kuhse J, Betz H (1995) Targeting of glycine receptor subunits to gephyrin-rich domains in transfected human embryonic kidney cells. Mol Cell Neurosci 6:450-461.

Kirsch J, Wolters I, Triller A, Betz H (1993) Gephyrin antisense oligonucleotides prevent glycine receptor clustering in spinal neurons. Nature 366:745-748.

Kirsch J, Langosch D, Prior P, Littauer UZ, Schmitt B, Betz H (1991) The 93-kDa glycine receptor-associated protein binds to tubulin. J Biol Chem 266:22242-22245.

Klausberger T, Sarto I, Ehya N, Fuchs K, Furtmuller R, Mayer B, Huck S, Sieghart W (2001) Alternate use of distinct intersubunit contacts controls GABAA receptor assembly and stoichiometry. J Neurosci 21:9124-9133.

Kleckner NW, Dingledine R (1988) Requirement for glycine in activation of NMDA-receptors expressed in Xenopus oocytes. Science 241:835-837.

Kneussel M, Betz H (2000) Clustering of inhibitory neurotransmitter receptors at developing postsynaptic sites: the membrane activation model. Trends Neurosci 23:429-435.

Kneussel M, Hermann A, Kirsch J, Betz H (1999) Hydrophobic interactions mediate binding of the glycine receptor beta-subunit to gephyrin. J Neurochem 72:1323-1326.

Kostelidou K, Trakas N, Zouridakis M, Bitzopoulou K, Sotiriadis A, Gavra I, Tzartos SJ (2006) Expression and characterization of soluble forms of the extracellular domains of the the beta, gamma and epsilon subunits of the human muscle acetylcholine receptor. FEBS Journal 273:3557-3568.

Koulen P, Brandstatter JH, Enz R, Bormann J, Wassle H (1998) Synaptic clustering of GABA(C) receptor rho-subunits in the rat retina. Eur J Neurosci 10:115-127.

Kriegler S, Sudweeks S, Yakel JL (1999) The Nicotinic alpha 4 Receptor Subunit Contributes to the Lining of the Ion Channel Pore When Expressed with the 5-HT3 Receptor Subunit. J Biol Chem 274:3934-3936.

Krishtal OA, Osipchuk Yu V, Vrublevsky SV (1988) Properties of glycine-activated conductances in rat brain neurones. Neurosci Lett 84:271-276.

Kuhse J, Schmieden V, Betz H (1990a) Identification and functional expression of a novel ligand binding subunit of the inhibitory glycine receptor. J Biol Chem 265:22317-22320.

Kuhse J, Schmieden V, Betz H (1990b) A single amino acid exchange alters the pharmacology of neonatal rat glycine receptor subunit. Neuron 5:867-873.

Kuhse J, Betz H, Kirsch J (1995) The inhibitory glycine receptor: architecture, synaptic localization and molecular pathology of a postsynaptic ion-channel complex. Curr Opin Neurobiol 5:318-323.

Kuhse J, Laube B, Magalei D, Betz H (1993) Assembly of the inhibitory glycine receptor: identification of amino acid sequence motifs governing subunit stoichiometry. Neuron 11:1049-1056.

Kuhse J, Kuryatov A, Maulet Y, Malosio ML, Schmieden V, Betz H (1991) Alternative splicing generates two isoforms of the alpha 2 subunit of the inhibitory glycine receptor. FEBS Lett 283:73-77.

Langosch D, Thomas L, Betz H (1988) Conserved quaternary structure of ligand-gated ion channels: the postsynaptic glycine receptor is a pentamer. Proc Natl Acad Sci U S A 85:7394-7398.

Larson A, Beitz A (1988) Glycine potentiates strychnine-induced convulsions: role of NMDA receptors. J Neurosci 8:3822-3826.

Lasalde JA, Tamamizu S, Butler DH, Vibat CR, Hung B, McNamee MG (1996) Tryptophan substitutions at the lipid-exposed transmembrane segment M4 of Torpedo californica acetylcholine receptor govern channel gating. Biochemistry 35:14139-14148.

Laube B, Langosch D, Betz H, Schmieden V (1995) Hyperekplexia mutations of the glycine receptor unmask the inhibitory subsite for beta-amino-acids. Neuroreport 6:897-900.

Laube B, Maksay G, Schemm R, Betz H (2002) Modulation of glycine receptor function: a novel approach for therapeutic intervention at inhibitory synapses? Trends Pharmacol Sci 23:519-527.

Le Novere N, Grutter T, Changeux JP (2002) Models of the extracellular domain of the nicotinic receptors and of agonist- and Ca2+-binding sites. Proc Natl Acad Sci U S A 99:3210-3215.

152

Lees JG, Miles AJ, Wien F, Wallace BA (2006) A reference database for circular dichroism spectroscopy covering fold and secondary structure space. Bioinformatics 22:1955-1962.

Legendre P (1997) Pharmacological Evidence for Two Types of Postsynaptic Glycinergic Receptors on the Mauthner Cell of 52-h-Old Zebrafish Larvae. J Neurophysiol 77:2400-2415.

Legendre P (2001) The glycinergic inhibitory synapse. Cell Mol Life Sci 58:760-793.

Legendre P, Korn H (1994) Glycinergic Inhibitory Synaptic Currents and Related Receptor Channels in the Zebrafish Brain. European Journal of Neuroscience 6:1544-1557.

Legendre P, Muller E, Badiu CI, Meier J, Vannier C, Triller A (2002) Desensitization of Homomeric alpha 1 Glycine Receptor Increases with Receptor Density. Mol Pharmacol 62:817-827.

Leite JF, Cascio M (2001) Structure of ligand-gated ion channels: critical assessment of biochemical data supports novel topology. Mol Cell Neurosci 17:777-792.

Leite JF, Amoscato AA, Cascio M (2000) Coupled proteolytic and mass spectrometry studies indicate a novel topology for the glycine receptor. J Biol Chem 275:13683-13689.

Lester HA, Dibas MI, Dahan DS, Leite JF, Dougherty DA (2004) Cys-loop receptors: new twists and turns. Trends Neurosci 27:329-336.

Lewis TM, Sivilotti LG, Colquhoun D, Gardiner RM, Schoepfer R, Rees M (1998) Properties of human glycine receptors containing the hyperekplexia mutation alpha1(K276E), expressed in Xenopus oocytes. The Journal of Physiology 507:25-40.

Li L, Lee Y-H, Pappone P, Palma A, McNamee MG (1992) Site-specific mutations of nicotinic acetylcholine receptor at the lipid- protein interface dramatically alter ion channel gating. Biophysical Journal 62:61-63.

Liang FQ, Walline R, Earnest DJ (1998) Circadian rhythm of brain-derived neurotrophic factor in the rat suprachiasmatic nucleus. Neurosci Lett 242:89-92.

Lindstrom JM (2003) Nicotinic acetylcholine receptors of muscles and nerves: comparison of their structures, functional roles, and vulnerability to pathology. Ann N Y Acad Sci 998:41-52.

Llinas RR, Ribary U, Jeanmonod D, Kronberg E, Mitra PP (1999) Thalamocortical dysrhythmia: A neurological and neuropsychiatric syndrome characterized by magnetoencephalography. Proc Natl Acad Sci U S A 96:15222-15227.

Lobley A, Whitmore L, Wallace BA (2002) DICHROWEB: an interactive website for the analysis of protein secondary structure from circular dichroism spectra. Bioinformatics 18:211-212.

Luscher B, Keller CA (2004) Regulation of GABAA receptor trafficking, channel activity, and functional plasticity of inhibitory synapses. Pharmacology & Therapeutics 102:195-221.

Lynch JW (2004) Molecular structure and function of the glycine receptor chloride channel. Physiol Rev 84:1051-1095.

Lynch JW, Han N-LR, Haddrill J, Pierce KD, Schofield PR (2001) The Surface Accessibility of the Glycine Receptor M2-M3 Loop Is Increased in the Channel Open State. J Neurosci 21:2589-2599.

Lynch JW, Rajendra S, Pierce KD, Handford CA, Barry PH, Schofield PR (1997) Identification of intracellular and extracellular domains mediating signal transduction in the inhibitory glycine receptor chloride channel. Embo J 16:110-120.

Maksay G, Bikadi Z, Simonyi M (2003) Binding interactions of antagonists with 5-hydroxytryptamine3A receptor models. J Recept Signal Transduct Res 23:255-270.

Maksay G, Simonyi M, Bikadi Z (2004) Subunit rotation models activation of serotonin 5-HT3AB receptors by agonists. J Comput Aided Mol Des 18:651-664.

Malosio M, Grenningloh G, Kuhse J, Schmieden V, Schmitt B, Prior P, Betz H (1991a) Alternative splicing generates two variants of the alpha 1 subunit of the inhibitory glycine receptor. J Biol Chem 266:2048-2053.

Malosio ML, Marqueze-Pouey B, Kuhse J, Betz H (1991b) Widespread expression of glycine receptor subunit mRNAs in the adult and developing rat brain. Embo J 10:2401-2409.

Mammoto A, Sasaki T, Asakura T, Hotta I, Imamura H, Takahashi K, Matsuura Y, Shirao T, Takai Y (1998) Interactions of drebrin and gephyrin with profilin. Biochem Biophys Res Commun 243:86-89.

Mannuzzu LM, Moronne MM, Isacoff EY (1996) Direct physical measure of conformational rearrangement underlying potassium channel gating. Science 271:213-216.

Mantipragada SB, Horvath LI, Arias HR, Schwarzmann G, Sandhoff K, Barrantes FJ, Marsh D (2003) Lipid-Protein Interactions and Effect of Local Anesthetics in Acetylcholine Receptor-Rich Membranes from Torpedo marmorata Electric Organ. Biochemistry 42:9167-9175.

Mao D, Wallace BA (1984) Differential light scattering and absorption flattening optical effects are minimal in the circular dichroism spectra of small unilamellar vesicles. Biochemistry 23:2667-2673.

Mao D, Wachter E, Wallace BA (1982) Folding of the mitochondrial proton adenosinetriphosphatase proteolipid channel in phospholipid vesicles. Biochemistry 21:4960-4968.

Maricq AV, Peterson AS, Brake AJ, Myers RM, Julius D (1991) Primary structure and functional expression of the 5HT3 receptor, a serotonin-gated ion channel. Science 254:432-437.

Martin M, Czajkowski C, Karlin A (1996) The contributions of aspartyl residues in the acetylcholine receptor gamma and delta subunits to the binding of agonists and competitive antagonists. J Biol Chem 271:13497-13503.

Marti-Renom MA, Stuart AC, Fiser A, Sanchez R, Melo F, Sali A (2000) Comparative protein structure modeling of genes and genomes. Annu Rev Biophys Biomol Struct 29:291-325.

Martyn JA, White DA, Gronert GA, Jaffe RS, Ward JM (1992) Up-and-down regulation of skeletal muscle acetylcholine receptors. Effects on neuromuscular blockers. Anesthesiology 76:822-843.

Marvizon JC, Vazquez J, Garcia Calvo M, Mayor F, Jr., Ruiz Gomez A, Valdivieso F, Benavides J (1986) The glycine receptor: pharmacological studies and mathematical modeling of the allosteric interaction between the glycine- and strychnine-binding sites. Mol Pharmacol 30:590-597.

Matzenbach B, Maulet Y, Sefton L, Courtier B, Avner P, Guenet JL, Betz H (1994) Structural analysis of mouse glycine receptor alpha subunit genes. Identification and chromosomal localization of a novel variant. J Biol Chem 269:2607-2612.

McCarthy M, Moore M (1992) Effects of lipids and detergents on the conformation of the nicotinic acetylcholine receptor from Torpedo californica. J Biol Chem 267:7655-7663.

McLafferty FW, Fridriksson EK, Horn DM, Lewis MA, Zubarev RA (1999) BIOCHEMISTRY:Biomolecule Mass Spectrometry. Science 284:1289-1290.

Meyer G, Kirsch J, Betz H, Langosch D (1995) Identification of a gephyrin binding motif on the glycine receptor beta subunit. Neuron 15:563-572.

Michels G, Moss SJ (2007) GABA A Receptors: Properties and Trafficking. Critical Reviews in Biochemistry and Molecular Biology 42:3 - 14.

Middleton RE, Cohen JB (1991) Mapping of the acetylcholine binding site of the nicotinic acetylcholine receptor: [3H]nicotine as an agonist photoaffinity label. Biochemistry 30:6987-6997.

Mielke DL, Wallace BA (1988) Secondary structural analyses of the nicotinic acetylcholine receptor as a test of molecular models. J Biol Chem 263:3177-3182.

Mitterauer B (2000) Clock genes, feedback loops and their possible role in the etiology of bipolar disorders: an integrative model. Med Hypotheses 55:155-159.

Mitterauer B (2001) The loss of ego boundaries in schizophrenia: a neuromolecular hypothesis. Med Hypotheses 56:614-621.

Miyazawa A, Fujiyoshi Y, Unwin N (2003) Structure and gating mechanism of the acetylcholine receptor pore. Nature 423:949-955.

Miyazawa A, Fujiyoshi Y, Stowell M, Unwin N (1999) Nicotinic acetylcholine receptor at 4.6 A resolution: transverse tunnels in the channel. Journal of Molecular Biology 288:765-786.

Mody I, Pearce RA (2004) Diversity of inhibitory neurotransmission through GABAA receptors. Trends in Neurosciences 27:569-575.

Mohler H (2006) GABA-A Receptors in Central Nervous System Disease: Anxiety, Epilepsy, and Insomnia. Journal of Receptors and Signal Transduction 26:731 - 740.

Moorhouse AJ, Jacques P, Barry PH, Schofield PR (1999) The startle disease mutation Q266H, in the second transmembrane domain of the human glycine receptor, impairs channel gating. Mol Pharmacol 55:386-395.

Mori M, Gahwiler BH, Gerber U (2002) Beta-alanine and taurine as endogenous agonists at glycine receptors in rat hippocampus in vitro. J Physiol 539:191-200.

Morr J, Rundstrom N, Betz H, Langosch D, Schmitt B (1995) Baculovirus-driven expression and purification of glycine receptor alpha 1 homo-oligomers. FEBS Lett 368:495-499.

Moss SJ, Smart TG (2001) Constructing inhibitory synapses. Nat Rev Neurosci 2:240-250.

Ochoa ELM, Dalziel AW, McNamee MG (1983) Reconstitution of acetylcholine receptor function in lipid vesicles of defined composition. Biochimica et Biophysica Acta (BBA) - Biomembranes 727:151-162.

Oja SS, Saransaari P (1996) Kinetic analysis of taurine influx into cerebral cortical slices from adult and developing mice in different incubation conditions. Neurochem Res 21:161-166.

Oliet SH, Piet R, Poulain DA (2001) Control of glutamate clearance and synaptic efficacy by glial coverage of neurons. Science 292:923-926.

Opella SJ, Marassi FM, Gesell JJ, Valente AP, Kim Y, Oblatt-Montal M, Montal M (1999) Structures of the M2 channel-lining segments from nicotinic acetylcholine and NMDA receptors by NMR spectroscopy. 6:374-379.

Ortiz-Miranda SI, Lasalde JA, Pappone PA, McNamee MG (1997) Mutations in the M4 Domain of the Torpedo californica Nicotinic Acetylcholine Receptor Alter Channel Opening and Closing. Journal of Membrane Biology 158:17-30.

Pan Z-H, Zhang D, Zhang X, Lipton SA (2000) Evidence for coassembly of mutant GABAC rho-1;1 with GABAA gamma-2S, glycine alpha-1;1 and glycine alpha-2 receptor subunits in vitro. European Journal of Neuroscience 12:3137-3145.

Parri HR, Gould TM, Crunelli V (2001) Spontaneous astrocytic Ca2+ oscillations in situ drive NMDAR-mediated neuronal excitation. Nat Neurosci 4:803-812.

Parsons CG, Danysz W, Hesselink M, Hartmann S, Lorenz B, Wollenburg C, Quack G (1998) Modulation of NMDA receptors by glycine--introduction to some basic aspects and recent developments. Amino Acids 14:207-216.

Pedersen S, Cohen J (1990) d-Tubocurrarine Binding Sites are Located at {alpha}-gamma and {alpha}- delta Subunit Interfaces of the Nicotinic Acetylcholine Receptor. PNAS 87:2785-2789.

Peterson GL (1977) A simplification of the protein assay method of Lowry et al. which is more generally applicable. Anal Biochem 83:346-356.

Pfeiffer F, Betz H (1981) Solubilizticz of the glycine receptor from rat spinal cord. Brain Res 226:273-279.

Pfeiffer F, Graham D, Betz H (1982) Purification by affinity chromatography of the glycine receptor of rat spinal cord. J Biol Chem 257:9389-9393.

Pourcho RG (1996) Neurotransmitters in the retina. Curr Eye Res 15:797-803.

Pribilla I, Takagi T, Langosch D, Bormann J, Betz H (1992) The atypical M2 segment of the beta subunit confers picrotoxinin resistance to inhibitory glycine receptor channels. Embo J 11:4305-4311.

Prior P, Schmitt B, Grenningloh G, Pribilla I, Multhaup G, Beyreuther K, Maulet Y, Werner P, Langosch D, Kirsch J (1992) Primary structure and alternative splice variants of gephyrin, a putative glycine receptor-tubulin linker protein. Neuron 8:1161-1170.

Provencher SW, Glockner J (1981) Estimation of globular protein secondary structure from circular dichroism. Biochemistry 20:33-37.

Psaridi-Linardaki L, Mamalaki A, Remoundos M, Tzartos SJ (2002) Expression of soluble ligand- and antibody-binding extracellular domain of human muscle acetylcholine receptor alpha subunit in yeast Pichia pastoris. Role of glycosylation in alpha-bungarotoxin binding. J Biol Chem 277:26980-26986.

Raines DE, Krishnan NS (1998) Agonist binding and affinity state transitions in reconstituted nicotinic acetylcholine receptors revealed by single and sequential mixing stopped-flow fluorescence spectroscopies. Biochimica et Biophysica Acta (BBA) - Biomembranes 1374:83-93.

Rajendra S, Lynch JW, Schofield PR (1997) The glycine receptor. Pharmacol Ther 73:121-146.

Rajendra S, Lynch JW, Pierce KD, French CR, Barry PH, Schofield PR (1994) Startle disease mutations reduce the agonist sensitivity of the human inhibitory glycine receptor. J Biol Chem 269:18739-18742.

Rajendra S, Lynch JW, Pierce KD, French CR, Barry PH, Schofield PR (1995a) Mutation of an arginine residue in the human glycine receptor transforms [beta]-alanine and taurine from agonists into competitive antagonists. Neuron 14:169-175.

Rajendra S, Vandenberg RJ, Pierce KD, Cunningham AM, French PW, Barry PH, Schofield PR (1995b) The unique extracellular disulfide loop of the glycine receptor is a principal ligand binding element. Embo J 14:2987-2998.

Ramanoudjame G, Du M, Mankiewicz KA, Jayaraman V (2006) Allosteric mechanism in AMPA receptors: a FRET-based investigation of conformational changes. Proc Natl Acad Sci U S A 103:10473-10478.

Rankin SE, Addona GH, Kloczewiak MA, Bugge B, Miller KW (1997) The cholesterol dependence of activation and fast desensitization of the nicotinic acetylcholine receptor. Biophys J 73:2446-2455.

Rees MI, Andrew M, Jawad S, Owen MJ (1994) Evidence for recessive as well as dominant forms of startle disease (hyperekplexia) caused by mutations in the {alpha}1 subunit of the inhibitory glycine receptor. Hum Mol Genet 3:2175-2179.

Rees MI, Lewis TM, Kwok JB, Mortier GR, Govaert P, Snell RG, Schofield PR, Owen MJ (2002) Hyperekplexia associated with compound heterozygote mutations in the beta-subunit of the human inhibitory glycine receptor (GLRB). Hum Mol Genet 11:853-860.

Rees MI, Lewis TM, Vafa B, Ferrie C, Corry P, Muntoni F, Jungbluth H, Stephenson JB, Kerr M, Snell RG, Schofield PR, Owen MJ (2001) Compound heterozygosity and nonsense mutations in the alpha(1)-subunit of the inhibitory glycine receptor in hyperekplexia. Hum Genet 109:267-270.

Reeves DC, Sayed MF, Chau PL, Price KL, Lummis SC (2003) Prediction of 5-HT3 receptor agonist-binding residues using homology modeling. Biophys J 84:2338-2344.

Robitaille R (1995) Purinergic receptors and their activation by endogenous purines at perisynaptic glial cells of the frog neuromuscular junction. J Neurosci 15:7121-7131.

Robitaille R (1998) Modulation of synaptic efficacy and synaptic depression by glial cells at the frog neuromuscular junction. Neuron 21:847-855.

Robitaille R, Jahromi BS, Charlton MP (1997) Muscarinic Ca2+ responses resistant to muscarinic antagonists at perisynaptic Schwann cells of the frog neuromuscular junction. J Physiol 504 (Pt 2):337-347.

Rochon D, Rousse I, Robitaille R (2001) Synapse-glia interactions at the mammalian neuromuscular junction. J Neurosci 21:3819-3829.

Rubenstein JL, Merzenich MM (2003) Model of autism: increased ratio of excitation/inhibition in key neural systems. Genes Brain Behav 2:255-267.

Rundstrom N, Schmieden V, Betz H, Bormann J, Langosch D (1994) Cyanotriphenylborate: subtype-specific blocker of glycine receptor chloride channels. Proc Natl Acad Sci U S A 91:8950-8954.

Russell RB, Eggleston DS (2000) New roles for structure in biology and drug discovery. Nat Struct Biol 7 Suppl:928-930.

Ryan SE, Baenziger JE (1999) A Structure-Based Approach to Nicotinic Receptor Pharmacology. Mol Pharmacol 55:348-355.

Ryan SE, Demers CN, Chew JP, Baenziger JE (1996) Structural Effects of Neutral and Anionic Lipids on the Nicotinic Acetylcholine Receptor. An infrared difference spectroscopy study. J Biol Chem 271:24590-24597.

Ryan SG, Buckwalter MS, Lynch JW, Handford CA, Segura L, Shiang R, Wasmuth JJ, Camper SA, Schofield P, O'Connell P (1994) A missense mutation in the gene encoding the alpha 1 subunit of the inhibitory glycine receptor in the spasmodic mouse. Nat Genet 7:131-135.

Sabatini DM, Barrow RK, Blackshaw S, Burnett PE, Lai MM, Field ME, Bahr BA, Kirsch J, Betz H, Snyder SH (1999) Interaction of RAFT1 with gephyrin required for rapamycin-sensitive signaling. Science 284:1161-1164.

Sali A, Blundell TL (1993) Comparative protein modelling by satisfaction of spatial restraints. J Mol Biol 234:779-815.

Sanes DH, Geary WA, Wooten GF, Rubel EW (1987) Quantitative distribution of the glycine receptor in the auditory brain stem of the gerbil. J Neurosci 7:3793-3802.

Santiago J, Guzman GR, Rojas LV, Marti R, Asmar-Rovira GA, Santana LF, McNamee M, Lasalde-Dominicci JA (2001) Probing the Effects of Membrane Cholesterol in the

Torpedo californica Acetylcholine Receptor and the Novel Lipid-exposed Mutation alpha C418W in Xenopus Oocytes. J Biol Chem 276:46523-46532.

Sargent PB (1993) The Diversity of Neuronal Nicotinic Acetylcholine Receptors. Annual Review of Neuroscience 16:403-443.

Sassoe-Pognetto M, Panzanelli P, Sieghart W, Fritschy JM (2000) Colocalization of multiple GABA(A) receptor subtypes with gephyrin at postsynaptic sites. J Comp Neurol 420:481-498.

Saul B, Schmieden V, Kling C, Mulhardt C, Gass P, Kuhse J, Becker CM (1994) Point mutation of glycine receptor alpha 1 subunit in the spasmodic mouse affects agonist responses. FEBS Lett 350:71-76.

Saul B, Kuner T, Sobetzko D, Brune W, Hanefeld F, Meinck HM, Becker CM (1999) Novel GLRA1 missense mutation (P250T) in dominant hyperekplexia defines an intracellular determinant of glycine receptor channel gating. J Neurosci 19:869-877.

Savitzky A, Golay MJE (1964) Smoothing and Differentiation of data by a simplified least squares procedures. Anal Chem 36:1627-1639.

Schmieden V, Betz H (1995) Pharmacology of the inhibitory glycine receptor: agonist and antagonist actions of amino acids and piperidine carboxylic acid compounds. Mol Pharmacol 48:919-927.

Schmieden V, Kuhse J, Betz H (1992) Agonist pharmacology of neonatal and adult glycine receptor alpha subunits: identification of amino acid residues involved in taurine activation. Embo J 11:2025-2032.

Schmieden V, Kuhse J, Betz H (1993) Mutation of glycine receptor subunit creates beta-alanine receptor responsive to GABA. Science 262:256-258.

Schmieden V, Grenningloh G, Schofield PR, Betz H (1989) Functional expression in Xenopus oocytes of the strychnine binding 48 kd subunit of the glycine receptor. Embo J 8:695-700.

Schmitt B, Knaus P, Becker CM, Betz H (1987) The Mr 93,000 polypeptide of the postsynaptic glycine receptor complex is a peripheral membrane protein. Biochemistry 26:805-811.

Schofield CM, Jenkins A, Harrison NL (2003) A Highly Conserved Aspartic Acid Residue in the Signature Disulfide Loop of the {alpha}1 Subunit Is a Determinant of Gating in the Glycine Receptor. J Biol Chem 278:34079-34083.

Schofield PR, Darlison MG, Fujita N, Burt DR, Stephenson FA, Rodriguez H, Rhee LM, Ramachandran J, Reale V, Glencorse TA, et al. (1987) Sequence and functional expression of the GABA A receptor shows a ligand-gated receptor super-family. Nature 328:221-227.

Schrattenholz A, Pfeiffer S, Pejovic V, Rudolph R, Godovac-Zimmermann J, Maelicke A (1998) Expression and Renaturation of the N-terminal Extracellular Domain of Torpedo Nicotinic Acetylcholine Receptor alpha -Subunit. J Biol Chem 273:32393-32399.

Seitanidou T, Triller A, Korn H (1988) Distribution of glycine receptors on the membrane of a central neuron: an immunoelectron microscopy study. J Neurosci 8:4319-4333.

Selvin PR, Hearst JE (1994) Luminescence energy transfer using a terbium chelate: improvements on fluorescence energy transfer. Proc Natl Acad Sci U S A 91:10024-10028.

Selvin PR, Rana TM, Hearst JE (1994) Luminescence Resonance Energy Transfer. J Am Chem Soc 116:6029-6030.

Shan Q, Nevin ST, Haddrill JL, Lynch JW (2003) Asymmetric contribution of alpha and beta subunits to the activation of alpha/beta heteromeric glycine receptors. Journal of Neurochemistry 86:498-507.

Shank RP, Aprison MH (1970) The metabolism in vivo of glycine and serine in eight areas of the rat central nervous system. Journal of Neurochemistry 17:1461-1475.

Shepherd GM, Erulkar SD (1997) Centenary of the synapse: from Sherrington to the molecular biology of the synapse and beyond. Trends Neurosci 20:385-392.

Shiang R, Ryan SG, Zhu YZ, Hahn AF, O'Connell P, Wasmuth JJ (1993) Mutations in the alpha 1 subunit of the inhibitory glycine receptor cause the dominant neurologic disorder, hyperekplexia. Nat Genet 5:351-358.

Shiang R, Ryan SG, Zhu YZ, Fielder TJ, Allen RJ, Fryer A, Yamashita S, O'Connell P, Wasmuth JJ (1995) Mutational analysis of familial and sporadic hyperekplexia. Ann Neurol 38:85-91.

Shivers BD, Killisch I, Sprengel R, Sontheimer H, Kohler M, Schofield PR, Seeburg PH (1989) Two novel GABAA receptor subunits exist in distinct neuronal subpopulations. Neuron 3:327-337.

Sieghart W, Fuchs K, Tretter V, Ebert V, Jechlinger M, Hoger H, Adamiker D (1999) Structure and subunit composition of GABAA receptors. Neurochemistry International 34:379-385.

Sine SM (2002) The nicotinic receptor ligand binding domain. J Neurobiol 53:431-446.

Sine SM, Engel AG (2006) Recent advances in Cys-loop receptor structure and function. Nature 440:448-455.

Sine SM, Kreienkamp HJ, Bren N, Maeda R, Taylor P (1995) Molecular dissection of subunit interfaces in the acetylcholine receptor: identification of determinants of alpha-conotoxin M1 selectivity. Neuron 15:205-211.

Singer JH, Berger AJ (2000) Development of inhibitory synaptic transmission to motoneurons. Brain Res Bull 53:553-560.

Sinz A (2003) Chemical cross-linking and mass spectrometry for mapping three-dimensional structures of proteins and protein complexes. J Mass Spectrom 38:1225-1237.

Sinz A (2006) Chemical cross-linking and mass spectrometry to map three-dimensional protein structures and protein-protein interactions. Mass Spectrom Rev 25:663-682.

Sixma TK, Smit AB (2003) Acetylcholine binding protein (AChBP): a secreted glial protein that provides a high-resolution model for the extracellular domain of pentameric ligand-gated ion channels. Annu Rev Biophys Biomol Struct 32:311-334.

Smit AB, Brejc K, Syed N, Sixma TK (2003) Structure and function of AChBP, homologue of the ligand-binding domain of the nicotinic acetylcholine receptor. Ann N Y Acad Sci 998:81-92.

Smit AB, Celie PH, Kasheverov IE, Mordvintsev DY, van Nierop P, Bertrand D, Tsetlin V, Sixma TK (2006) Acetylcholine-binding proteins: functional and structural homologs of nicotinic acetylcholine receptors. J Mol Neurosci 30:9-10.

Smit AB, Syed NI, Schaap D, van Minnen J, Klumperman J, Kits KS, Lodder H, van der Schors RC, van Elk R, Sorgedrager B, Brejc K, Sixma TK, Geraerts WP (2001) A glia-derived acetylcholine-binding protein that modulates synaptic transmission. Nature 411:261-268.

Smith GB, Olsen RW (2000) Deduction of amino acid residues in the GABA(A) receptor alpha subunits photoaffinity labeled with the benzodiazepine flunitrazepam. Neuropharmacology 39:55-64.

Sontheimer H, Becker CM, Pritchett DB, Schofield PR, Grenningloh G, Kettenmann H, Betz H, Seeburg PH (1989) Functional chloride channels by mammalian cell expression of rat glycine receptor subunit. Neuron 2:1491-1497.

Speranskiy K, Cascio M, Kurnikova M (2007) Homology modeling and molecular dynamics simulations of the glycine receptor ligand binding domain. Proteins 67:950-960.

Sreerama N, Woody RW (2000) Estimation of protein secondary structure from circular dichroism spectra: comparison of CONTIN, SELCON, and CDSSTR methods with an expanded reference set. Anal Biochem 287:252-260.

Srinivasan S, Nichols CJ, Lawless GM, Olsen RW, Tobin AJ (1999) Two Invariant Tryptophans on the alpha 1 Subunit Define Domains Necessary for GABAA Receptor Assembly. J Biol Chem 274:26633-26638.

Steiger JL, Russek SJ (2004) GABAA receptors: building the bridge between subunit mRNAs, their promoters, and cognate transcription factors. Pharmacology & Therapeutics 101:259-281.

Stephenson FA, Duggan MJ, Pollard S (1990) The gamma 2 subunit is an integral component of the gamma-aminobutyric acidA receptor but the alpha 1 polypeptide is the principal site of the agonist benzodiazepine photoaffinity labeling reaction. J Biol Chem 265:21160-21165.

Strata F, Cherubini E (1994) Transient expression of a novel type of GABA response in rat CA3 hippocampal neurones during development. J Physiol 480 (Pt 3):493-503.

Stryer L (1978) Fluorescence Energy Transfer as a Spectroscopic Ruler. Annual Review of Biochemistry 47:819-846.

Sun J, Kaback HR (1997) Proximity of Periplasmic Loops in the Lactose Permease of Escherichia coli Determined by Site-Directed Cross-Linking. Biochemistry 36:11959-11965.

Sunshine C, McNamee MG (1994) Lipid modulation of nicotinic acetylcholine receptor function: the role of membrane lipid composition and fluidity. Biochimica et Biophysica Acta (BBA) - Biomembranes 1191:59-64.

Takahashi T, Momiyama A, Hirai K, Hishinuma F, Akagi H (1992) Functional correlation of fetal and adult forms of glycine receptors with developmental changes in inhibitory synaptic receptor channels. Neuron 9:1155-1161.

Tamamizu S, Guzman GR, Santiago J, Rojas LV, McNamee MG, Lasalde-Dominicci JA (2000) Functional Effects of Periodic Tryptophan Substitutions in the α M4 Transmembrane Domain of the Torpedo californica Nicotinic Acetylcholine Receptor. Biochemistry 39:4666-4673.

Tang P, Mandal PK, Xu Y (2002) NMR Structures of the Second Transmembrane Domain of the Human Glycine Receptor alpha 1 Subunit: Model of Pore Architecture and Channel Gating. Biophys J 83:252-262.

Tapia J, Aguayo L (1998) Changes in the properties of developing glycine receptors in cultured mouse spinal neurons. Synapse 28:185-194.

Taylor PM, Connolly CN, Kittler JT, Gorrie GH, Hosie A, Smart TG, Moss SJ (2000) Identification of residues within GABA(A) receptor alpha subunits that mediate specific assembly with receptor beta subunits. J Neurosci 20:1297-1306.

Teichberg VI (1991) Glial glutamate receptors: likely actors in brain signaling. Faseb J 5:3086-3091.

Thompson JD, Higgins DG, Gibson TJ (1994) CLUSTAL W: improving the sensitivity of progressive multiple sequence alignment through sequence weighting, position-specific gap penalties and weight matrix choice. Nucleic Acids Res 22:4673-4680.

Tierney ML, Unwin N (2000) Electron microscopic evidence for the assembly of soluble pentameric extracellular domains of the nicotinic acetylcholine receptor. J Mol Biol 303:185-196.

Tillman TS, Cascio M (2003) Effects of membrane lipids on ion channel structure and function. Cell Biochem Biophys 38:161-190.

Tretter V, Ehya N, Fuchs K, Sieghart W (1997) Stoichiometry and assembly of a recombinant GABAA receptor subtype. J Neurosci 17:2728-2737.

Triller A, Cluzeaud F, Pfeiffer F, Betz H, Korn H (1985) Distribution of glycine receptors at central synapses: an immunoelectron microscopy study. J Cell Biol 101:683-688.

Trudell J (2002) Unique assignment of inter-subunit association in GABA(A) alpha 1 beta 3 gamma 2 receptors determined by molecular modeling. Biochim Biophys Acta 1565:91-96.

Tsetlin VI, Dergousova NI, Azeeva EA, Kryukova EV, Kudelina IA, Shibanova ED, Kasheverov IE, Methfessel C (2002) Refolding of the Escherichia coli expressed extracellular domain of alpha 7 nicotinic acetylcholine receptor. Eur J Biochem 269:2801-2809.

Turecek R, Trussell LO (2001) Presynaptic glycine receptors enhance transmitter release at a mammalian central synapse. 411:587-590.

Turecek R, Trussell LO (2002) Reciprocal developmental regulation of presynaptic ionotropic receptors. PNAS 99:13884-13889.

Ulens C, Hogg RC, Celie PH, Bertrand D, Tsetlin V, Smit AB, Sixma TK (2006) Structural determinants of selective alpha-conotoxin binding to a nicotinic acetylcholine receptor homolog AChBP. Proc Natl Acad Sci U S A 103:3615-3620.

Unwin N (1995) Acetylcholine receptor channel imaged in the open state. 373:37-43.

Unwin N (2003) Structure and action of the nicotinic acetylcholine receptor explored by electron microscopy. FEBS Letters, 126th Nobel Symposium Membrane Proteins: Structure, Function and Assembly 555:91-95.

Unwin N (2005) Refined structure of the nicotinic acetylcholine receptor at 4A resolution. J Mol Biol 346:967-989.

Unwin N, Miyazawa A, Li J, Fujiyoshi Y (2002) Activation of the Nicotinic Acetylcholine Receptor Involves a Switch in Conformation of the [alpha] Subunits. Journal of Molecular Biology 319:1165-1176.

Vafa B, Lewis TM, Cunningham AM, Jacques P, Lynch JW, Schofield PR (1999) Identification of a new ligand binding domain in the alpha1 subunit of the inhibitory glycine receptor. J Neurochem 73:2158-2166.

van den Pol AN, Gorcs T (1988) Glycine and glycine receptor immunoreactivity in brain and spinal cord. J Neurosci 8:472-492.

van Hooft JA, Spier AD, Yakel JL, Lummis SCR, Vijverberg HPM (1998) Promiscuous coassembly of serotonin 5-HT3 and nicotinic alpha 4 receptor subunits into Ca2+-permeable ion channels. PNAS 95:11456-11461.

Vandenberg R, Rajendra S, French C, Barry P, Schofield P (1993) The extracellular disulfide loop motif of the inhibitory glycine receptor does not form the agonist binding site. Mol Pharmacol 44:198-203.

Vandenberg RJ, Handford CA, Schofield PR (1992a) Distinct agonist- and antagonist-binding sites on the glycine receptor. Neuron 9:491-496.

Vandenberg RJ, French CR, Barry PH, Shine J, Schofield PR (1992b) Antagonism of ligand-gated ion channel receptors: two domains of the glycine receptor alpha subunit form the strychnine-binding site. Proc Natl Acad Sci U S A 89:1765-1769.

Verdoorn TA, Draguhn A, Ymer S, Seeburg PH, Sakmann B (1990) Functional properties of recombinant rat GABAA receptors depend upon subunit composition. Neuron 4:919-928.

Vincent A, Palace J, Hilton-Jones D (2001) Myasthenia gravis. Lancet 357:2122.

Volterra A, Magistretti P, Haydon P (2002) The tripartite synapse ?glia in synaptic transmission.: Oxford (UK): Oxford University Press.

Vriend G (1990) WHAT IF: a molecular modeling and drug design program. J Mol Graph 8:52-56, 29.

Waldvogel HJ, Baer K, Snell RG, During MJ, Faull RL, Rees MI (2003) Distribution of gephyrin in the human brain: an immunohistochemical analysis. Neuroscience 116:145-156.

Wallace BA, Lees JG, Orry AJ, Lobley A, Janes RW (2003) Analyses of circular dichroism spectra of membrane proteins. Protein Sci 12:875-884.

Wang D, Moore S (1977) Polyspermine-ribonuclease prepared by cross-linkage with dimethyl suberimidate. Biochemistry 16:2937-2942.

Wang LY, MacDonald JF (1995) Modulation by magnesium of the affinity of NMDA receptors for glycine in murine hippocampal neurones. J Physiol 486 (Pt 1):83-95.

Wassef A, Baker J, Kochan LD (2003) GABA and schizophrenia: a review of basic science and clinical studies. J Clin Psychopharmacol 23:601-640.

Watanabe E, Akagi H (1995) Distribution patterns of mRNAs encoding glycine receptor channels in the developing rat spinal cord. Neuroscience Research 23:377-382.

Wells GB, Anand R, Wang F, Lindstrom J (1998) Water-soluble Nicotinic Acetylcholine Receptor Formed by alpha 7 Subunit Extracellular Domains. J Biol Chem 273:964-973.

Werman R, Davidoff RA, Aprison MH (1967) Is Glycine a Neurotransmitter?: Inhibition of Motoneurones by Iontophoresis of Glycine. 214:681-683.

West AP, Jr., Bjorkman PJ, Dougherty DA, Lester HA (1997) Expression and circular dichroism studies of the extracellular domain of the alpha subunit of the nicotinic acetylcholine receptor. J Biol Chem 272:25468-25473.

Whitehead KJ, Manning J-P, Smith CGS, Bowery NG (2001) Determination of the extracellular concentration of glycine in the rat spinal cord dorsal horn by quantitative microdialysis. Brain Research 910:192-194.

Whitmore L, Wallace BA (2004) DICHROWEB, an online server for protein secondary structure analyses from circular dichroism spectroscopic data. Nucleic Acids Res 32:W668-673.

Wilbur DS (1992) Radiohalogenation of proteins: an overview of radionuclides, labeling methods, and reagents for conjugate labeling. Bioconjug Chem 3:433-470.

Wilke K, Gaul R, Klauck SM, Poustka A (1997) A Gene in Human Chromosome Band Xq28 (GABRE) Defines a Putative New Subunit Class of the GABAANeurotransmitter Receptor. Genomics 45:1-10.

Williams DB, Akabas MH (1999) gamma -Aminobutyric Acid Increases the Water Accessibility of M3 Membrane-Spanning Segment Residues in gamma -Aminobutyric Acid Type A Receptors. Biophys J 77:2563-2574.

Williams DB, Akabas MH (2000) Benzodiazepines Induce a Conformational Change in the

Region of the gamma -Aminobutyric Acid Type A Receptor alpha 1-Subunit M3 Membrane-Spanning Segment. Mol Pharmacol 58:1129-1136.

Yan D, White MM (2005) Spatial orientation of the antagonist granisetron in the ligand-binding site of the 5-HT3 receptor. Mol Pharmacol 68:365-371.

Yao Y, Wang J, Viroonchatapan N, Samson A, Chill J, Rothe E, Anglister J, Wang ZZ (2002) Yeast expression and NMR analysis of the extracellular domain of muscle nicotinic acetylcholine receptor alpha subunit. J Biol Chem 277:12613-12621.

Ye J-H (2000) Physiology and pharmacology of native glycine receptors in developing rat ventral tegmental area neurons. Brain Research 862:74-82.

Young AB, Snyder SH (1973) Strychnine binding associated with glycine receptors of the central nervous system. Proc Natl Acad Sci U S A 70:2832-2836.

Young MM, Tang N, Hempel JC, Oshiro CM, Taylor EW, Kuntz ID, Gibson BW, Dollinger G (2000) High throughput protein fold identification by using experimental constraints derived from intramolecular cross-links and mass spectrometry. PNAS 97:5802-5806.

Zhou L, Chillag KL, Nigro MA (2002) Hyperekplexia: a treatable neurogenetic disease. Brain Dev 24:669-674.